ENGINEERING STUDY

# Sediment Transport and Scour Analysis

## San Jacinto River, Stage 4 North and South Levees


**Prepared for:**

RIVERSIDE COUNTY FLOOD CONTROL & WATER CONSERVATION DISTRICT

&

SAN JACINTO

CITY OF SAN JACINTO

**Prepared by:**

PACE

Advanced Water Engineering

Job# 9020E
April 2011
(February 2011 - Revised)
(June 2010 - Revised)
(November 2009 - Revised)

Contact Person:
Bruce M. Phillips, PE

## Sediment Transport and Scour Analysis

# San Jacinto River, Stage 4 North and South Levees

**Amended April 2011**
(Revised February 2011)
(Revised June 2010)
(Revised November 2009)

*Prepared For:*

**Riverside County Flood Control and Water Conservation District**
1995 Market Street
Riverside, CA 92501
(951) 955-1200

and

**City of San Jacinto**
595 S. San Jacinto Ave.
San Jacinto, CA 92583
(951) 487-7330

*Prepared By:*


PACE
Advanced Water Engineering

**Pacific Advanced Civil Engineering, Inc.**
17520 Newhope Street, Suite 200
Fountain Valley, CA 92708

*Contact Person:*

Bruce Phillips, PE


#9020E

# Table of Contents

## List of Figures

## List of Tables

# 1 Introduction

The following technical investigation provides a detailed and focused evaluation of the fluvial characteristics and long-term stability of the San Jacinto River located in San Jacinto, Riverside County, California. The Creek study reach is located in the San Jacinto Mountains in central Riverside County, California (Figure 1-1). San Jacinto River within the study reach is from Olmstead Street to approximately 8,200 feet downstream of Sanderson Avenue, and is approximately 5.5 miles in length. The River lies within a contributing drainage of the 700 square-mile area of Southern California. The existing floodplain generally consists of an alluvial stream system within the San Jacinto River Watershed. Modifications to existing levees are planned and may result in changes in streambed response. The intent of this analysis is to evaluate these impacts from (1) fluvial modifications of the riverbed from single hypothetical storm events, and (2) changes in the floodplain fluvial operation over the long-term.

## 1.1 Study Location

The study portion of the San Jacinto River extends from approximately Olmstead Street downstream of the Lake Park Drive Bridge to upstream of the Laborde Canyon confluence, or a total study reach length of approximately 5.5 miles. The State Street and Sanderson Avenue Bridges are located approximately 10,000 feet from each other. The only significant confluence in the study reach is located at Massacre Canyon upstream of the State Street Bridge. The total tributary watershed area to the downstream portion of this study reach for San Jacinto River is approximately 675 square miles. This portion of San Jacinto is a natural alluvial stream system, although it has experienced a variety of human activity, including the construction of bridge crossings, historic sand/gravel mining operations, and agricultural activities, that have all influenced the fluvial mechanics.


**Figure 1-1** - Aerial Photograph Depicting the Study Site

## 1.2 Proposed Project Facilities

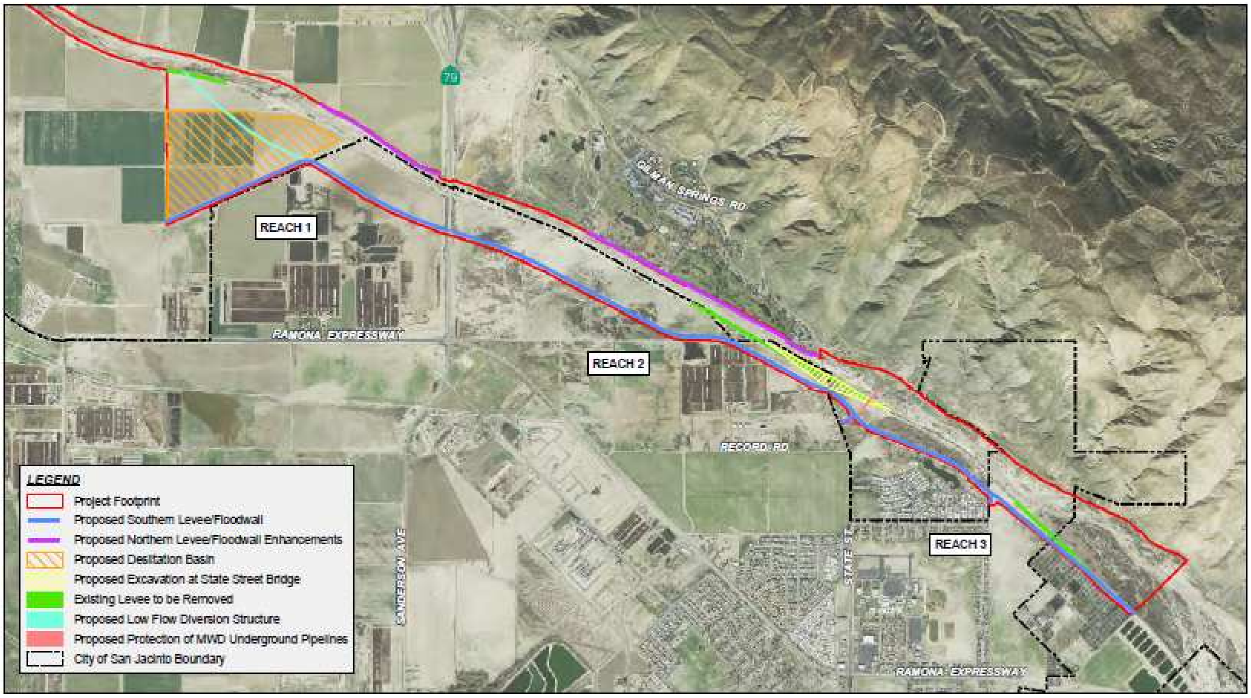


## 1.3 Types of Adjustment

Modifications to the Creek system are measured as vertical bed adjustment in feet. Positive adjustment indicates bed aggradation while negative adjustment indicates bed degradation. Several types of adjustment are considered in this study including general adjustment, long-term adjustment, and other scour. General adjustment consists of scour that occurs during an individual discharge event, and may be considered as the difference between sediment inflow and outflow. That is, if sediment inflow into a given reach is higher than sediment outflow for the same reach, aggradation will occur. In contrast, if sediment outflow exceeds inflow for a given reach, degradation will occur, or the bed may become armored. Long-term adjustment consists of fluvial processes that occur over many rainy seasons and contribute fluctuation of bed elevation of a river or creek. Other scour is comprised of local scour, bend scour, low-flow incisement, and bed form formation. These are discussed in detail in the different sections of the report.

# 2 Study Area Description

## 2.1 Overview

This section provides basic information about the following characteristics of San Jacinto River study area within the study reach:

- Watershed Description
- Geologic Setting
- Climate
- Study Area Description

The interrelated watershed, geologic, hydraulic, and hydrologic characteristics of a stream combine to determine its unique geomorphology. These types of data for this portion of San Jacinto River were used to define specific stream reaches for more detailed analyses.

## 2.2 San Jacinto Watershed Description

The San Jacinto River watershed is located in central Riverside County, California and encompasses a drainage area of approximately 700 square miles (RCFCD 1994). The San Jacinto River has several tributaries including Bautista, Poppet and Potrero Creeks, as well as Perris Valley Drain and Salt Creek (RCFCD 1975, RCFCD 1994). The River is approximately 59.5 miles long from the headwaters to Railroad Canyon Dam, and is tributary to Santa Ana River through Lake Elsinore and the Temescal Wash; however, Lake Elsinore seldom attains stages where lake overflow reaches the Santa Ana River (RCFCD 1975, RCFCD 1994).

## 2.3 Geologic Setting

Two major faults confine portions of the watersheds. The Casa Loma and San Jacinto faults are oriented in a northwesterly direction, and between the faults resides the San Jacinto Valley. The valley floor is comprised primarily of alluvial deposits. At the western end of the valley a natural sump is present (RCFCD 1975, RCFCD 1994).

The higher elevations of the watershed are comprised of granitic, shallow, stony soils. The middle elevations consist of partially consolidated clay shales overlain by gravels. The valley floor and lower elevations are made up of alluvium that varies from coarse soils at the upstream hills to fine, sandy clays in downstream reaches (RCFCD 1975, RCFCD 1994).

## 2.4 Climate

Climate within the watershed varies by geography. Mountainous areas have cold winters and mild summers, while valley floors have hot, dry summers, and mild winters. Snow may occur in the mountains during winter with average precipitation of approximately 35 inches. Precipitation in the valley averages approximately 11 inches. Precipitation for the watershed primarily occurs in the winter months and most of the runoff in the watershed is produced from these storms. Runoff is produced in the River primarily during and immediately after intense or prolonged precipitation with intense periods of rainfall (RCFCD 1975, RCFCD 1994).

## 2.5 Study Area

The present study area rests primarily in the City of San Jacinto between the watershed's San Jacinto Valley and Soboba-Gilman sub-areas. The Poppet and Bautista confluences are upstream of the study reach.

# 3 Hydrology

### 3.1 Watershed Description

The San Jacinto River watershed is mainly located in Central Riverside County, California. The watershed encompasses a drainage area of approximately 700 square miles. San Jacinto River is the major stream in the watershed. The headwater of San Jacinto River generates from the San Bernardino National Forest and drains southwesterly to Lake Elsinore. No major tributaries exist in the study area. (Figure 3.1)


**Figure 3-1** - Regional Watersheds

### 3.2 Flood History - San Jacinto River

A long history of recurrent but infrequent flood problems in Southern California is revealed in records kept by missions and other historical sources, including diaries from Mission Fathers, early travelers, and settlers. There are accounts of floods occurring as far back as 1770. Of these early Southern California accounts, the floods of 1780, 1825, 1862, 1884, 1891, and 1916 were of major proportions. The 1916 event saw levels in Lake Elsinore reach stages such that flow from San Jacinto reached Santa Ana River (RCFCD 1975, RCFCD 1994). Floods occurring since 1851 have been described in more detail than previous floods and provide some basis for determining the relative magnitudes of major flood events and their recurrence intervals. Recorded data from 1897 to present show medium to large winter floods occurring in January 1910, January 1916, February 1937, March 1938, January 1943, January and February 1969, February and March 1978, February 1980, March 1983, January, February and March 1995, and December, January and February 1998. Among these events, gage data on San Jacinto River upstream of the project site (USGS 11069500 San Jacinto River near San Jacinto) indicates discharges exceeding 10,000 cfs on the following dates: February 1927, February 1937, March 1938, and February 1980. The 1938 event was particularly significant in Riverside County history since this event ultimately lead to the formation of the Flood Control District. The Federal Register (V. 22, N. 139, p. 39802) cites that the San Jacinto Levee project (1961) provided sufficient protection from the 1969 event. The 1980 event, although smaller in discharge, caused the levee to fail and resulted in severe flooding in the City of San Jacinto. However, it is unknown if the levee failure was from overtopping or not.

### 3.3 Historic Hydrologic Data

Eight USGS stream gages are available for San Jacinto River. These gages provide data from 1916 onward. Of the available gages only three are located on the River above the study reach, and of these three gages, only one (11069500) has sufficient length of record to provide adequate data for statistical analysis. The San Jacinto gage records discharges for the upper 142 square miles of the watershed, and includes 74 records between 1920 and 2006. At State Street there exists a gage (11070150) recording discharges for the upper 252 square miles of the watershed, however, this gage only has approximately 10 years of discharge data. Data from USGS gage 11069500 is used in this study.

A Spearman-Conley test was conducted on the data set to evaluate whether trends in the flood record exist and test for the nonhomogeneity of a flood record. The Spearman-Conley test statistic, $R_{sc}$, is given as (McCuen 1998):

$$R_s = 1 - \frac{6\sum_{i=1}^{n} d_i^2}{n^3 - n}$$

where I is the sample size, and $d_{R_{s,i}}$ is the i[th] difference in ranks of the test series. For San Jacinto River within the study reach the test statistic was calculated as $R_{sc}$=0.07880. At a 5% level of significance, the results of the Spearman-Conley test suggest that there has not been a systematic change to the watershed hydrology over time, and that the flood record is stationary. The analysis is shown in Table 3.1.

Critical values for the Spearman-Conley statistic are readily available for sample sizes between 5 and 30. The statistic for the San Jacinto Creek was calculated using the complete data set, 74 data pairs. To approximate a critical value for a sample size of 74, the critical values presented in McCuen for a 5% significance (Hydrologic Analysis and Design, 2005) were plotted versus the corresponding sample size and an exponential trendline was fitted to the tail of the curve (corresponding to sample sizes n = 21 – 30). The resulting trendline equation was used to calculate an approximate critical value for a sample size of n = 74. The calculated critical value of RCR = 0.1213 is greater than the value of the statistic calculated for the data set, RSC = 0.0788. This implies that there is no trending in the data set caused by imperviousness.

A Log-Pearson Type III frequency analysis was performed on the USGS gage 11069500 data (McCuen 1998). Based on the Weibull plotting position formula, the data is shown in Table 3.2. Using the data to determine the P=0.01 return period event gives a discharge of Q=26,907 cfs. The RCFCD (1975) study determined that the P=0.01 design discharge is Q=57,250 cfs, and that discharge is considered the design discharge for this study as required by RCFCD. Since the gage location and the RCFCD study design discharge location are not coincidentally located, the gage data must be scaled up to the design discharge. Scaling the calculated value up to the RCFCD value to account for differences in watershed area gives a ratio of discharges of 2.13:1. That is, 2.13:1:57,250:26,907. The peak discharge hydrograph is assumed to take a SCS hydrograph shape since no single event data is available for the USGS gage

11069500. The scaled 100-year design hydrograph for the study reach is based on USGS gage 11069500 is shown in Figure 3.2.

Long-term gage data for 11069500 is only available as daily mean data for the period of record of the gage. To convert the daily average discharge data to daily peak discharge data a relationship between average and peak must be formulated, although it is unclear if any relationship exists. Figure 3.2 shows the annual maximum daily peak discharge plotted against the annual maximum daily average discharge. Only days where the annual peak discharge coincides with the annual peak average discharge are used. The figure shows that an exponential relationship exists for the data given as $Q_{PEAK}=2.25\ Q_{AVG}{}^{0.99}$, which for the purposes of the present study can be simplified to the linear relationship $Q_{PEAK}=2.25\ Q_{AVG}$. The power relationship has a correlation coefficient of $r^2=0.72$. Since this relationship will scale the daily discharge more conservatively (higher ratio) than the ratio of daily average discharge to the design discharge the present study uses the ratio of 2.25:1 to scale all long-term gage data for long-term analysis. It is assumed for purposes of this study that all events less than the P=0.01 event scale at the same ratio for all return periods. While it is recognized that this assumption is unlikely to be observed in the field, the lack of supporting hydrology data from other studies or gages provides that this is the best estimate available at the time of writing. The scaled long-term data set with no-report records removed is shown in Figure 3.3A. Confidence intervals of the data are shown in Figure 3.3B, and the figure indicates that all of the data points reside within the 95% confidence interval.

**Table 3-1 -** Spearman-Conley Test of Discharge at Gage 11069500: 1921-2006

| Spearman-Connley Analysis of USGS Gage 11069500 | | | | | | |
|---|---|---|---|---|---|---|
| Year | Annual $Q_{max}=Y_t$ | Offset $Y_t = X_t$ | Rank $y_i = r_{yi}$ | Rank $x_i = r_{xi}$ | $d_i = ry_i - rx_i$ | $d_i^2$ |
| 3/13/1921 | 324 | | | | | |
| 2/10/1922 | 2180 | 324 | 15 | 34 | -19 | 361 |
| 12/13/1922 | 630 | 2180 | 28 | 15 | 13 | 169 |
| 3/6/1924 | 238 | 630 | 43 | 28 | 15 | 225 |
| 12/23/1924 | 113 | 238 | 59 | 43 | 16 | 256 |
| 4/6/1926 | 2700 | 113 | 12 | 59 | -47 | 2209 |
| 2/16/1927 | 45000 | 2700 | 1 | 12 | -11 | 121 |
| 12/30/1927 | 42 | 45000 | 72 | 1 | 71 | 5041 |
| 5/5/1930 | 203 | 42 | 47 | 72 | -25 | 625 |
| 8/31/1931 | 6000 | 203 | 7 | 47 | -40 | 1600 |
| 12/28/1931 | 3150 | 6000 | 10 | 7 | 3 | 9 |
| 4/29/1933 | 94 | 3150 | 63 | 10 | 53 | 2809 |
| 1/1/1934 | 295 | 94 | 36 | 63 | -27 | 729 |
| 2/6/1935 | 280 | 295 | 40 | 36 | 4 | 16 |
| 2/11/1936 | 287 | 280 | 38 | 40 | -2 | 4 |
| 2/6/1937 | 14000 | 287 | 4 | 38 | -34 | 1156 |
| 3/2/1938 | 14300 | 14000 | 3 | 4 | -1 | 1 |
| 3/27/1939 | 220 | 14300 | 44 | 3 | 41 | 1681 |
| 1/8/1940 | 470 | 220 | 32 | 44 | -12 | 144 |
| 3/5/1941 | 820 | 470 | 24 | 31 | -7 | 49 |
| 3/20/1942 | 101 | 820 | 62 | 24 | 38 | 1444 |
| 3/4/1943 | 1420 | 101 | 20 | 62 | -42 | 1764 |
| 3/7/1944 | 66 | 1420 | 64 | 20 | 44 | 1936 |
| 2/2/1945 | 800 | 66 | 25 | 64 | -39 | 1521 |
| 12/22/1945 | 2000 | 800 | 17 | 25 | -8 | 64 |
| 11/23/1946 | 117 | 2000 | 57 | 17 | 40 | 1600 |
| 4/4/1948 | 60 | 117 | 65 | 57 | 8 | 64 |
| 3/20/1949 | 56 | 60 | 67 | 65 | 2 | 4 |
| 2/7/1950 | 200 | 56 | 48 | 67 | -19 | 361 |
| 7/18/1951 | 44 | 200 | 71 | 48 | 23 | 529 |
| 12/30/1951 | 1600 | 44 | 19 | 71 | -52 | 2704 |
| 1/8/1953 | 115 | 1600 | 58 | 19 | 39 | 1521 |
| 1/25/1954 | 786 | 115 | 26 | 58 | -32 | 1024 |
| 2/17/1955 | 340 | 786 | 34 | 26 | 8 | 64 |
| 1/27/1956 | 1080 | 340 | 23 | 33 | -10 | 100 |
| 1/13/1957 | 292 | 1080 | 37 | 23 | 14 | 196 |
| 3/22/1958 | 1780 | 292 | 18 | 37 | -19 | 361 |
| 2/16/1959 | 715 | 1780 | 27 | 18 | 9 | 81 |

**Table 3-1 -** Spearman-Conley Test of Discharge at Gage 11069500: 1921-2006 (continued)

| Spearman-Connley Analysis of USGS Gage 11069500 | | | | | | |
|---|---|---|---|---|---|---|
| Year | Annual $Q_{max}$=$Y_t$ | Offset $Y_t$ = $X_t$ | Rank $y_i$ = $r_{yi}$ | Rank $x_i$ = $r_{xi}$ | $d_i$ = $ry_i$ - $rx_i$ | $d_i^2$ |
| 12/10/1959 | 185 | 715 | 49 | 27 | 22 | 484 |
| 8/19/1961 | 215 | 185 | 45 | 49 | -4 | 16 |
| 9/22/1962 | 119 | 215 | 55 | 45 | 10 | 100 |
| 2/10/1963 | 160 | 119 | 51 | 55 | -4 | 16 |
| 4/1/1964 | 129 | 160 | 53 | 51 | 2 | 4 |
| 4/10/1965 | 126 | 129 | 54 | 53 | 1 | 1 |
| 11/22/1965 | 6300 | 126 | 6 | 54 | -48 | 2304 |
| 12/6/1966 | 5720 | 6300 | 8 | 6 | 2 | 4 |
| 3/8/1968 | 118 | 5720 | 56 | 8 | 48 | 2304 |
| 1/25/1969 | 7410 | 118 | 5 | 56 | -51 | 2601 |
| 3/2/1970 | 506 | 7410 | 31 | 5 | 26 | 676 |
| 11/29/1970 | 45 | 506 | 70 | 30 | 40 | 1600 |
| 12/25/1971 | 368 | 45 | 33 | 70 | -37 | 1369 |
| 12/4/1972 | 278 | 368 | 41 | 32 | 9 | 81 |
| 4/2/1974 | 255 | 278 | 42 | 41 | 1 | 1 |
| 3/8/1975 | 112 | 255 | 60 | 42 | 18 | 324 |
| 9/24/1976 | 515 | 112 | 30 | 60 | -30 | 900 |
| 1/3/1977 | 55 | 515 | 68 | 29 | 39 | 1521 |
| 1/15/1978 | 4500 | 55 | 9 | 68 | -59 | 3481 |
| 2/21/1979 | 2050 | 4500 | 16 | 9 | 7 | 49 |
| 2/21/1980 | 17300 | 2050 | 2 | 16 | -14 | 196 |
| 2/9/1981 | 208 | 17300 | 46 | 2 | 44 | 1936 |
| 2/10/1982 | 2900 | 208 | 11 | 46 | -35 | 1225 |
| 3/1/1983 | 2420 | 2900 | 13 | 11 | 2 | 4 |
| 8/31/1988 | 181 | 2420 | 50 | 13 | 37 | 1369 |
| 3/1/1991 | 2410 | 181 | 14 | 50 | -36 | 1296 |
| 1/26/1997 | 284 | 2410 | 39 | 14 | 25 | 625 |
| 2/22/1998 | 1120 | 284 | 22 | 39 | -17 | 289 |
| 7/11/1999 | 151 | 1120 | 52 | 22 | 30 | 900 |
| 2/21/2000 | 60 | 151 | 65 | 52 | 13 | 169 |
| 2/28/2001 | 52 | 60 | 69 | 65 | 4 | 16 |
| 12/14/2001 | 0.61 | 52 | 73 | 69 | 4 | 16 |
| 3/15/2003 | 310 | 0.61 | 35 | 73 | -38 | 1444 |
| 2/27/2004 | 110 | 310 | 61 | 35 | 26 | 676 |
| 1/11/2005 | 1310 | 110 | 21 | 61 | -40 | 1600 |
| 2/28/2006 | 517 | 1310 | 29 | 21 | 8 | 64 |
| | | | | | sum $d_i^2$ = | 62204 |
| | | | | | Number of values (n) = | 74 |
| | | | | | $R_{sc}$ = | 0.07880 |

**Table 3-2 -** Log-Pearson Analysis of Peak Discharge at Gage 11069500: 1921-2006

| Date | Discharge | LOG(Q) | Scaled Discharge | LOG(ScaledQ) |
|---|---|---|---|---|
| 3/13/1921 | 324 | 2.51 | 689.37 | 2.84 |
| 2/10/1922 | 2180 | 3.34 | 4638.37 | 3.67 |
| 12/13/1922 | 630 | 2.80 | 1340.45 | 3.13 |
| 3/6/1924 | 238 | 2.38 | 506.39 | 2.70 |
| 12/23/1924 | 113 | 2.05 | 240.43 | 2.38 |
| 4/6/1926 | 2700 | 3.43 | 5744.77 | 3.76 |
| 2/16/1927 | 45000 | 4.65 | 95746.11 | 4.98 |
| 12/30/1927 | 42 | 1.62 | 89.36 | 1.95 |
| 5/5/1930 | 203 | 2.31 | 431.92 | 2.64 |
| 8/31/1931 | 6000 | 3.78 | 12766.15 | 4.11 |
| 12/28/1931 | 3150 | 3.50 | 6702.23 | 3.83 |
| 4/29/1933 | 94 | 1.97 | 200.00 | 2.30 |
| 1/1/1934 | 295 | 2.47 | 627.67 | 2.80 |
| 2/6/1935 | 280 | 2.45 | 595.75 | 2.78 |
| 2/11/1936 | 287 | 2.46 | 610.65 | 2.79 |
| 2/6/1937 | 14000 | 4.15 | 29787.68 | 4.47 |
| 3/2/1938 | 14300 | 4.16 | 30425.99 | 4.48 |
| 3/27/1939 | 220 | 2.34 | 468.09 | 2.67 |
| 1/8/1940 | 470 | 2.67 | 1000.01 | 3.00 |
| 3/5/1941 | 820 | 2.91 | 1744.71 | 3.24 |
| 3/20/1942 | 101 | 2.00 | 214.90 | 2.33 |
| 3/4/1943 | 1420 | 3.15 | 3021.32 | 3.48 |
| 3/7/1944 | 66 | 1.82 | 140.43 | 2.15 |
| 2/2/1945 | 800 | 2.90 | 1702.15 | 3.23 |
| 12/22/1945 | 2000 | 3.30 | 4255.38 | 3.63 |
| 11/23/1946 | 117 | 2.07 | 248.94 | 2.40 |
| 4/4/1948 | 60 | 1.78 | 127.66 | 2.11 |
| 3/20/1949 | 56 | 1.75 | 119.15 | 2.08 |
| 2/7/1950 | 200 | 2.30 | 425.54 | 2.63 |
| 7/18/1951 | 44 | 1.64 | 93.62 | 1.97 |
| 12/30/1951 | 1600 | 3.20 | 3404.31 | 3.53 |
| 1/8/1953 | 115 | 2.06 | 244.68 | 2.39 |
| 1/25/1954 | 786 | 2.90 | 1672.37 | 3.22 |
| 2/17/1955 | 340 | 2.53 | 723.42 | 2.86 |
| 1/27/1956 | 1080 | 3.03 | 2297.91 | 3.36 |
| 1/13/1957 | 292 | 2.47 | 621.29 | 2.79 |
| 3/22/1958 | 1780 | 3.25 | 3787.29 | 3.58 |
| 2/16/1959 | 715 | 2.85 | 1521.30 | 3.18 |

**Original:**

| Return | P | K | QBAR + KS | Q |
|---|---|---|---|---|
| 1.00 | 1.00 | -3.85 | -0.39 | 0 |
| 2.00 | 0.50 | 0.01 | 2.65 | 442 |
| 5.00 | 0.20 | 0.84 | 3.30 | 1997 |
| 10.00 | 0.10 | 1.27 | 3.64 | 4352 |
| 50.00 | 0.02 | 2.02 | 4.23 | 16790 |
| 100.00 | 0.01 | 2.28 | 4.43 | 26907 |
| 500.00 | 0.00 | 2.81 | 4.84 | 69345 |

**$Q_{100}$ (RCFCD Design Discharge):** 57250

**Scale Factor:** 2.13

**Scaled:**

| Return | P | K | QBAR + KS | Q |
|---|---|---|---|---|
| 1.00 | 1.00 | -3.85 | -0.06 | 1 |
| 2.00 | 0.50 | 0.01 | 2.97 | 857 |
| 5.00 | 0.20 | 0.84 | 3.63 | 3935 |
| 10.00 | 0.10 | 1.27 | 3.97 | 8703 |
| 50.00 | 0.02 | 2.02 | 4.55 | 35036 |
| 100.00 | 0.01 | 2.28 | 4.76 | 57250 |
| 500.00 | 0.00 | 2.81 | 5.17 | 154561 |

**Table 3-2 -** Log-Pearson Analysis of Peak Discharge at Gage 11069500: 1921-2006 (continued)

| Date | Discharge | LOG(Q) | Scaled Discharge | LOG(ScaledQ) |
|---|---|---|---|---|
| 12/10/1959 | 185 | 2.27 | 393.62 | 2.60 |
| 8/19/1961 | 215 | 2.33 | 457.45 | 2.66 |
| 9/22/1962 | 119 | 2.08 | 253.20 | 2.40 |
| 2/10/1963 | 160 | 2.20 | 340.43 | 2.53 |
| 4/1/1964 | 129 | 2.11 | 274.47 | 2.44 |
| 4/10/1965 | 126 | 2.10 | 268.09 | 2.43 |
| 11/22/1965 | 6300 | 3.80 | 13404.46 | 4.13 |
| 12/6/1966 | 5720 | 3.76 | 12170.39 | 4.09 |
| 3/8/1968 | 118 | 2.07 | 251.07 | 2.40 |
| 1/25/1969 | 7410 | 3.87 | 15766.19 | 4.20 |
| 3/2/1970 | 506 | 2.70 | 1076.61 | 3.03 |
| 11/29/1970 | 45 | 1.65 | 95.75 | 1.98 |
| 12/25/1971 | 368 | 2.57 | 782.99 | 2.89 |
| 12/4/1972 | 278 | 2.44 | 591.50 | 2.77 |
| 4/2/1974 | 255 | 2.41 | 542.56 | 2.73 |
| 3/8/1975 | 112 | 2.05 | 238.30 | 2.38 |
| 9/24/1976 | 515 | 2.71 | 1095.76 | 3.04 |
| 1/3/1977 | 55 | 1.74 | 117.02 | 2.07 |
| 1/15/1978 | 4500 | 3.65 | 9574.61 | 3.98 |
| 2/21/1979 | 2050 | 3.31 | 4361.77 | 3.64 |
| 2/21/1980 | 17300 | 4.24 | 36809.06 | 4.57 |
| 2/9/1981 | 208 | 2.32 | 442.56 | 2.65 |
| 2/10/1982 | 2900 | 3.46 | 6170.30 | 3.79 |
| 3/1/1983 | 2420 | 3.38 | 5149.01 | 3.71 |
| 8/31/1988 | 181 | 2.26 | 385.11 | 2.59 |
| 3/1/1991 | 2410 | 3.38 | 5127.74 | 3.71 |
| 1/26/1997 | 284 | 2.45 | 604.26 | 2.78 |
| 2/22/1998 | 1120 | 3.05 | 2383.01 | 3.38 |
| 7/11/1999 | 151 | 2.18 | 321.28 | 2.51 |
| 2/21/2000 | 60 | 1.78 | 127.66 | 2.11 |
| 2/28/2001 | 52 | 1.72 | 110.64 | 2.04 |
| 12/14/2001 | 0.61 | -0.21 | 1.30 | 0.11 |
| 3/15/2003 | 310 | 2.49 | 659.58 | 2.82 |
| 2/27/2004 | 110 | 2.04 | 234.05 | 2.37 |
| 1/11/2005 | 1310 | 3.12 | 2787.28 | 3.45 |
| 2/28/2006 | 517 | 2.71 | 1100.02 | 3.04 |

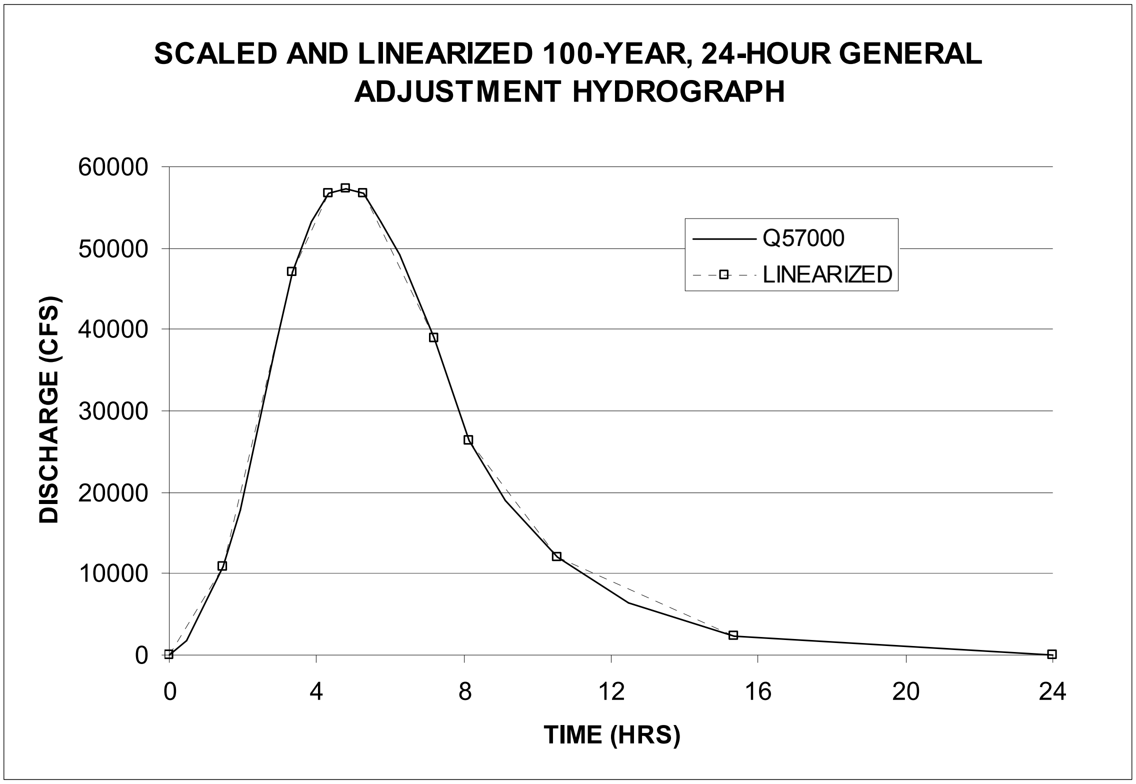


**Figure 3-2 -** Scaled SCS Hydrograph Discharge at Gage 11069500

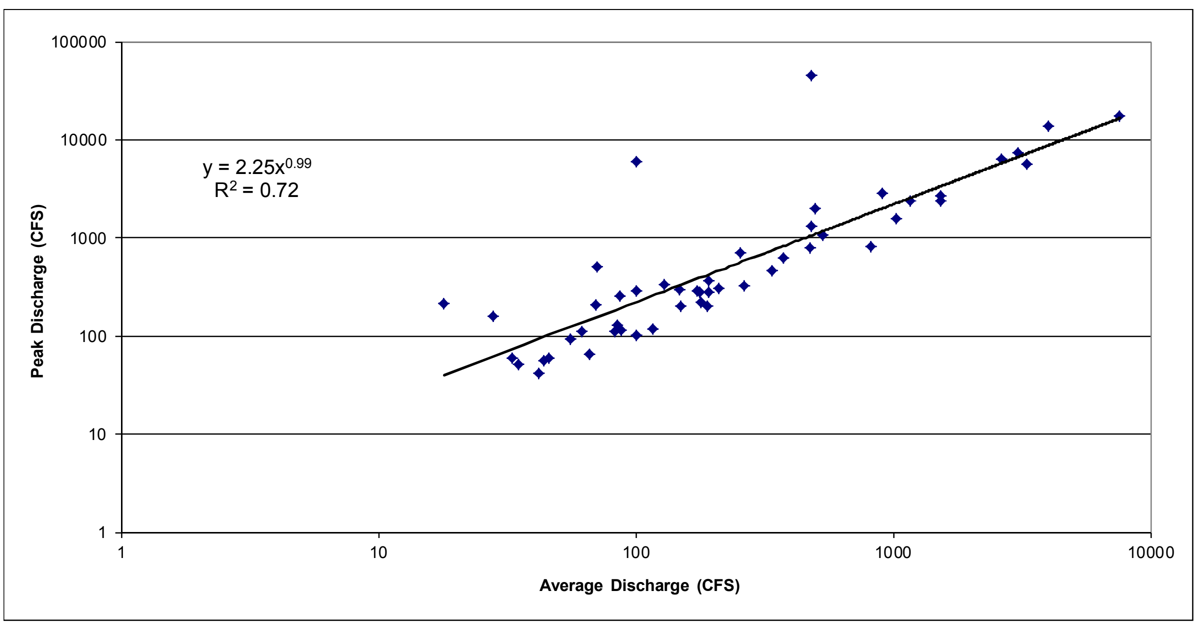


**Figure 3-3A** - Daily Mean Discharge Data Discharge at Gage 11069500: Un-scaled and Scaled Data 1921-2006

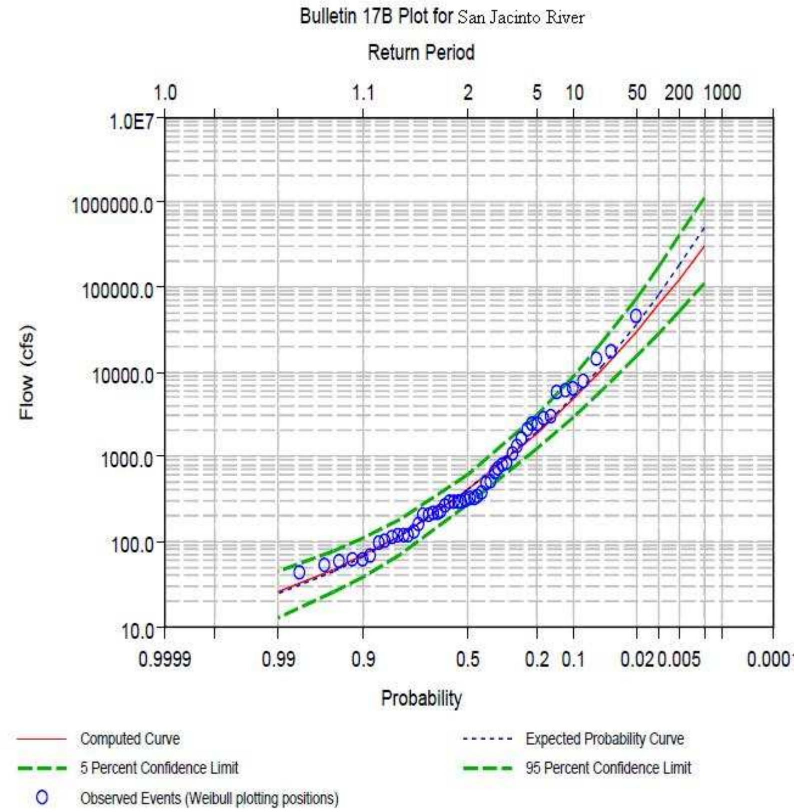


**Figure 3-3B** - Daily Mean Discharge Data Discharge at Gage 11069500: Un-scaled and Scaled Data 1921-2006

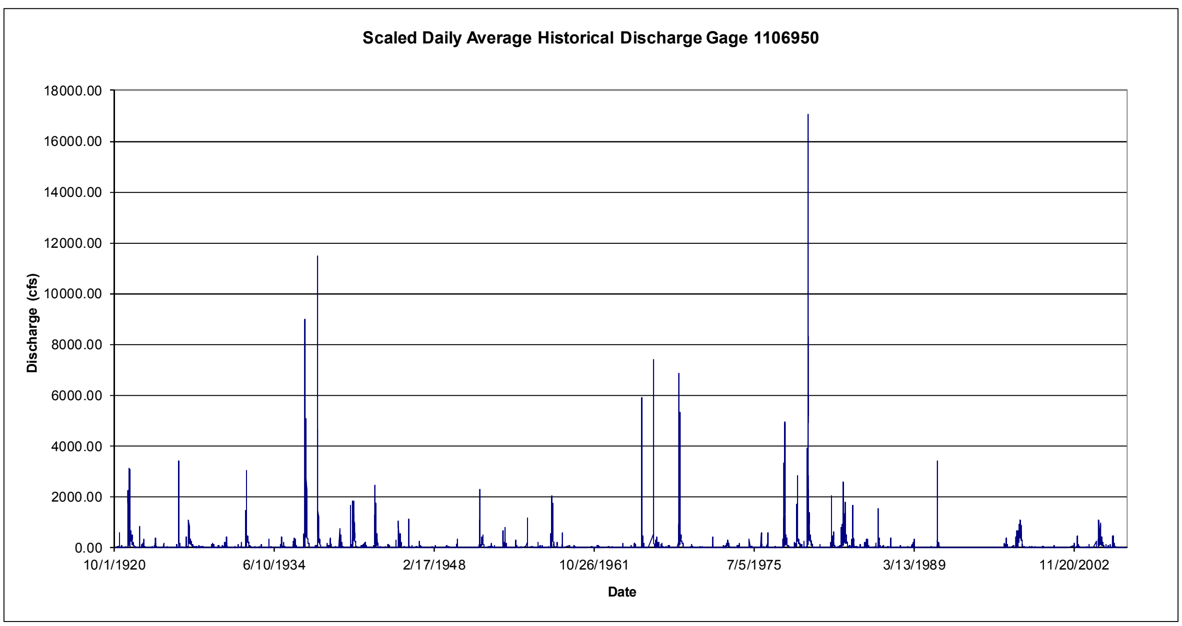


**Figure 3-4** - Scaled Daily Average Discharge at Gage 11069500: 1921-2006

## 3.4 Levee Design Discharge

The approved 100-year discharge utilized by Riverside County Flood Control and Water Conservation for the design of the levee system corresponds to $Q_{design}$ **= 57,250 cfs.** This value corresponds to the hydrology generated in the 1975 study prepared by the District.

# 4 Sediment Characterization and Analysis

## 4.1 Sediment Data Collection

To characterize the sediment of the streambed and by extension the material available for transport during discharge events, a sediment grain size analysis was conducted. The goal of the analysis is to gain a statistical representation of the size distribution of soil components of the streambed. Grain size distribution analysis is a powerful tool because the results can represent both a qualitative description of soil make up as well as quantitative input for further predictive measures, such as fluvial modeling.

High quality sediment collection for the San Jacinto River along the study reach was conducted by CHJ, Inc. and detailed in the July 2008 report. Within the Creek, 52 samples were collected positioned along various Creek subreaches at two depths: 0 and 5 feet. Samples were taken in the active and recently active bed within the River channel, and on the overbank areas. Please see sample location exhibit in the Appendix and reduced version of the exhibit is illustrated on the following page, which also includes the HEC-RAS cross-section locations as a relative indicator.

## 4.2 Sediment Gradation Analysis

Generally, grain size distribution analysis is broken down into three distinct steps. The first step is to dry the samples. Drying is accomplished in a desiccator or similar apparatus. The second step is to sieve or otherwise separate the sediment by particle size. Finally, fine material (smaller than standard mesh 200) is analyzed using hydrometric techniques. The sediment distributions are plotted on semi-log plots by percent finer for a given sample size. For this study, no fine material is included in analysis because fine material (< 0.075 mm) is generally transported as wash load, which is not of concern here. Samples, which visually appear on plots to be very unlike other samples from the same reach, have been removed from the distribution data. Six samples have been removed from the one-foot sample depth data and 21 samples have been removed from the five-foot sample depth data. The large number of outliers in the five-foot sample data may indicate more variability in grain size distribution with increasing depth, although this is presently unclear. The removed samples are indicated in the soil gradation data in the Appendix.

In early sediment model testing, all data was used. The use of the complete sediment data caused irregular bed fluctuations. To prevent these fluctuations, the sediment data was entered using average sediment values. Averaging is accomplished by taking the mean of the samples for each grain size and creating a composite mean plot. Averaging provides a single representative sediment grain size distribution that can be used for numerical modeling or other analysis. Two distinct grain size distributions were found by examining the raw sediment data. The separation between these two distributions is located at the Massacre Creek confluence. A plot of grain size distributions for each similar sampling distribution is presented in Figures 4.1A-B. Both distributions are used in the final modeling.

**Figure 4-1 –** Sediment sample locations relative to the proposed levee and HEC-RAS cross-sections

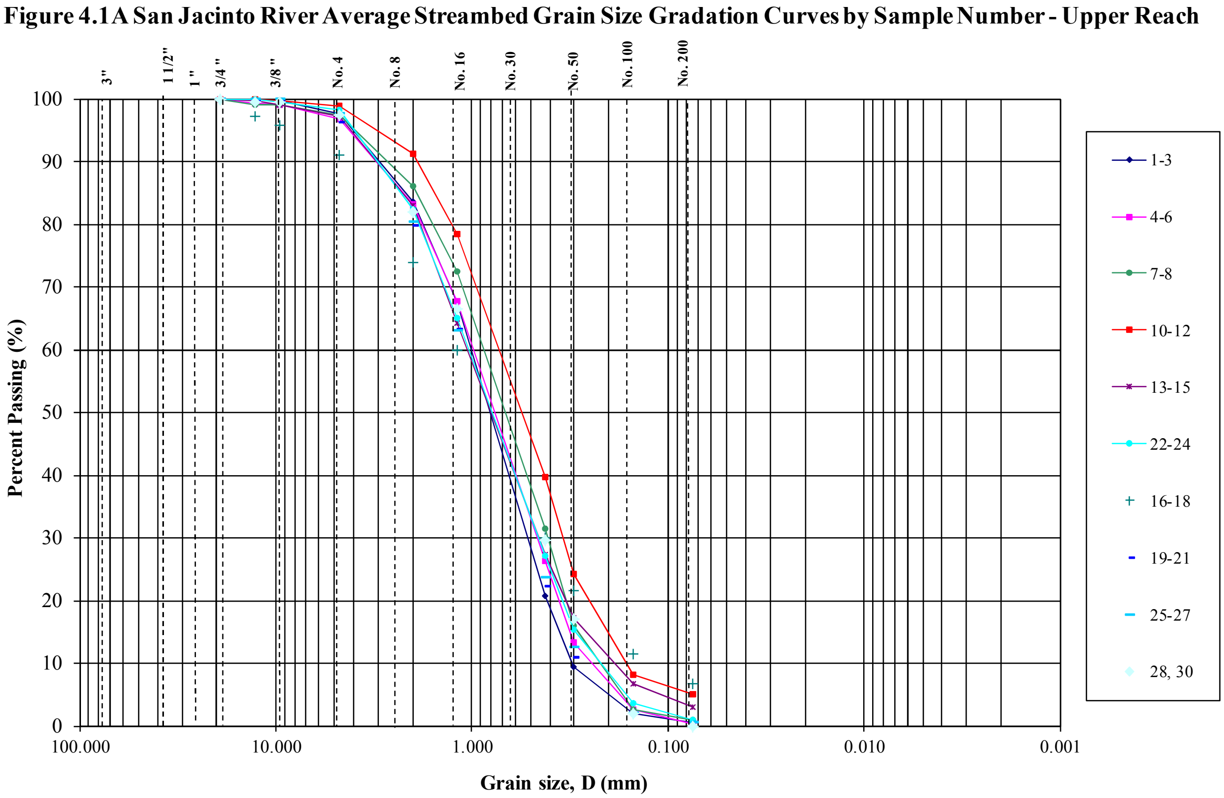


**Figure 4-1A** - Raw Grain Size Distribution, Upper Reach

**Figure 4.1b San Jacinto River Average Streambed Grain Size Gradation Curves by Sample Number - Lower Reach**

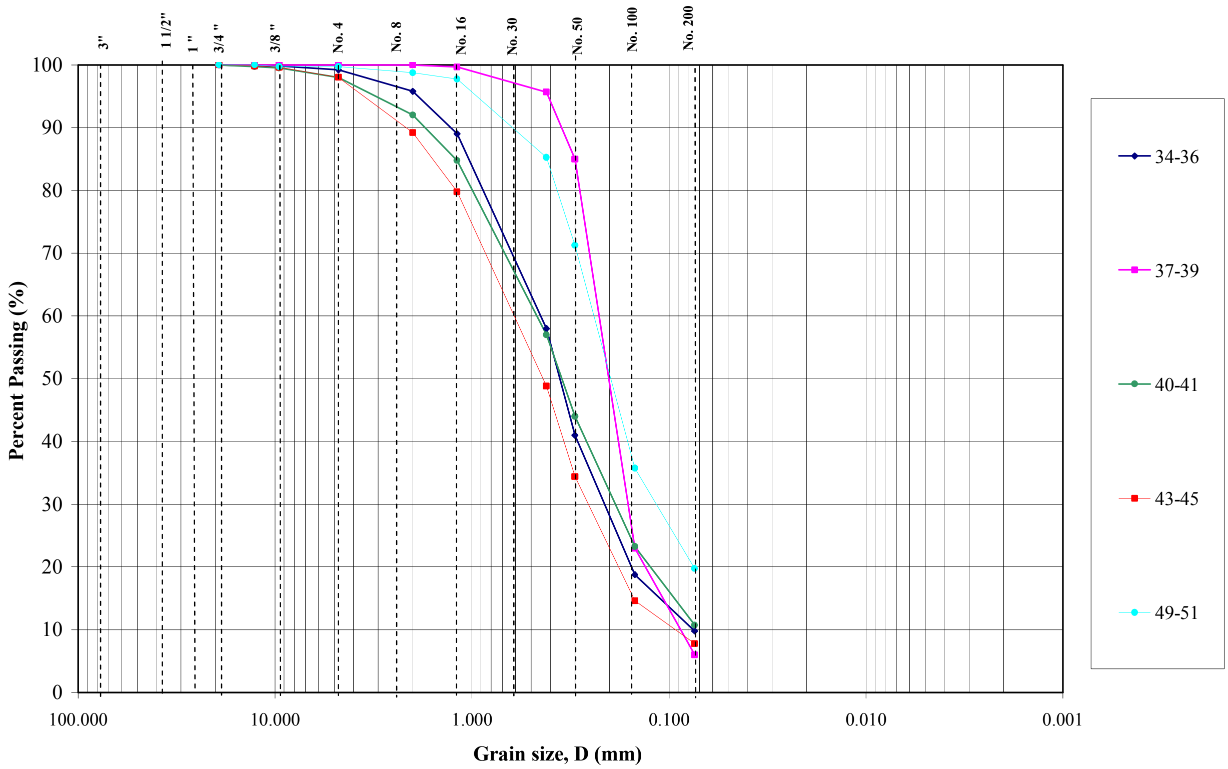


**Figure 4-1B** - Raw Grain Size Distribution, Lower Reach

## 4.3 Sediment Characterization

The bed of the main channel in the upper reach of the study area is composed primarily of sand and gravel. The bed of the main channel in the lower reach, in contrast, is composed primarily of sands and gravels, but has more fine material accounting for approximately 10 percent of the sample distribution. The change in particle size in the along-stream direction indicates the influence of the confluence on the local grain size distribution. The $D_{50}$ values for all samples ranged from 0.20 to 0.95 mm. The average $D_{50}$ for all samples is 0.80 and 0.30 mm for the upstream and downstream reaches, respectively. A comparison of Figure 4.1A and B with Figure 4.2A and B, respectively, indicates that averaging retains the essential character of the sampled soil.

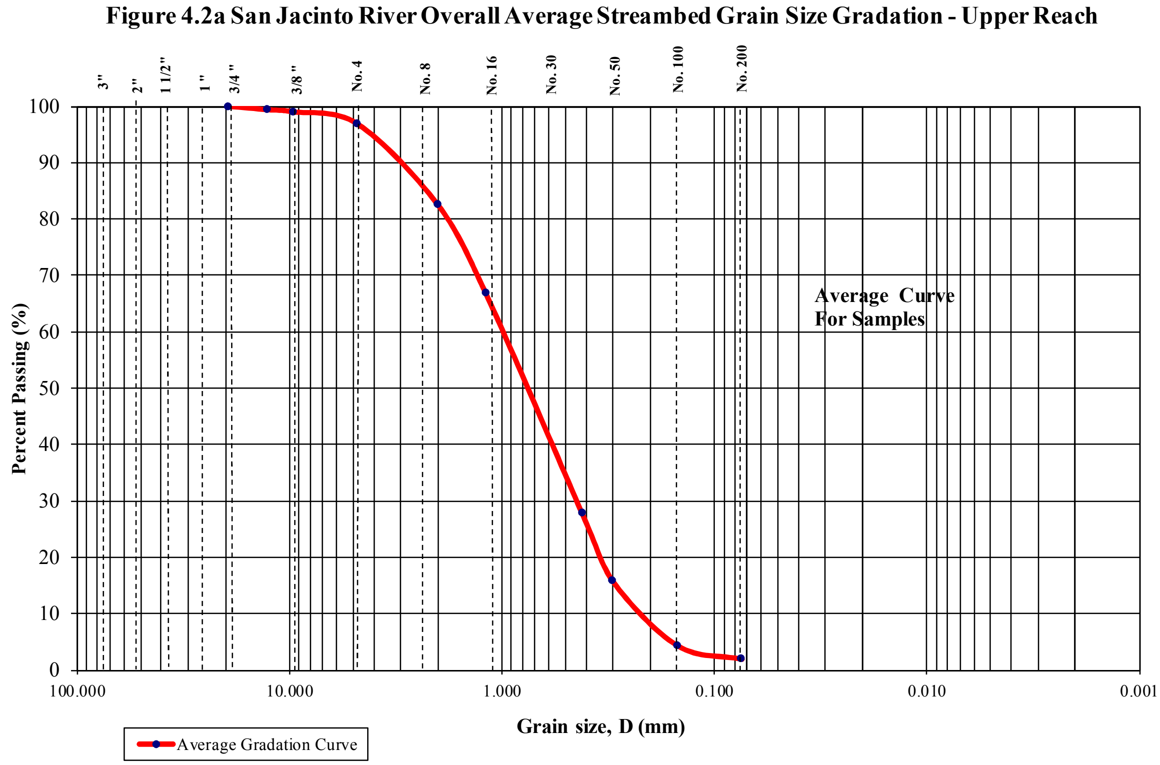


**Figure 4-2A -** Average Grain Size Distribution, Upper Reach

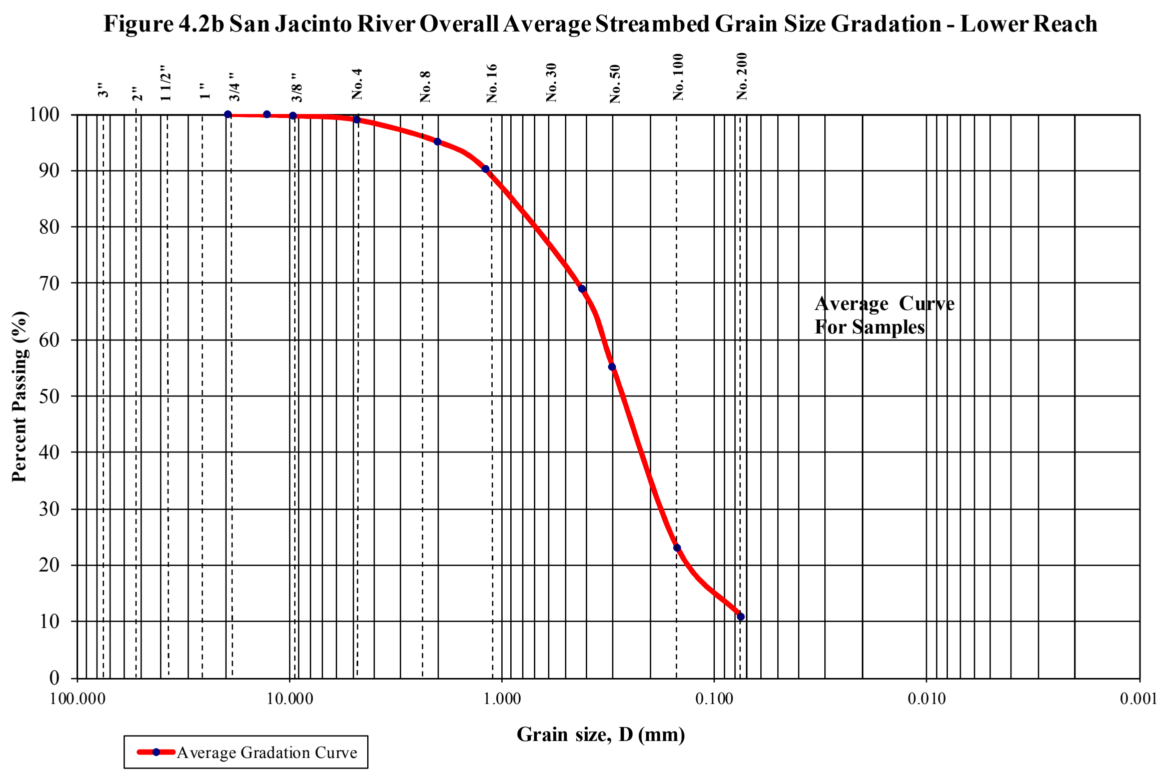


**Figure 4-2B -** Average Grain Size Distribution, Lower Reach

# 5 Previous Studies

Numerous regional watershed hydrology, floodplain hydraulics, and sediment transport studies have been done for San Jacinto River watershed over the last few decades. Since hydraulics and fluvial mechanics are the main subjects of this report, only four of the previous studies are discussed.

**RCFCD, 1975 -** The purpose of the 1975 RCFCD study was to determine the 100-year discharge within San Jacinto River. The report details areas of the watershed including climate, hydrology, hydraulics and geology. The report describes the presence of the ACOE and RCFCD bank protection and channel improvements downstream of Bautista Canyon, as well as agricultural levees and embankments in the vicinity of the City of San Jacinto. Also of significance to the present study, the RCFCD report describes the presence of storage areas or depressions in the watershed valleys. The report discusses historic discharge events and the extent of discharge records available at the time of publication. The work of the study focuses on the creation of unit hydrographs for each sub-area of the watershed. Alternatives for master planning were also analyzed. In the study's existing condition the 100-year, 24-hour discharge at Massacre Canyon is 57,250 cfs.

**RCFCD, 1994 -** The 1994 RCFCD study revisits the 1975 study for the purpose of designing 10.5 miles of channel improvements within the River. The methodology and structure of the 1994 study are very similar to that of the 1975 study. Ultimately the study found a discharge of 59,100 cfs was the appropriate design discharge value for the 100-year, 24-hour event at Massacre Canyon. The difference in design discharges is attributed to a change in loss rates in the HEC-1 model resulting from land development within the modeled watershed.

**RCFCD, 2000 -** The report sought to define the habitat impacts to a 10.6 mile earthen channel, which reclaimed 6,000 ac from the San Jacinto River floodplain, based on pre- and post-project hydraulics within the study reach. The study utilized a HEC-RAS model developed by WEST Consultants. The model was calibrated using gage data and discrete discharge events. USGS gage 11069500 was used to calibrate the upper watershed. The study found that in the existing conditions the 2- and 5- year events can be contained within the channel, but the 10- and 20-year events will spill over into the floodplain.

**USBR, 2008** – "Supper San Jacinto River Sediment Transport Study, San Jacinto River, California" is a report which evaluated the effects of sediment delivery for a proposed channel with levees to reconnect Mystic Lake and the San Jacinto River. The proposed channel design extended from Sanderson Avenue to Bridge Street and includes a series of five drop structures with a constant downstream slope of S=0.0010. The purpose of the report was to analyze the flow of sediment through the designed channel to the terminus just upstream of Bridge Street near Mystic Lake. The sediment transport analyses included a sediment "budget" based on dividing the channel into a series of reaches and also performing a moveable bed model using SRH-1D to estimate the amount of streambed vertical adjustment. The results indicated that the general trends were similar between the sediment budget analysis and the SRH-1D model. Aggradation is predicted in all portions of the channel and corresponds to 1-foot from 3-years of flow similar to the three years of flow experienced during the 87-year duration simulated. The sediment inflow upstream tributary to the channel was assumed to be "capacity limited."

# 6 Bridge Descriptions

## 6.1 Existing Condition

There are two different bridges crossing along the study reach for this portion of the San Jacinto River, which include (1) State Street, and (2) Sanderson Avenue Bridge. Additional reference data and information on the bridges is provided in the *Technical Appendix*. The **State Street Bridge** was designed in 1996 and is a 19-span (20-bents including the abutments) design with five circular columns at each bent that traverses San Jacinto River at State Street. The five circular columns at each bent are inline with each other, parallel to the direction of flow, and the spacing ranges from 12.5 feet to 15.5 feet between them. The span width between the bents is 17 spans at 40-feet, and the span at the two abutments is reduced to 32.5 feet. The bridge has a 0.018 grade from south to north that varies along its approximate 745-foot span. The pier pairs (bents) reside 141 feet from one another. The bridge is skewed slightly across the span, and the five circular columns at each bent are perpendicular to the flow. The bridge elevation ranges from approximately 1509 feet on the south bank to approximately 1517 feet on the north bank. The piers have a 2-foot width at the base. The longitudinal width of the bridge roadway deck is 36 feet. The following cross-section represents the bridge geometry generated in the design HEC-RAS model from Webb Associates.

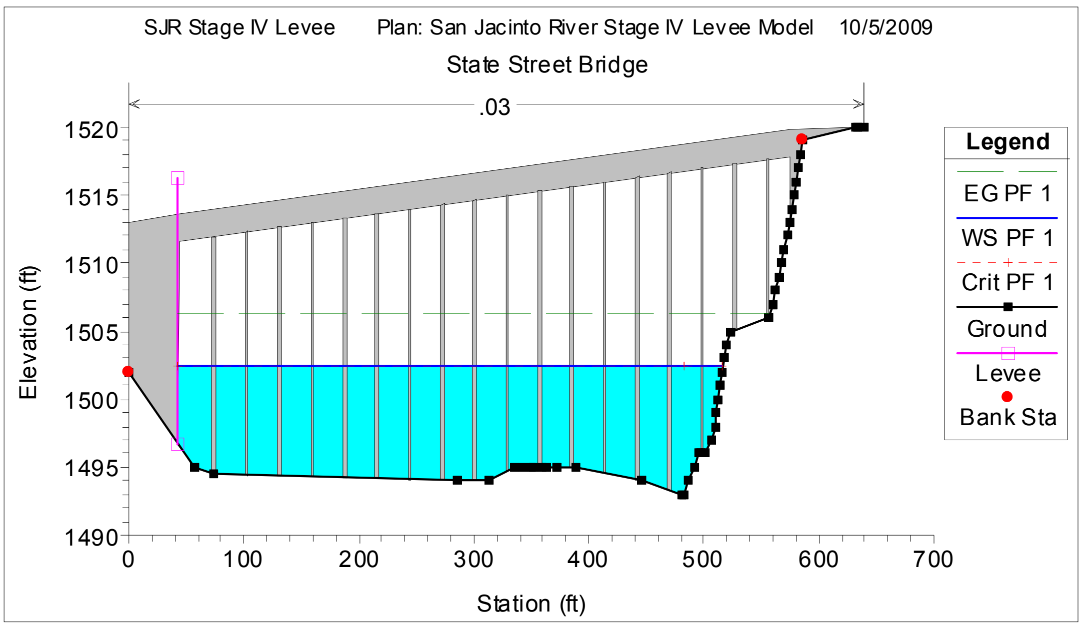


**Figure 6-1 -** State Street Bridge cross-section geometry utilized for the HEC-RAS model

The **Sanderson Avenue Bridge** was designed in 1993 and is an eight span with pier wall design with circular noses that traverses San Jacinto River at Sanderson Avenue. The bridge has a 0.8% grade from south to north that varies along its approximate 1226-foot span. The spacing between the bents or spans is 144 feet from one another and reduced to a span of 110 feet from each embankment abutment. The bridge is skewed across the span with a skew angle of 17 degrees. Both abutments and the piers (bents) are aligned with the direction of flow. The bridge elevation ranges from approximately 1464 feet on the south bank to approximately 1490 feet on the north bank. The pier walls have a three-foot width at the base with 1.5-foot radius circular noses supported by three rows of piles below the pier foundation. The bridge is 71.6 feet wide and each pier wall is 68.5 feet in length. Bridge plans are included in the Appendix.

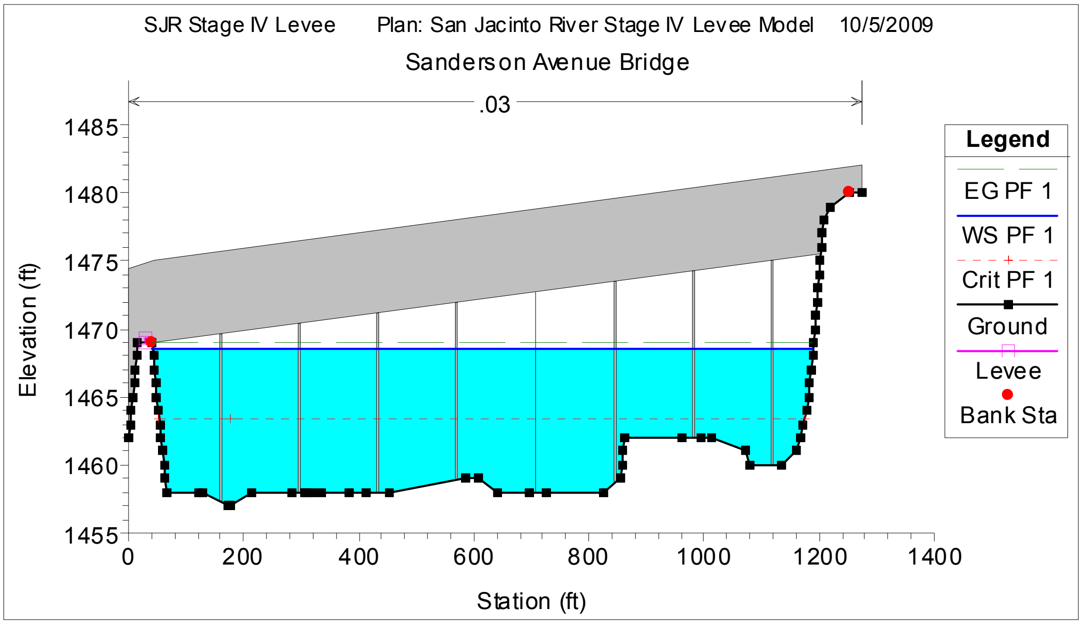


**Figure 6-2** – Sanderson Avenue Bridge cross-section geometry from HEC-RAS model

## 6.2 Proposed Condition

No proposed improvements associated with the bridges exist at this time to change the existing bridge structures. The existing and proposed conditions HEC-RAS model reflect the same bridge geometries.

# 7 Floodplain Hydraulics Analysis

## 7.1 Procedure

Hydraulic modeling was performed by Albert A. Webb Associates (RCFCD-approved HEC-RAS model) using HEC-RAS, computer modeling software developed by the U.S. Army Corps of Engineers (ACOE). HEC-RAS is a rigid boundary hydraulic model, which assumes the channel bed does not fluctuate. Movable bed analysis based on sediment transport was performed using ACOE HEC-6T by PACE, discussed below. HEC-RAS executes a one-dimensional solution of the energy equation, where energy losses are evaluated by friction through Manning's equation and contraction/expansion based on the coefficient and change in velocity head. When bridges and confluences are present, the momentum equation is used to manage these situations of rapidly varying water surface profile. The "mixed flow" option is available to accommodate the potential for subcritical and supercritical flow regimes within the model.

The channel cross-section data is provided in the HEC-RAS model for the project site at varying reach lengths varying from approximately 300 to 800 feet within the study reach. A varying Manning's coefficient is applied to the study reach and a discharge selected for analysis. The design discharge, $Q_{100}$=57,250 cfs is the design discharge utilized in the model, as required by RCFCD. Boundary conditions for the design 100-year discharge are entered to initiate hydraulic calculations. Finally, the model is computed based on "subcritical" flow.

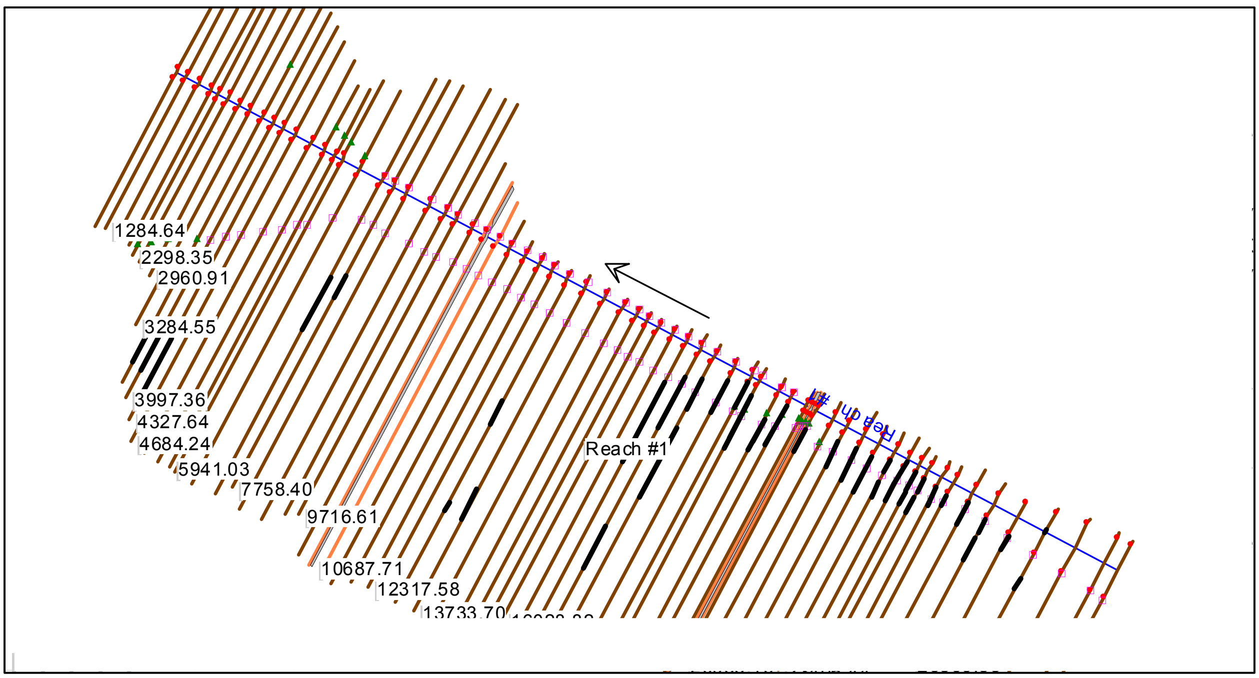


**Figure 7-1** – HEC-RAS plan general cross-section layout of existing conditions illustrating cross-section width and channel bank station and river stationing for the model. Pink points indicate channel bank station and darken line along cross-section indicates blocked flow locations.

The main purpose of the baseline analysis is to serve as a basis of comparison for the post-development analysis. The analysis was completed by Albert A. Webb & Associates, and is included here for completeness. Since these were the approved HEC-RAS models, and in order to maintain and be consistent with the original design, the HEC-RAS models were not modified or corrected. The existing condition analysis shows that flow depths for the 100-year event range from 1.5 to 12.3 feet and channel velocity ranges from 1.1 to 13.3 fps. A complete summary of the hydraulic results is presented in the Appendix.

### 7.4 Proposed Condition Analysis

The "proposed conditions" HEC-RAS floodplain hydraulic analysis was also completed by Albert A. Webb & Associates. The proposed condition model differs from the existing condition model in that the proposed condition model includes improvements to the levees and grading of the channel, primarily removing existing levee embankments to generate fill for the proposed levee. This proposed conditions model for the proposed levee was originally generated by utilizing the levee option within HEC-RAS to set vertical walls at the levee location. The corresponding HEC-RAS cross-sections were manually adjusted to insert the levee a fixed points as part of the cross-section. The proposed condition analysis shows that flow depths for the 100-year event range from 3.0 to 12.9 feet, and channel velocity ranges from 2.5 to 13.4 fps. The numerically average velocity along the reach is 6.0 fps and the average maximum depth (thalweg or minimum elevation to the water surface) is approximately 7.3 feet.

### 7.5 Comparison of Existing and Proposed Conditions HEC-RAS Models

A comparison was prepared of the results from the existing and proposed conditions 100-year (Q=57,250 cfs) HEC-RAS models in order to evaluate hydraulic characteristics and determine the effect of the levee on the existing floodplain. However, the comparison was made with the models without the bridges since this reflects the proposed models that will be utilized in the development of the HEC-6T model and provides a useful comparison of how the "rigid boundary" hydraulics should perform in the HEC-6T model. The comparison also allowed determining if the model was accurately modeling the proposed facilities and if the changes illustrated in the model hydraulic characteristics reflect the anticipated response of the floodplain. Table 7-1 compares the flow depths and velocities from the two conditions and the differences that arise as a result. Negative values in the table indicate a decrease from existing conditions while a positive value indicates an increase from existing conditions. The comparison in the table illustrates that the maximum change in water surface was a 6.05 foot increase, velocity was a 6.58 fps increase, and top width was 8,965 feet decrease. The water surface profile model illustrated that the encroachment of the levee will reduce the effective floodplain width and the corresponding reduced channel width will result in increased water surface elevations and velocities. The amount of floodplain encroachment is illustrated in the channel in the floodplain top width so large increase in the water surface and velocity is expected. A more detailed review of the "cause-and-effect" illustrated in the changes between the existing proposed conditions floodplain hydraulic characteristics are discussed in the following section.

**Table 7-1** -Comparison of Existing and Proposed HEC-RAS Model Characteristic Hydraulic Parameters

| Section No. | Existing Conditions Hydraulics | | | Proposed Conditions Hydraulics | | | Difference | | |
|---|---|---|---|---|---|---|---|---|---|
| | Water Surface | Vel | Top Width | W.S. | Vel | Top Width | Vel | W.S. | Top Width |
| | (ft) | (fps) | (ft) | (ft) | (ft/s) | (ft) | (fps) | (ft) | (ft) |
| 30361.69 | 1545 | 5.43 | 1719.39 | 1543.11 | 7.96 | 1715.25 | **-2.53** | **1.89** | **4.14** |
| 29945.89 | 1542.4 | 6.12 | 1619.86 | 1540.62 | 8.61 | 1998.06 | **-2.49** | **1.78** | **-378.2** |
| 29025.39 | 1538.8 | 5.31 | 1642.82 | 1537.13 | 6.9 | 2057.51 | **-1.59** | **1.67** | **-414.69** |
| 28104.69 | 1533.31 | 7.45 | 1326.64 | 1531.51 | 11.03 | 1476.1 | **-3.58** | **1.8** | **-149.46** |
| 27263.37 | 1527.77 | 8.24 | 1076.92 | 1526.09 | 9.31 | 1509.53 | **-1.07** | **1.68** | **-432.61** |
| 26500.53 | 1526.48 | 6.3 | 831.4 | 1524.64 | 6.93 | 1528.05 | **-0.63** | **1.84** | **-696.65** |
| 25846.05 | 1524.74 | 8.86 | 651.95 | 1523.61 | 7.74 | 2320.95 | **1.12** | **1.13** | **-1669** |
| 25246.64 | 1522.53 | 9.49 | 788.96 | 1521.35 | 10.25 | 1046.57 | **-0.76** | **1.18** | **-257.61** |
| 24895.09 | 1521.27 | 8 | 897.52 | 1520.52 | 8.01 | 1594.13 | **-0.01** | **0.75** | **-696.61** |

| Section No. | Existing Conditions Hydraulics | | | Proposed Conditions Hydraulics | | | Difference | | |
|---|---|---|---|---|---|---|---|---|---|
| | Water Surface | Vel | Top Width | W.S. | Vel | Top Width | Vel | W.S. | Top Width |
| | (ft) | (fps) | (ft) | (ft) | (ft/s) | (ft) | (fps) | (ft) | (ft) |
| 24469.84 | 1519.46 | 8.4 | 812.33 | 1518.27 | 11.58 | 1702.65 | **-3.18** | **1.19** | **-890.32** |
| 24190.24 | 1518.28 | 8.58 | 738.84 | 1517.02 | 11.46 | 1382.65 | **-2.88** | **1.26** | **-643.81** |
| 23817.09 | 1516.2 | 9.27 | 778.11 | 1515.1 | 11.3 | 822.22 | **-2.03** | **1.1** | **-44.11** |
| 23406.44 | 1514.06 | 8.41 | 1026.08 | 1511.96 | 13.34 | 1074.98 | **-4.93** | **2.1** | **-48.9** |
| 22909.46 | 1512.53 | 6.75 | 1280.17 | 1510.91 | 6.23 | 1921.47 | **0.52** | **1.62** | **-641.3** |
| 22448.18 | 1510.56 | 8.35 | 1360.54 | 1509.31 | 9.81 | 2628.05 | **-1.46** | **1.25** | **-1267.51** |
| 21912.02 | 1508.6 | 7.74 | 1337.8 | 1507.83 | 9.14 | 2545.59 | **-1.4** | **0.77** | **-1207.79** |
| 21459.26 | 1506.66 | 8.6 | 1219.96 | 1506.33 | 9.83 | 2649.98 | **-1.23** | **0.33** | **-1430.02** |
| 20953.16 | 1503.57 | 11.52 | 622.55 | 1503.59 | 12.5 | 2213.07 | **-0.98** | **-0.02** | **-1590.52** |
| 20853.6* | 1503.31 | 10.89 | 660.19 | 1502.79 | 12.63 | 2308.16 | **-1.74** | **0.52** | **-1647.97** |
| 20754.2* | 1503.06 | 10.35 | 748.95 | 1501.67 | 12.78 | 2424.45 | **-2.43** | **1.39** | **-1675.5** |
| 20654.72 | 1502.71 | 10.44 | 811.25 | 1501.13 | 11.23 | 2449.09 | **-0.79** | **1.58** | **-1637.84** |
| 20179.46 | 1500.1 | 11.87 | 1043.46 | 1498.38 | 11.85 | 2058.36 | **0.02** | **1.72** | **-1014.9** |
| 19813.26 | 1498.18 | 11.01 | 1129.54 | 1496.62 | 10.33 | 2907.58 | **0.68** | **1.56** | **-1778.04** |
| 19200.76 | 1496.64 | 7.44 | 1251.92 | 1494.81 | 7.04 | 3655.46 | **0.4** | **1.83** | **-2403.54** |
| 18929.32 | 1496.26 | 6.27 | 1203.49 | 1494.07 | 6.76 | 3664.03 | **-0.49** | **2.19** | **-2460.54** |
| 18399.16 | 1495 | 6.45 | 1218.25 | 1491.99 | 8.72 | 4612.19 | **-2.27** | **3.01** | **-3393.94** |
| 17768.32 | 1492.23 | 7.31 | 1222.92 | 1486.79 | 7.3 | 4278.02 | **0.01** | **5.44** | **-3055.1** |
| 17330.97 | 1490.12 | 7.16 | 1216.68 | 1485.62 | 3.11 | 6371.09 | **4.05** | **4.5** | **-5154.41** |
| 16913.42 | 1487.89 | 7.57 | 1208.16 | 1483.58 | 6.91 | 6952.97 | **0.66** | **4.31** | **-5744.81** |
| 16476.12 | 1485.92 | 7.71 | 1205.32 | 1481.58 | 2.4 | 5806.81 | **5.31** | **4.34** | **-4601.49** |
| 16028.82 | 1484.2 | 7.32 | 1198.92 | 1479.09 | 5.08 | 6292.41 | **2.24** | **5.11** | **-5093.49** |
| 15682.82 | 1482.61 | 7.36 | 1188.58 | 1477.98 | 1.66 | 5517.43 | **5.7** | **4.63** | **-4328.85** |
| 15347.98 | 1481.51 | 7.11 | 1189.66 | 1476.19 | 1.74 | 6478.43 | **5.37** | **5.32** | **-5288.77** |
| 14920.48 | 1480.37 | 7.29 | 1192.13 | 1474.35 | 0.71 | 5917.42 | **6.58** | **6.02** | **-4725.29** |
| 14335.42 | 1478.58 | 6.8 | 1203.11 | 1472.53 | 1.92 | 6655.34 | **4.88** | **6.05** | **-5452.23** |
| 13733.7 | 1476.34 | 7.49 | 1215 | 1470.4 | 1.14 | 5461.81 | **6.35** | **5.94** | **-4246.81** |
| 13200.36 | 1474.79 | 7.29 | 1184.9 | 1468.91 | 2.95 | 7120.68 | **4.34** | **5.88** | **-5935.78** |
| 12726.18 | 1472.63 | 7.91 | 1164.09 | 1467.53 | 2.91 | 7148.4 | **5** | **5.1** | **-5984.31** |
| 12317.58 | 1470.9 | 7.75 | 1174.9 | 1466.74 | 2.94 | 7145.54 | **4.81** | **4.16** | **-5970.64** |
| 11871.18 | 1469.54 | 7.95 | 1162.66 | 1466.16 | 2.13 | 7242.81 | **5.82** | **3.38** | **-6080.15** |
| 11396.58 | 1467.95 | 8.15 | 1187.56 | 1465.22 | 4.08 | 7088.92 | **4.07** | **2.73** | **-5901.36** |
| 11003.2* | 1466.77 | 7.74 | 1183.22 | 1464.14 | 4.55 | 6932.09 | **3.19** | **2.63** | **-5748.87** |
| 10609.8* | 1465.8 | 7.21 | 1194.98 | 1462.82 | 5.36 | 6461.58 | **1.85** | **2.98** | **-5266.6** |
| 10216.47 | 1464.98 | 6.69 | 1190.91 | 1461.75 | 4.29 | 5752.65 | **2.4** | **3.23** | **-4561.74** |
| 9716.61 | 1464.1 | 6.09 | 1276.5 | 1460.67 | 4.09 | 7140.67 | **2** | **3.43** | **-5864.17** |
| 9359.16 | 1463.37 | 5.73 | 1292.21 | 1459.63 | 5.17 | 8529.61 | **0.56** | **3.74** | **-7237.4** |

**Table 7-1** -Comparison of Existing and Proposed HEC-RAS Model Characteristic Hydraulic Parameters

| Table 7-1 -Comparison of Existing and Proposed HEC-RAS Model Characteristic Hydraulic Parameters | | | | | | | | | |
|---|---|---|---|---|---|---|---|---|---|
| **Section No.** | **Existing Conditions Hydraulics** | | | **Proposed Conditions Hydraulics** | | | **Difference** | | |
| | **Water Surface** | **Vel** | **Top Width** | **W.S.** | **Vel** | **Top Width** | **Vel** | **W.S.** | **Top Width** |
| | **(ft)** | **(fps)** | **(ft)** | **(ft)** | **(ft/s)** | **(ft)** | **(fps)** | **(ft)** | **(ft)** |
| 8867.34 | 1462.45 | 5.47 | 1332.89 | 1458.01 | 4.19 | 7002.57 | **1.28** | **4.44** | **-5669.68** |
| 8175.9 | 1461.06 | 5.62 | 1362.4 | 1456.71 | 2.98 | 8959.28 | **2.64** | **4.35** | **-7596.88** |
| 7758.4 | 1459.54 | 6.41 | 1304.5 | 1455.93 | 4.23 | 9173.26 | **2.18** | **3.61** | **-7868.76** |
| 7418.76 | 1457.8 | 7.85 | 1285.85 | 1455.29 | 3.96 | 10251.4 | **3.89** | **2.51** | **-8965.55** |
| 6710.68 | 1455.14 | 6.65 | 3133.79 | 1453.37 | 5.2 | 5826.47 | **1.45** | **1.77** | **-2692.68** |
| 6166.06 | 1453.46 | 5.91 | 2928.91 | 1452.36 | 3.73 | 9358.32 | **2.18** | **1.1** | **-6429.41** |
| 5941.03 | 1452.62 | 6.38 | 2782.49 | 1451.94 | 3 | 8069.79 | **3.38** | **0.68** | **-5287.3** |
| 5609.07 | 1451.83 | 5.2 | 2892.68 | 1451.48 | 3.73 | 9095.6 | **1.47** | **0.35** | **-6202.92** |
| 5183.62 | 1451.19 | 4.29 | 2901.26 | 1450.88 | 4.18 | 8694.14 | **0.11** | **0.31** | **-5792.88** |
| 4684.24 | 1450.67 | 3.62 | 3773.95 | 1450.28 | 2.89 | 6641.65 | **0.73** | **0.39** | **-2867.7** |
| 4327.64 | 1450.36 | 3.41 | 4191.18 | 1449.95 | 2.58 | 6628.78 | **0.83** | **0.41** | **-2437.6** |
| 3997.36 | 1450.1 | 3.23 | 4354.21 | 1449.84 | 1.38 | 7090.03 | **1.85** | **0.26** | **-2735.82** |
| 3670.6 | 1449.68 | 2.39 | 6818.94 | 1449.66 | 2.19 | 6706.95 | **0.2** | **0.02** | **111.99** |
| 3284.55 | 1449.54 | 1.54 | 6085.08 | 1449.49 | 1.57 | 6058.96 | **-0.03** | **0.05** | **26.12** |
| 2960.91 | 1449.21 | 3.07 | 6037.41 | 1449.2 | 2.82 | 6037.11 | **0.25** | **0.01** | **0.3** |
| 2580.91 | 1448.65 | 2.9 | 5726 | 1448.65 | 2.93 | 5725.77 | **-0.03** | **0** | **0.23** |
| 2298.35 | 1448.25 | 2.63 | 5745.02 | 1448.24 | 2.63 | 5743.79 | **0** | **0.01** | **1.23** |
| 2072.69 | 1448.01 | 2.34 | 5728.93 | 1448 | 2.34 | 5727.41 | **0** | **0.01** | **1.52** |
| 1677.04 | 1447.4 | 2.59 | 5527.61 | 1447.39 | 2.59 | 5526.66 | **0** | **0.01** | **0.95** |
| 1284.64 | 1446.53 | 2.92 | 3985.08 | 1446.53 | 2.92 | 3985 | **0** | **0** | **0.08** |
| 1000 | 1445.85 | 3.35 | 4258.75 | 1445.85 | 3.35 | 4258.75 | **0** | **0** | **0** |

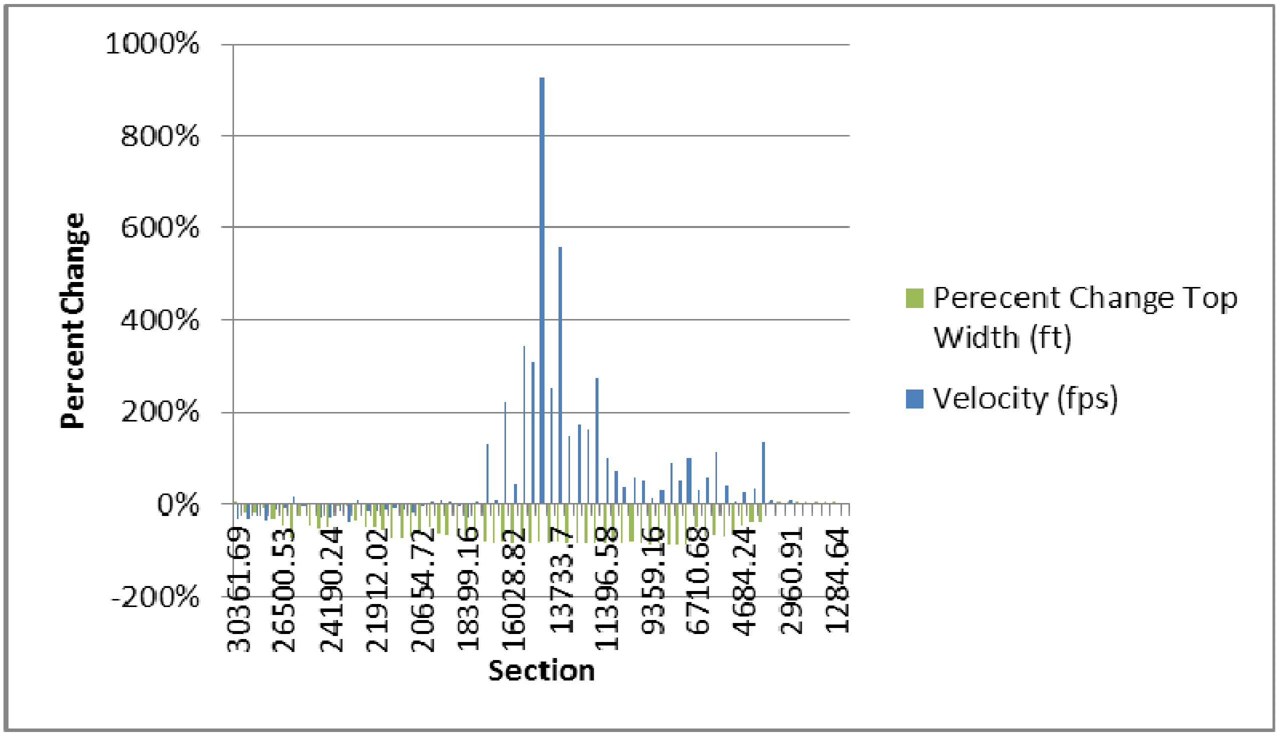


**Figure 7-2 -** Comparison between Existing and Proposed Conditions HEC-RAS Model results evaluating change in **Velocity** and **Top Width** trends

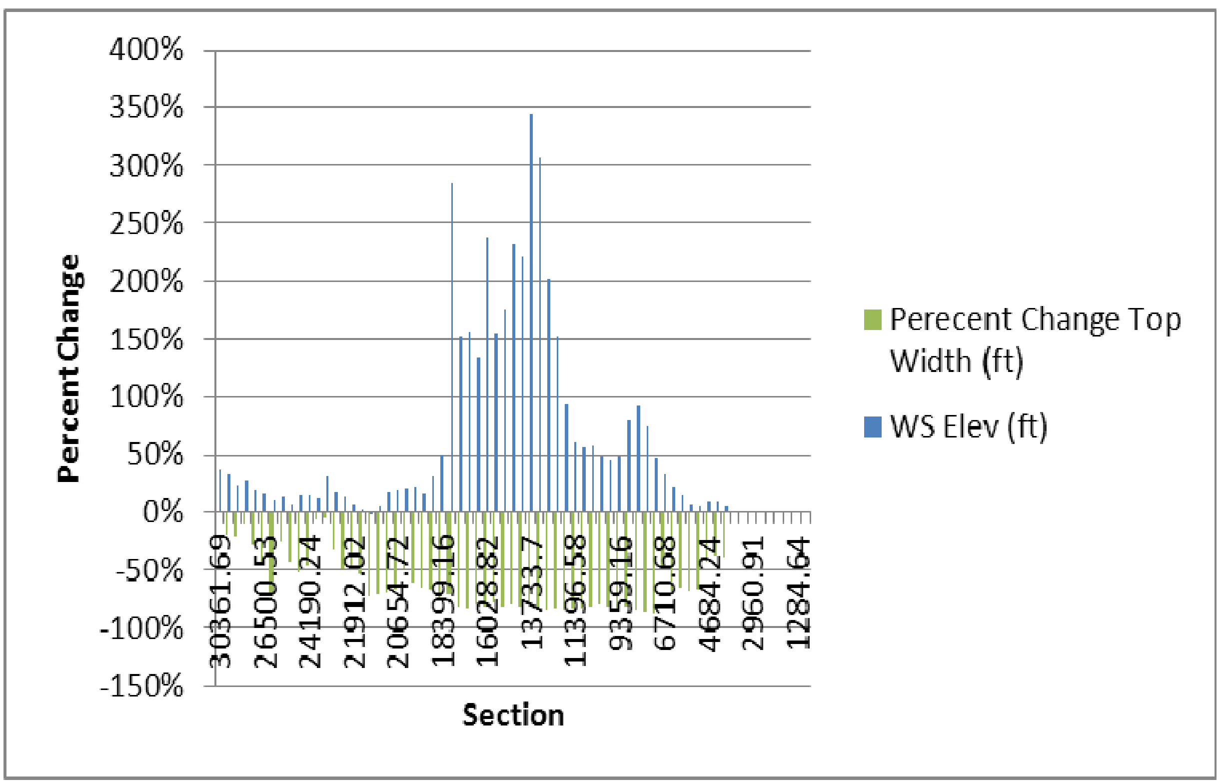


**Figure 7-3 -** Comparison of Percentage Change between Existing and Proposed Conditions HEC-RAS Models evaluating change in **Top-width** vs. **Water Surface** elevation or **Depth** trends

### 7.5.1 Discussion of Hydraulic Changes and Influences Between Existing and Proposed HEC-RAS

The expected influence illustrated in the hydraulic model between the existing and proposed floodplain is that the proposed levee will reduce the floodplain width. The levee encroaches within the overbank and reduces a large flat overbank area that had originally been flooded in the existing conditions. The encroachment will reduce the effective hydraulic width and hydraulic cross-section, so the water surface will increase and the velocity will increase. For example, examining the cross-section (Sta. 149+20) where the maximum increase in velocity of 6.58 fps (0.71 fps to 7.29 fps) occurs where the cross-section width has been reduced by 4,725 (an 80% reduction in the floodplain width) and there is a corresponding increase in the water surface depth of 6.05 feet. This is shown graphically in a comparison of the existing and proposed cross-sections for Sta 149+20 (section no. 32) below.

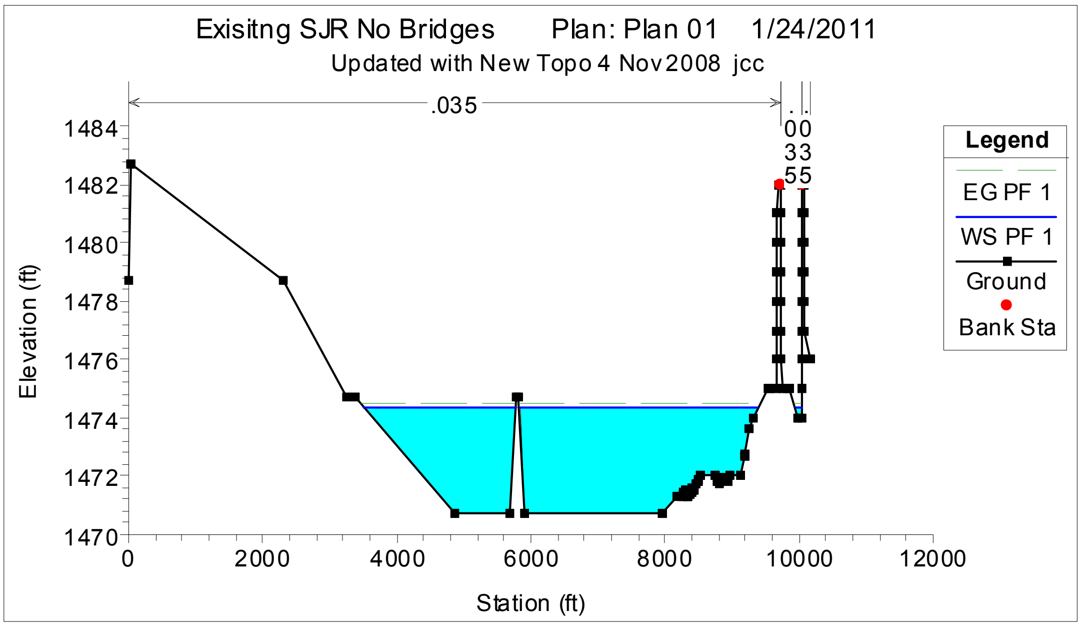


**Figure 7-4** – Existing HEC-RAS cross-section for River Sta. 149+20 where a significant portion of the flow is located in the left overbank and below the existing main channel earthen levees to the right of the section. However, note the floodplain width and then compare to the width in the proposed conditions illustrated in the next section

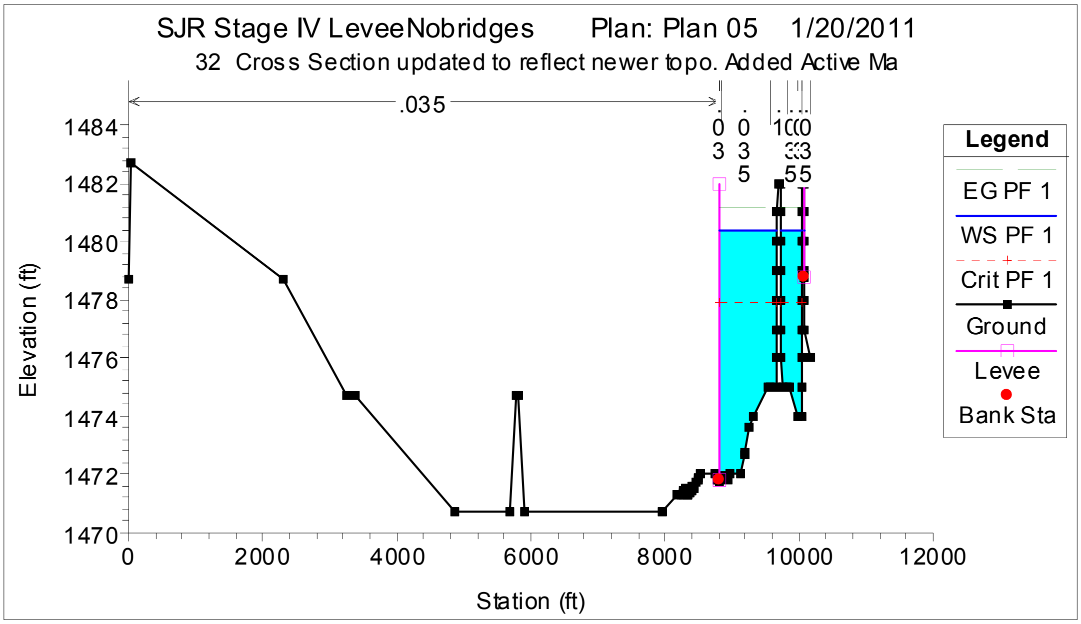


**Figure 7-5 –** Cross-section geometry for HEC-RAS model with **proposed** levee encroachment with the floodplain at River Station 149+20. Notice that the floodplain width now relocated to the right side of the section with the reduced width that has increased the flow depth.

However, the comparison of results indicates there are several locations where the trend in the hydraulics change is the opposite from anticipated for a levee encroachment. There are several where there is a reduction in the top width and the water surface increases as expected, but the velocity decreases rather than increases. The reason for this is that in the "proposed conditions" HEC-RAS developed by Webb they had incorporated modifications to the horizontal variation of the Manning's roughness coefficient different from the existing conditions. The reduced effective floodplain was modified to account for an "active maintenance section" and a corresponding "no touch zone" required by the environmental regulatory permitting agencies avoiding disturbance of vegetation. The regulatory "no touch zone" utilized an increased Manning's roughness coefficient of n=0.10 reflecting an unmaintained dense vegetation in the future, while the existing floodplain used a constant n = 0.035. If the width of the "no touch zone" within the reduced width floodplain represented a significant portion of the width, then this affects the hydraulics through a decrease in the friction slope and corresponding decrease in the velocity rather than the typical increase. However, if the "no touch zone" was only a small percentage of the width, then the encroachment effect would reflect the influence of the baseline Manning's coefficient and the velocity as well as the depth would increase.

The location where the hydraulic trend is opposite and the velocity decreases rather than increases with the encroachment occurs at 23 of the 67 sections in the HEC-RAS model. An example of this occurs at HEC-RAS Sta. 234+06 (Section 51) where a maximum velocity reduction of 4.93 fps occurs, changing from 13.34 fps in the existing conditions to 8.41 fps even though there is a 1,026 foot floodplain width reduction from the levee encroachment. The influence of the portion of the section with the increase Manning's roughness coefficient of n=0.10 is illustrated in the comparison of the "existing" and "proposed" cross-sections from the HEC-RAS models shown below.

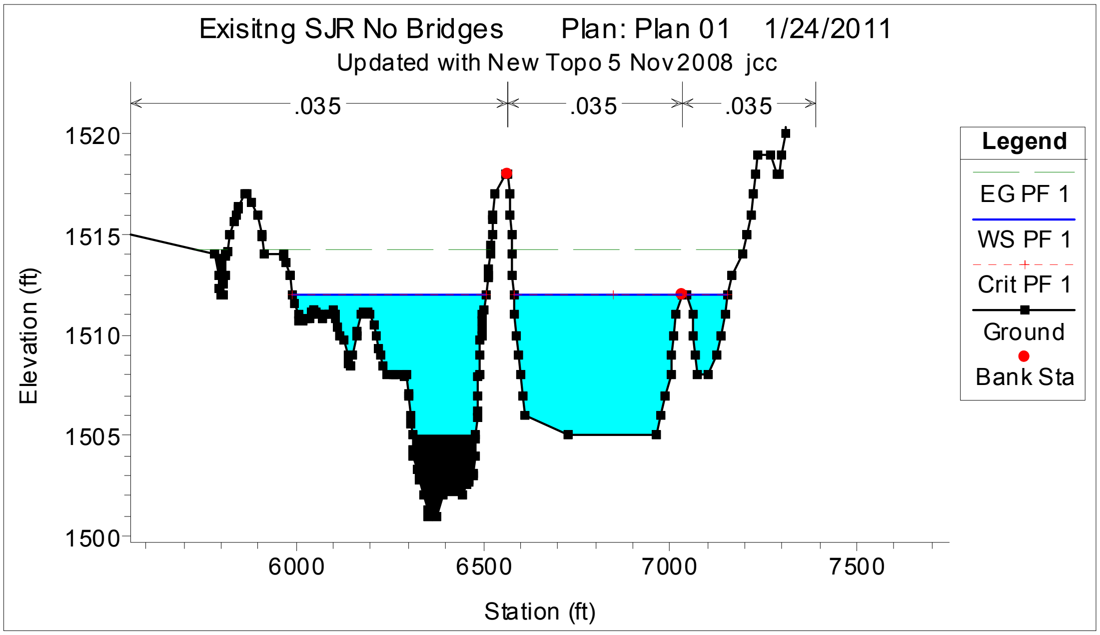


**Figure 7-6** – Existing conditions HEC-RAS model cross-section geometry for River Station 234+06 which can be compared to the proposed conditions with levee encroachment in the next figure. Notice the locations and horizontal limits of the manning's roughness indicated at the top of the figure.

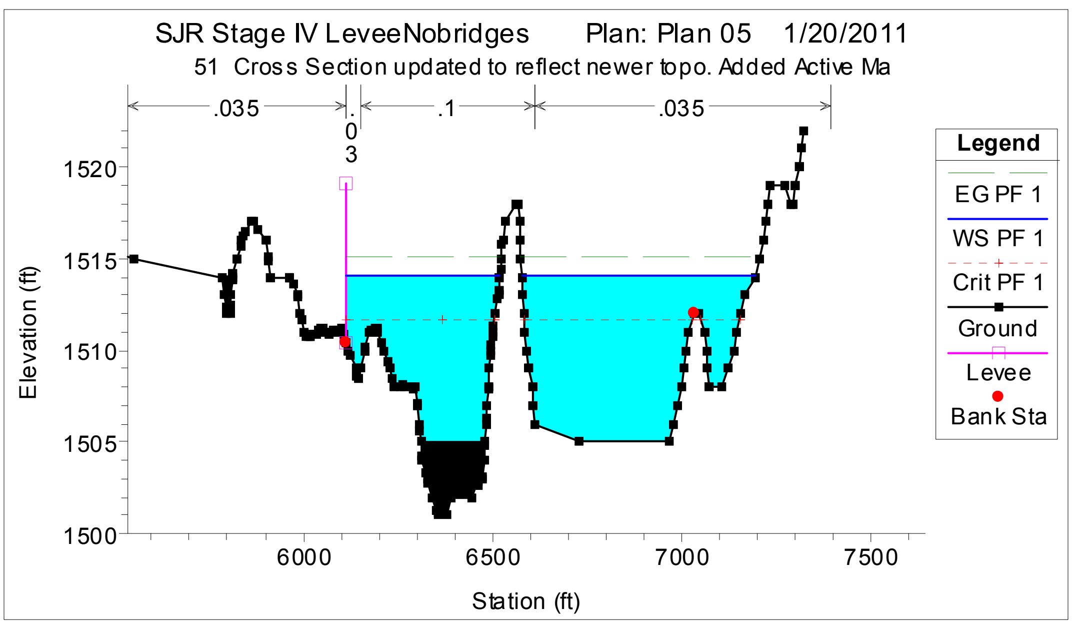


**Figure 7-7** – Proposed conditions HEC-RAS model cross-section 234+06 which illustrates the portion of the floodplain which has an increased manning's coefficient to n=0.10 to reflect future non-maintenance area. The roughness coefficient has increased from the existing conditions

This comparison illustrates within this section that the "no touch zone" represents a significant portion of the floodplain width and will dominate the hydraulic friction loss with the large increased Manning's roughness coefficient even though there is an encroachment or reduction in the floodplain width from the levee. The width reduction is relatively minor compared to the large amount of the effective floodplain width with the larger Manning's roughness coefficient.

### 7.5.2 <u>Other Hydraulic Influences / Issues in HEC-RAS Models</u>

Reviewing both the existing and proposed conditions HEC-RAS models that had been developed for the District illustrated some items that will influence the accuracy of the results. A key item illustrated in the floodplain hydraulics in both models was the majority of the cross-sections encountered **"divided flow"** which indicates that there is an obstruction which creates an "island effect" and splits the flow on either side of the obstruction. HEC-RAS cannot accurately compute the water surface with "divided flow" if this occurs at several consecutive sections since HEC-RAS assumes (1) the water surface elevation is the same on each side of the obstruction, and (2) computes a different flow distribution at each section which will change the amount of flow on each side of the obstruction. This occurred in both the "existing" and "proposed conditions" HEC-RAS model. This is illustrated in the following section for the "proposed" conditions which illustrates the embankment that will remain within the effective active floodplain section that creates the divided flow. There are three primary locations where multiple consecutive sections of divided flow conditions occur which include (1) HEC-RAS Sta. 258+46 to 224+48, nine sections, (2) Sta. 189+29 to 127+26, fourteen section, and (3) Sta.93+59 to 10+00, twenty-one sections. A more accurate would be to create separate independent HEC-RAS model for each side of the divided flow area since they operate as independent hydraulic streams, however, this was the District approved HEC-RAS model.

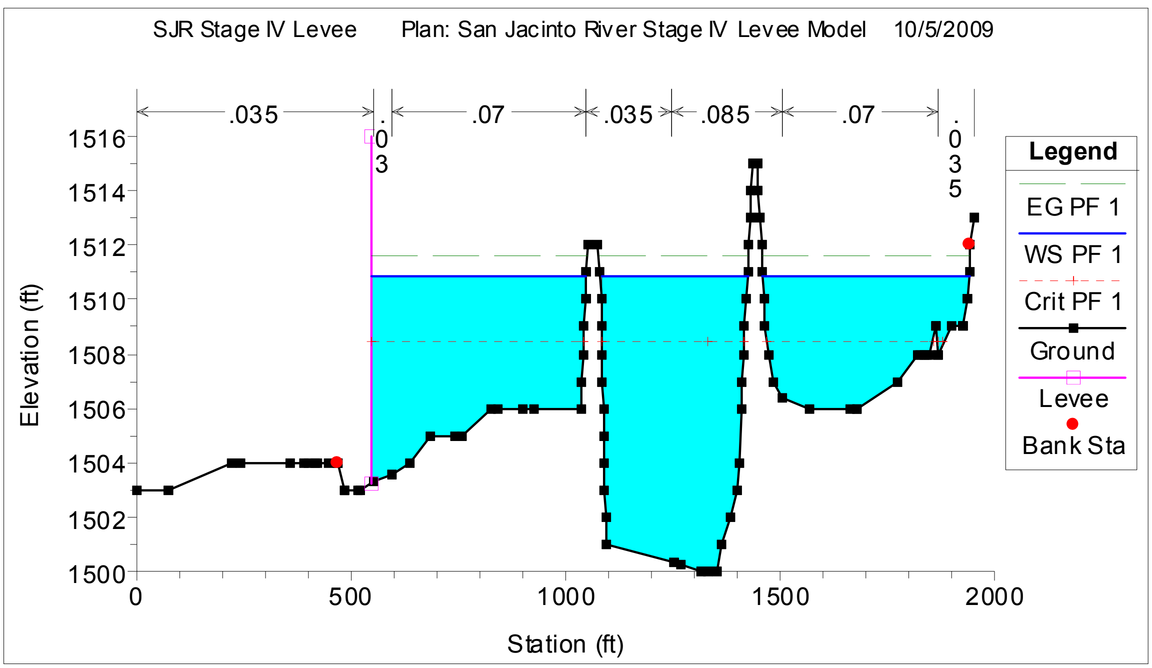


**Figure 7-8** – Proposed conditions HEC-RAS cross-section geometry illustrating the divided flow with the "islands" projecting above the water surface. The divided geometry is associated with the existing earthen berms within the floodplain of previous levee. Cross-section geometry reflects the final HEC-RAS model from Webb and Associates so cross-section station are not the same as those used in this final report.

# 8 HEC-18 Bridge Hydraulics & Scour

## 8.1 Modeling

The bridge routines in HEC-RAS allow the modeler to analyze a bridge with several different methods. The bridge routines have the ability to model low flow, combined low and weir flow, pressure flow, and submerged flow. HEC-RAS computes the energy losses at bridges in three steps. First, losses downstream of the bridge are calculated at the expansion in the flow. Next, the losses associated with the structure are calculated, and, finally, losses occurring upstream of the bridge are determined. A brief description follows.

### *8.1.1 Contraction Scour*

Contraction scour at the bridges can be evaluated both in HEC-RAS and within HEC-6T independently. The results of the magnitudes of the different analysis from the two models are compared and the larger of the two values will be utilized as the contraction scour value. The geometry of the cross-sections upstream and at the bridge have been utilized in the development of the HEC-6T model so it will evaluate contraction scour based on sediment continuity. In order to determine the type of contraction scour that is occurring with HEC-RAS, sediment transport upstream of the contraction must be established. HEC-RAS calculates the critical velocity for motion ($V_C$) for the mean grain size and compares it with the mean velocity V upstream of the bridge. If the critical velocity is greater than the mean velocity ($V_C > V$), then clear-water contraction scour is assumed. In contrast, if the critical velocity is less than the mean velocity ($V_C < V$), then live-bed contraction scour is assumed. The critical velocity is calculated using the Laursen (1963) equation given by:

$$V_C = K_U\, y_1^{1/6}\, D_{50}^{1/3}$$

where $V_C$ is critical velocity above which material of size $D_{50}$ and smaller will be transported (fps), $y_1$ is the average depth of flow in the main channel (ft), $D_{50}$ is the mean particle size (ft), and $K_U$ is 11.17 (English units).

HEC No. 18 recommends using a modified version of Laursen's (1960) live-bed contraction scour equation (used for this study) given by:

$$y_2 = y_1\left[\frac{Q_2}{Q_1}\right]^{6/7}\left[\frac{W_1}{W_2}\right]^{K_1}$$

$$y_s = y_2 - y_0$$

where $y_s$ is average depth of contraction scour (ft), $y_2$ is average flow depth after scour in the contraction (ft), $y_1$ is the average flow depth in the main channel (ft), $y_0$ is the average depth in the at the contracted section before scour (ft), $Q_1$ is the flow in the main channel which is transporting sediment (cfs), $Q_2$ is the flow in the main channel in the contracted section which is transporting sediment (cfs), $W_1$ is the bottom width in the main channel (ft) which is approximated as the top width of the active flow area in HEC-RAS, $W_2$ is the bottom width of the main channel in the contracted section less pier widths (ft), approximated as the top width of the active flow area, and $k_1$ is the exponent for mode of bed material transport.

The recommended clear-water contraction scour equation by HEC No. 18 is an equation based on research from Laursen (1963):

$$y_S = \left[\frac{Q_2^2}{C D_m^{2/3} W_2^2}\right]^{3/7}$$

$$y_S = y_2 - y_0$$

where $D_m$ is the diameter of the smallest non-transportable particle in the bed material (1.25 $D_{50}$) in the contracted section (ft), $D_{50}$ is the median diameter of the bed material (ft), and C is 130 in English units.

### *8.1.2 Local Scour at Piers*

HEC No. 18 recommends the use of the Richardson (1990) equation for the computation of pier scour under both live-bed and clear-water conditions. The Richardson equation predicts maximum pier scour depths for both live-bed and clear-water pier scour. The Richardson equation is given as:

$$y_S = 2.0\, K_1 K_2 K_3 K_4\, a^{0.65}\, y_1^{0.35}\, Fr_1^{0.43}$$

where $y_S$ is depth of scour (ft), $K_1$ is correction factor for pier nose shape, $K_2$ is correction factor for angle of attack of flow, $K_3$ is correction factor for bed condition, $K_4$ is correction factor for armoring of bed material, a is pier width (ft), $y_1$ is flow depth (ft), and $Fr_1$ is the Froude number. HEC-RAS includes the addition of the pier width when computing pier scour.

### *8.1.3 Local Scour at Abutments*

HEC No. 18 recommends two equations for the computation of live-bed abutment scour. When the wetted embankment length (L) divided by the approach flow depth ($y_1$) is greater than 25, HEC No. 18 suggests using the HIRE equation (Richardson, 1990), but when the wetted embankment length divided by the approach depth is less than or equal to 25, the Froehlich (1989) should be used.

The HIRE equation is based on field data of scour at the end of spurs in the Mississippi River (obtained by USACE). The HIRE equation is given by:

$$y_S = 4 y_1 \left( \frac{K_1}{0.55} \right) K_2 Fr_1^{0.33}$$

where $y_S$ is scour depth (ft), $y_1$ is depth of flow at the toe of the abutment (ft) upstream of the bridge, $K_1$ is the correction factor for abutment shape, $K_2$ is the correction factor for angle of attack (θ) of flow with abutment (θ=90 when abutments are perpendicular to the flow, θ<90 if embankment points downstream, θ>90 if embankment points upstream; $K_2=(\theta/90)^{0.13}$), and $Fr_1$ is the Froude.

The Froehlich equation is given by:

$$y_S = 2.27\, K_1\, K_2\, (L')^{0.43}\, y_a^{0.57}\, Fr^{0.61} + y_a$$

where $y_S$ is scour depth (ft), $K_1$ is correction factor for abutment shape, $K_2$ is correction factor for angle of attack (θ) of flow with abutment (θ=90 when abutments are perpendicular to the flow, θ<90 if embankment points downstream, θ>90 if embankment points upstream; $K_2=(\theta/90)^{0.13}$), L' is length of abutment (embankment) projected normal to flow (ft), $y_a$ is average depth of flow (ft), Fr is the Froude number, $V_e$ is average velocity (fps), $Q_e$ is the flow obstructed by the abutment and embankment at the approach section (fps), and $A_e$ is the flow area of the approach section obstructed by the abutment and embankment ($ft^2$). It is important to note that the above form of the Froehlich equation is for design purposes. The addition of the average depth at the approach section, $y_a$, was added to the equation in order to envelope 98 percent of the data. If the equation is to be used in an analysis mode, Froehlich suggests dropping the addition of the approach depth ( $y_a$). HEC-RAS program always calculates the abutment scour with the ($+y_a$) included in the equation.

## 8.2 Parameters

In the present modeling the standard step approach is used for the modeling approach. Manning's values are prescribed following the initial model set-up described in Section 6. Contraction and expansion coefficients are set in the model as 0.3 and 0.5 in the vicinity of the bridges (one section downstream of the bridge and two sections upstream of the bridge), respectively, and 0.1 and 0.3 distant from structures, respectively. All other bridge data is taken from Caltrans as-built plans and were coded by Webb.

## 8.3 Results

The bridge hydraulic and scour computation results for the 100-year discharge are averaged for approximately 1,000 feet immediately upstream and downstream of **State Street Bridge** to account for any backwater effects. Upstream of State Street Bridge, the depth of flow is 10.0 feet and velocity is 11.9 fps for the proposed condition, while the depth of flow is 12.0 feet and velocity is 8.7 fps for the existing condition. Downstream of the bridge, the depth of flow is 9.3 feet and velocity is 13.0 fps for the proposed condition, while the depth of flow is 11.4 feet and velocity is 9.7 fps for the existing condition. These results are summarized in Table 8.1A and B. The hydraulics through the bridge were calculated using the energy method.

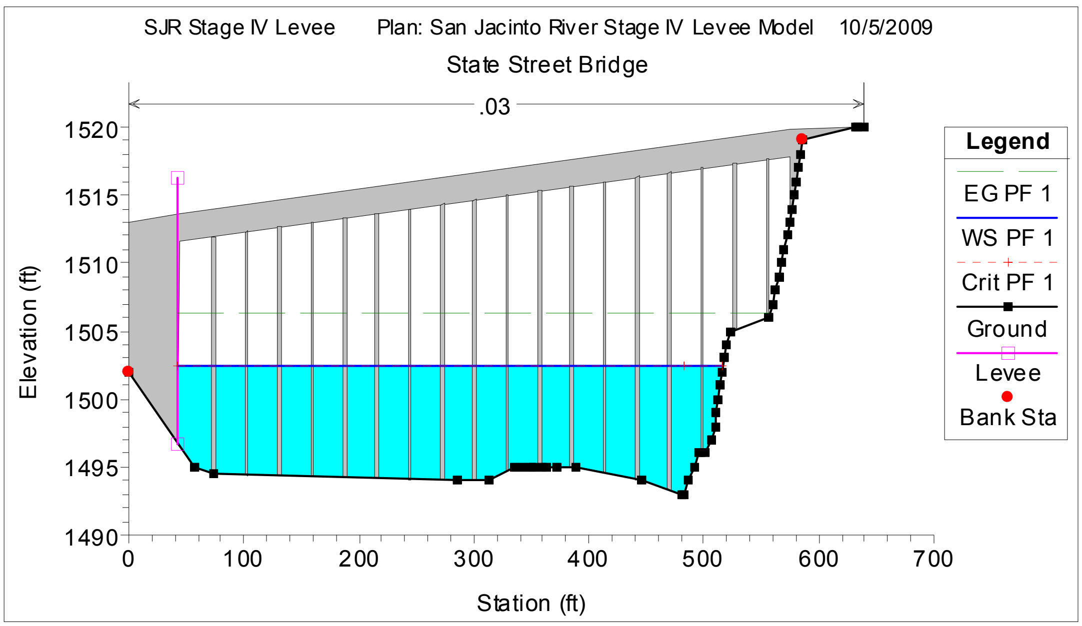


**Figure 8-1 –** State Street bridge HEC-RAS cross-section geometry

The 100-year hydraulic results are averaged for approximately 1,000 feet immediately upstream and downstream of Sanderson Avenue Bridge to account for any backwater effects. Upstream of **Sanderson Avenue Bridge**, the depth of flow is 6.3 feet and velocity is 9.3 fps for the proposed condition, while the depth of flow is 3.8 feet and velocity is 7.2 fps for the existing condition illustrating the effect of not all the flow going through the bridge at the existing conditions. Downstream of the bridge, the depth of flow is 8.2 feet and velocity is 7.4 fps for the proposed condition, while the depth of flow is 4.9 feet and velocity is 5.4 fps for the existing condition. The hydraulics through the bridge was calculated using the energy method. The major difference in the bridge hydraulics between the existing and proposed conditions is that **not all the flow during the 100-year event is going through the bridge in the existing conditions** because the flows flank around the existing levee and the bridge is perched. The hydraulics analysis indicated that at State Street approximately 80% of the flow goes through the bridge at the existing condition while only 50% of the flow goes through the Sanderson Bridge. The proposed new levee ensures that all the flow is confined and will go through the bridge which is the reason that there is a difference in the hydraulics between the two different conditions as indicated in the summary of bridge hydraulics.

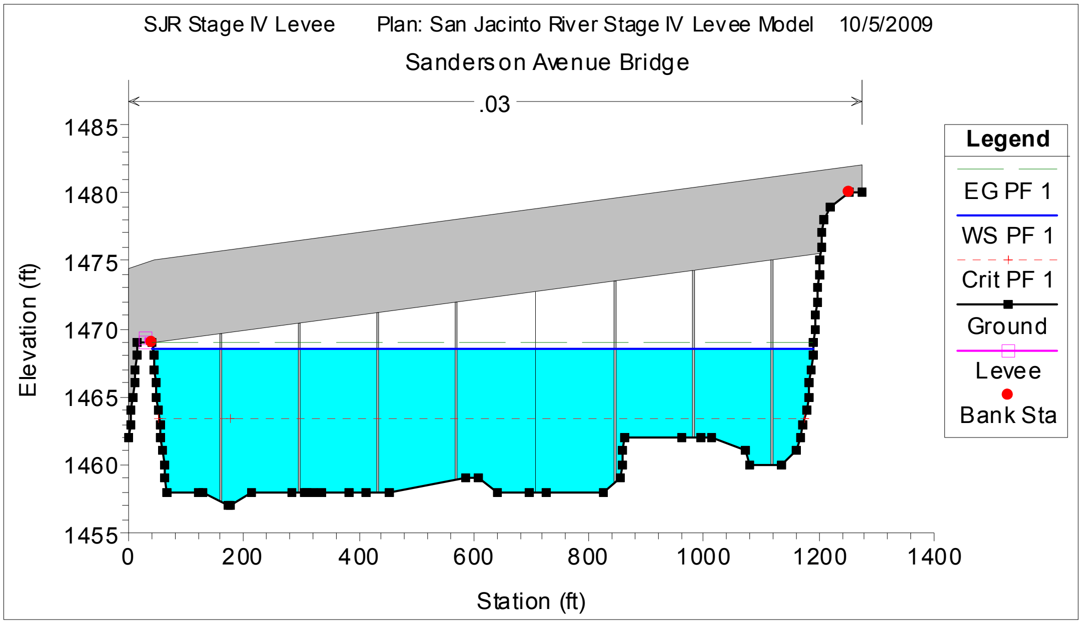


**Figure 8-2** – Sanderson Bridge HEC-RAS cross-section geometry

Table 8.2 shows a more detailed HEC-18 output (FHWA 2002) for both bridges as computed by HEC-RAS. Maximum scour is used for each component to be conservative. The pier scour for Sanderson Bridge was utilized in calculating the total toedown depth but can be deleted since the pier scour geometry is not within the zone of influence of the embankment scour.

**Table 8-1A** - Existing Conditions100-year Bridge Hydraulics San Jacinto River

| HEC-RAS BRIDGE HYDRAULICS OUTPUT - 100-YEAR | | | | |
|---|---|---|---|---|
| BRIDGE | VELOCITY | | DEPTH | |
| | U/S | D/S | U/S | D/S |
| STATE | 8.7 | 9.7 | 12.0 | 11.4 |
| SANDERSON | 7.2 | 5.4 | 3.8 | 4.9 |

**Table 8-1B** - Proposed Conditions 100-year Bridge Hydraulics San Jacinto River

| HEC-RAS BRIDGE HYDRAULICS OUTPUT -100-YEAR | | | | |
|---|---|---|---|---|
| BRIDGE | VELOCITY | | DEPTH | |
| | U/S | D/S | U/S | D/S |
| STATE | 11.9 | 13.0 | 10.0 | 9.3 |
| SANDERSON | 9.3 | 7.4 | 6.4 | 8.2 |

**Table 8-2A -** Existing Conditions 100-year Bridge HEC-18 Calculations San Jacinto River

| HEC-RAS HEC-18 CALCULATIONS OUTPUT | | | | | | |
|---|---|---|---|---|---|---|
| Component | State Street | | | Sanderson Avenue | | |
| Contraction Scour | Left | Channel | Right | Left | Channel | Right |
| Scour Depth Ys (ft): | 1.9 | 11.0 | - | 1.4 | 2.1 | - |
| Critical Velocity (ft/s): | 2.1 | 2.4 | - | 1.9 | 1.9 | - |
| Equation: | Live | Live | - | Live | Live | - |
| Pier Scour | | | | | | |
| Scour Depth Ys (ft): | | 4.23 | | | 4.28 | |
| Froude #: | | 0.22 | | | 0.32 | |
| Equation: | | CSU equation | | | CSU equation | |
| Abutment Scour | | | | | | |
| Scour Depth Ys (ft): | 0 | - | - | 0 | - | - |
| Froude #: | 0.15 | - | - | 0.24 | - | - |
| Equation: | HIRE | - | - | HIRE | - | - |
| Combined Scour Depths | | | | | | |
| Pier+Contraction (ft): | 6.1 | 15.2 | 4.2 | 5.6 | 6.4 | - |
| abutment+contraction (ft): | 1.9 | - | - | 1.4 | - | - |

**Table 8-2B -** Proposed Conditions Bridge HEC-18 Calculations San Jacinto River

| HEC-RAS HEC-18 CALCULATIONS OUTPUT | | | | | | |
|---|---|---|---|---|---|---|
| Component | State Street | | | Sanderson Avenue | | |
| Contraction Scour | Left | Channel | Right | Left | Channel | Right |
| Scour Depth Ys (ft): | 1.9 | 1.5 | - | 1.1 | 0.9 | - |
| Critical Velocity (ft/s): | 2.4 | 2.4 | - | 2.2 | 2.2 | - |
| Equation: | Live | Live | - | Live | Live | - |
| Pier Scour | | | | | | |
| Scour Depth Ys (ft): | | 3.37 | | | 3.43 | |
| Froude #: | | 0.42 | | | 0.27 | |
| Equation: | | CSU equation | | | CSU equation | |
| Abutment Scour | | | | | | |
| Scour Depth Ys (ft): | 0 | - | - | 0 | - | - |
| Froude #: | 0.50 | - | - | 0.44 | - | - |
| Equation: | HIRE | - | - | HIRE | - | - |
| Combined Scour Depths | | | | | | |
| Pier+Contraction (ft): | 6.7 | 6.3 | 4.8 | 5.9 | 5.7 | - |
| abutment+contraction (ft): | 1.9 | - | - | 1.1 | - | - |

### *8.3.1 <u>Comparison of HEC-18 vs. HEC-6T Contraction Scour Results</u>*

A comparison of the contraction scour results from HEC18 to the results of the General Scour analysis from HEC-6T indicated that HEC-18 computed a larger value. The 100-year General Scour value from HEC-6T model at the bridge sections will be replaced with the contraction scour values computed from HEC-18. The results are summarized in the following table for the main channel.

| **Table 8-3 –** Comparison of 100-year Bridge Contraction Scour Results from HEC-18 and HEC-6T General Scour | | | |
|---|---|---|---|
| **Bridge** | | **HEC-18 Contraction Scour** | **HEC-6T General Scour** |
| State Street | Existing | 11.0 | 2.4 |
| | Proposed | 1.5 | 0.2 |
| Sanderson | Existing | 2.1 | Aggrading |
| | Proposed | 0.9 | 0.0 |

# 9 General Adjustment

The ACOE HEC-6 model is a one-dimensional moveable bed open channel hydraulic and sediment model. The model was designed to simulate change in riverbed profiles resulting from sediment scour and deposition over long periods of time. The model segments hydrograph data into a progression of steady flow events with varied discharge and duration. Every segment of flow is used to calculate a water surface profile and associated hydraulic parameters (e.g. velocity, depth, etc.). From the hydraulic parameters potential sediment transport rates are estimated for each model reach and scour or deposition is next estimated so that cross-section shape can be updated. Sediment calculations are based on grain size distribution so that sorting and armoring can be considered. HEC-6 considers the interactions between sediment behavior in rivers with local hydraulics and bed geometry and conditions.

## 9.1 HEC-6 Model Theory and Limitations

Capability of a river to transport sediment in the model is based on yield from upstream locations. Computation of transport is partitioned into bed and suspended load after Einstein (1950). This assumes that the reach transports the same types of materials as those which comprise the bed (an alluvial reach), and thus reflects a record of the past and present sediment transport. Transport is constrained within the limits of the wetted perimeter.

A one-dimensional energy approximation to the equations of motion is used for hydraulic calculations in HEC-6. Manning's equation is utilized to incorporate bed friction. The model also uses both an up- and down-stream boundary condition with internal conditions optional. Flow conveyance, levee flow containment and ineffective flow are modeled in a manner similar to the Army Corps' HEC-2 model. Supercritical flow is approximated by normal depth and sediment transport is calculated using this criteria. Because the model is one-dimensional, there is no way to simulate meander development or specify lateral erosion.

Each cross-section (to the next downstream section) represents a sediment control volume and sediment continuity equations are evaluated for this volume. The only two sediment sources are considered by HEC-6 are the bed (sediment control volume) and sediment in the inflowing water. Only vertical adjustment of the bed is considered and is calculated through sediment continuity using iterations of the Exner equation. Krone's method (1962) is used for deposition of fines in HEC-6, and the method of Ariathurai and Krone (1976) is used for scour. Sediment transport functions are user selectable and 13 different equations are possible. Colby's method (1964) is used to adjust transport potential for high wash loads and armoring is simulated using Gessler's method (1970). Sediment boundary conditions operate such that inflowing sediment load is a function of inflow discharge. The total sediment discharge at each section, as well as the volume of deposition or scour at each section, is computed for all time steps.

The "T" enhancement (model build H6TV51322-07m) of the HEC-6 program, created by Mobile Boundary Hydraulics, is used in this study. Fundamental differences between the "T" and standard versions of the model are minimal and are described in the HEC-6T user's manual. Additional details describing model numerics are described in the HEC-6 user's manual. Details describing the implementation of specific model parameters and functions are described below.

## 9.2 HEC-6T Model Assembly

In this study, hydraulic representation of the creek bed is accomplished in several distinct steps. First, the HEC-RAS numerical model read directly into the HEC-6 program. In the standard version of the HEC-6 program the prepared version of the HEC-RAS model, described in Section 7, above, is used. However, the "T" enhancement allows direct importation of the geometry data. The model design (100-year) hydrograph, described above, is used for this study. The full hydrograph is linearized using splines to facilitate input into the model. Both the original and linearized 100-year, 24-hour hydrograph are illustrated in Figure 3-1. Sediment data is taken from the CHJ (2008) geotechnical investigation described in Section 4.

Sediment transport is calculated using the Toffaleti equation, chosen with assistance from the SAM.AID subroutine in the SAM software package (ACOE 2002). SAM.AID determines the most representative transport function based on the hydraulic parameters and percent finer data for a stream by comparing sediment and hydraulic data with the results of 20 peer-reviewed and widely acknowledged sediment transport studies. SAM.AID begins by comparing study parameters (V, D, $S_e$, $B_e$, $D_{50}$) with parameters in the transport function database. Comparison begins by determining if $D_{50}$ falls within one of the ranges identified in the database. Once the initial matches have been made in the database, the three best matched sediment transport function for the stream are listed along with the parameters that matched the data set. After SAM.AID has made its selections, the results are further compared to information published in Simons and Senturk (1992) and Yang and Huang (2001).

Sediment transport is calculated for grain sizes from 0.075 to 12.7 mm based on the sediment distribution presented in Section 4. The number of iterations of the Exner equation is determined by the model. A transmissive boundary condition is employed at the downstream boundary to minimize boundary condition errors. Water surface elevations at the downstream boundary are taken from the HEC-RAS model.

Sediment inflow for the upstream boundary condition is calculated using HEC-6T for four distinct discharges representing different discharges of the design hydrograph since there is not any available historical measured data on sediment discharges for specific storm events or information on sediment yields/delivery from the surrounding watersheds. The discharges that were used to develop the upstream sediment transport rating table were 2,390 cfs, 15,000 cfs, 30,000 cfs, and 60,000 cfs. The sediment inflow was determined by running the HEC-6T with the “recirculation option.” This assumes that sediment discharge at the upstream boundary is in steady state. The following graph which was generated from the recirculation analysis runs and illustrates the sediment transport rating curve for the upstream boundary condition.  These are the values from the LQ and LT cards used in the HEC6T model.

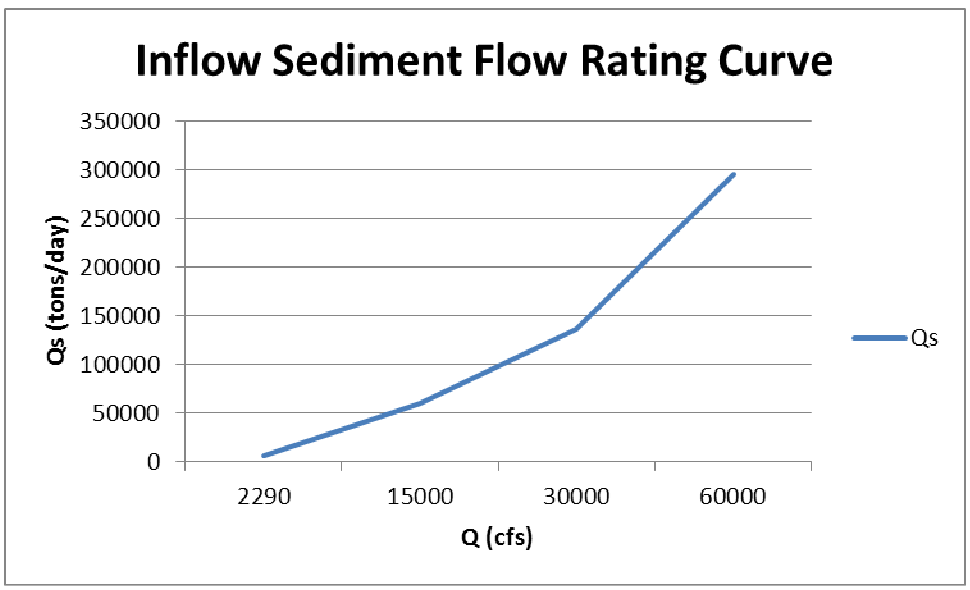


**Figure 9-1 –** Sediment inflow rating curve generated through HEC-6T recirculation analysis

While site visits of the study area (September 15, 2008, please see Appendix) indicate that the streambed is aggrading in the vicinity of the upstream boundary, the present method of assuming steady state was determined to be preferential to other methods (e.g. channel forming discharge) since the study area only receives very infrequent flows (Jaffe, 2009). A sensitivity analysis of the sediment inflow is described in *Section 9.4 - Sediment Input Data and Selection of Transport Functions*. In addition, the following figure indicates a plot of water flowrate vs. sediment transport rate for the inflowing sediment load at the upstream boundary condition based on the recirculation option for HEC-6T.

### 9.3 HEC-6T Rigid Bed Test and HEC-RAS Comparison

A test was run to determine how closely the hydraulics of the HEC-6T model, run in rigid bed mode, matches the hydraulics of parent HEC-RAS model from which the 6T model was built. It should be understood that the computational hydraulic engines of the HEC-RAS and HEC-6T models are different, despite being based on the same equations. The HEC-6T model is built on the engine from the HEC-2 model, and this engine is different than the one found in the HEC-RAS model. Therefore, while it is expected that the hydraulics of the two models will be different, even with the same geometries, the test is run knowing that some disparity between the two models will be apparent. The comparison was performed for the "proposed conditions" models without the bridges and using the 100-year flowrate of Q = 57,250 cfs. The HEC-RAS and HEC-6T will essentially have the same the same cross-section geometry at all the sections and additional hydraulic parameters such as roughness coefficients.

Table 9-9 provides a comparison of three different computed 100-year hydraulic characteristics from HEC-RAS and HEC-6T which can assist in illustrating general trends concerning the hydraulics. The hydraulic parameters that were compared included: (1) velocity, (2) top width (TW), and (3) the maximum depth at each section. In general, it should be expected that the differences in the hydraulic parameters would be within the range of 5-10% for conventional riverine system geometry. However, the comparison shown in the table illustrates large changes in the velocity between HEC-RAS and the HEC-6T model which range between 40% and 60%. The average change in velocity is approximately 15%. The top width change averaged about 10% with some localized changes over 40%. The average change in depth was about 9% between the models with the maximum change almost 50%. These three variables were graphed to evaluate trends in the changes and to assist in determining the background for these differences. The graphs provide useful insight into the reason for the changes. It appears that one of the major reasons for the locations where the large changes in velocity is <u>associated with the occurrence of "divided flow" at those locations</u>. Reviewing the HEC-RAS detailed computations at the individual sections indicated that over 70% of the cross-sections had divided flow occurring. The graph which presents the change in velocity illustrates two large groupings of velocity change and reviewing the hydraulics at this location the major common issue that occurs is divided flow because the cross-section geometry has an obstruction which creates one or several islands, as previously discussed in the hydraulics section of this report. HEC-RAS and HEC-6T treat divided flow differently in the computational process which accounts for this change. Locations where there is not divided flow then the results of the models appear to be within the normal acceptable range. Although there are these large changes in velocity between the two models we believe any differences will be accommodated within the safety factors for selection of the appropriate toe-down. Additional minor reasons for differences between the HEC-RAS and the HEC6-T model rigid boundary hydraulics include:

- HEC-6T or the HEC-2 computational hydraulic engine uses a "slope averaging method" to calculate the "friction slope" while the default method in HEC-RAS is the average conveyance method.
- Appropriate selection of the channel bank stations influences the hydraulic computations and averaging of the friction slope. The bank stations utilized were based on the approved HEC-RAS model, and modifications to those locations may be warranted based on the section geometry, however, the approved model was not adjusted. The channel markers generally reflected the original floodplain main channel section and an improved model would extend the channel markers to the left and right levee extents in the section.
- Neither the HEC-RAS nor HEC-6T model incorporated bridges within the models for the comparison analysis.

**Table 9-1 –** Comparison of HEC-RAS and HEC-6T Rigid Bed 100-Year Hydraulics

| Sect. No. | Invert Elev. | HEC-6T | | | | HEC-RAS | | | | DIFFERENCE (%) | | |
|---|---|---|---|---|---|---|---|---|---|---|---|---|
| | | Vel. (fps) | Top Width (ft) | W.S. Elev. | Max. Depth (ft) | Vel. (fps) | Top Width (ft) | W.S. Elev. | Max. Depth (ft) | $\Delta_{VEL}$ (%) | $\Delta_{TW}$ (%) | $\Delta_{DEPTH}$ (%) |
| 30361 | 1538 | 4.78 | 1721.2 | 1545.75 | 7.8 | 6.06 | 1719.4 | 1544.42 | 6.4 | 21.1 | -0.1 | -20.8 |
| 29945 | 1535 | 4.98 | 1629.0 | 1543.71 | 8.7 | 6.18 | 1619.9 | 1542.34 | 7.3 | 19.5 | -0.6 | -18.7 |
| 29025 | 1530 | 4.56 | 1543.5 | 1539.75 | 9.7 | 5.32 | 1642.8 | 1538.79 | 8.8 | 14.3 | 6.0 | -10.9 |
| 28104 | 1525 | 5.35 | 1337.9 | 1535.26 | 10.3 | 8.34 | 1326.6 | 1532.65 | 7.7 | 35.8 | -0.8 | -34.1 |
| 27263 | 1517 | 6.94 | 1073.3 | 1528.95 | 12.0 | 8.29 | 1076.9 | 1527.96 | 11.0 | 16.3 | 0.3 | -9.1 |
| 26500 | 1513 | 6.35 | 829.9 | 1526.63 | 13.6 | 6.6 | 831.4 | 1526.95 | 14.0 | 3.8 | 0.2 | 2.3 |
| 25846 | 1512.5 | 9.08 | 660.9 | 1524.48 | 12.0 | 9.28 | 652.0 | 1525.3 | 12.8 | 2.2 | -1.4 | 6.4 |
| 25246 | 1512 | 12.40 | 821.2 | 1521.42 | 9.4 | 10.7 | 789.0 | 1523.07 | 11.1 | -15.9 | -4.1 | 14.9 |
| 24895 | 1511 | 8.39 | 907.0 | 1520.43 | 9.4 | 8.77 | 897.5 | 1522.02 | 11.0 | 4.3 | -1.1 | 14.5 |
| 24469 | 1510 | 7.67 | 863.2 | 1519.09 | 9.1 | 9.49 | 812.3 | 1520.23 | 10.2 | 19.2 | -6.3 | 11.2 |
| 24190 | 1508 | 8.56 | 793.1 | 1518.03 | 10.0 | 9.94 | 738.8 | 1519.02 | 11.0 | 13.9 | -7.3 | 9.0 |
| 23817 | 1506 | 9.89 | 898.8 | 1516.18 | 10.2 | 11.65 | 778.1 | 1516.6 | 10.6 | 15.1 | -15.5 | 4.0 |
| 23406 | 1505 | 9.90 | 1095.1 | 1514.06 | 9.1 | 10.91 | 1026.1 | 1514.16 | 9.2 | 9.2 | -6.7 | 1.1 |
| 22909 | 1502 | 6.49 | 1101.8 | 1512.63 | 10.6 | 8.36 | 1280.2 | 1512.8 | 10.8 | 22.3 | 13.9 | 1.6 |
| 22448 | 1500 | 12.16 | 1439.5 | 1509.87 | 9.9 | 12.73 | 1360.5 | 1509.97 | 10.0 | 4.5 | -5.8 | 1.0 |
| 21912 | 1497.51 | 9.69 | 1338.3 | 1507.38 | 9.9 | 11.28 | 1337.8 | 1507.92 | 10.4 | 14.1 | 0.0 | 5.2 |
| 21459 | 1496 | 11.61 | 1245.7 | 1504.75 | 8.8 | 10.55 | 1220.0 | 1506.36 | 10.4 | -10.0 | -2.1 | 15.5 |
| 20953 | 1494.19 | 10.61 | 622.5 | 1502.99 | 8.8 | 11.24 | 622.6 | 1503.59 | 9.4 | 5.6 | 0.0 | 6.4 |
| 20853 | 1493.79 | 12.11 | 659.9 | 1501.59 | 7.8 | 10.41 | 660.2 | 1503.32 | 9.5 | -16.3 | 0.0 | 18.1 |
| 20754 | 1493.4 | 12.01 | 749.1 | 1501.05 | 7.7 | 9.86 | 749.0 | 1503.07 | 9.7 | -21.8 | 0.0 | 20.8 |
| 20654 | 1493 | 10.32 | 630.2 | 1501.10 | 8.1 | 10.3 | 811.3 | 1502.75 | 9.8 | -0.2 | 22.3 | 16.9 |
| 20179 | 1490 | 9.44 | 622.0 | 1499.65 | 9.6 | 13.4 | 1043.5 | 1500.02 | 10.0 | 29.5 | 40.4 | 3.7 |
| 19813 | 1489.4 | 12.64 | 656.2 | 1496.65 | 7.2 | 13.31 | 1129.5 | 1498 | 8.6 | 5.0 | 41.9 | 15.7 |
| 19200 | 1488.2 | 6.24 | 714.5 | 1494.72 | 6.5 | 8.36 | 1251.9 | 1496.3 | 8.1 | 25.4 | 42.9 | 19.5 |
| 18929 | 1488 | 4.35 | 710.9 | 1494.41 | 6.4 | 4.72 | 1203.5 | 1495.74 | 7.7 | 7.9 | 40.9 | 17.2 |
| 18399 | 1486 | 4.91 | 708.0 | 1492.23 | 6.2 | 5.36 | 1218.3 | 1494.25 | 8.3 | 8.5 | 41.9 | 24.5 |
| 17768 | 1485 | 2.95 | 895.7 | 1489.80 | 4.8 | 5.96 | 1222.9 | 1491.59 | 6.6 | 50.4 | 26.8 | 27.2 |
| 17330 | 1483 | 4.69 | 1099.4 | 1488.58 | 5.6 | 5.56 | 1216.7 | 1489.47 | 6.5 | 15.6 | 9.6 | 13.8 |
| 16913 | 1482 | 4.99 | 1230.0 | 1487.60 | 5.6 | 5.18 | 1208.2 | 1487.43 | 5.4 | 3.6 | -1.8 | -3.2 |
| 16476 | 1480 | 5.05 | 1257.9 | 1485.48 | 5.5 | 6.7 | 1205.3 | 1485.53 | 5.5 | 24.7 | -4.4 | 0.8 |
| 16028 | 1478 | 5.18 | 1260.7 | 1483.59 | 5.6 | 5.17 | 1198.9 | 1483.63 | 5.6 | -0.2 | -5.2 | 0.7 |
| 15682 | 1477 | 4.63 | 1255.0 | 1482.33 | 5.3 | 4.65 | 1188.6 | 1482.4 | 5.4 | 0.5 | -5.6 | 1.4 |
| 15347 | 1476 | 4.10 | 1252.7 | 1481.37 | 5.4 | 4.12 | 1189.7 | 1481.47 | 5.5 | 0.5 | -5.3 | 1.9 |
| 14920 | 1474 | 4.75 | 1244.2 | 1479.78 | 5.8 | 4.82 | 1192.1 | 1479.98 | 6.0 | 1.5 | -4.4 | 3.3 |
| 14335 | 1472 | 4.73 | 1262.0 | 1478.19 | 6.2 | 4.77 | 1203.1 | 1478.29 | 6.3 | 0.8 | -4.9 | 1.6 |
| 13733 | 1470 | 5.79 | 1245.5 | 1476.35 | 6.3 | 5.85 | 1215.0 | 1476.44 | 6.4 | 1.0 | -2.5 | 1.4 |
| 13200 | 1467 | 6.45 | 1226.0 | 1474.52 | 7.5 | 6.46 | 1184.9 | 1474.58 | 7.6 | 0.2 | -3.5 | 0.8 |
| 12726 | 1466 | 6.03 | 1214.9 | 1472.48 | 6.5 | 6.34 | 1164.1 | 1472.25 | 6.3 | 4.9 | -4.4 | -3.7 |
| 12317 | 1464 | 7.82 | 1174.7 | 1470.89 | 6.9 | 7.89 | 1174.9 | 1470.88 | 6.9 | 0.9 | 0.0 | -0.2 |

**Table 9-1 –** Comparison of HEC-RAS and HEC-6T Rigid Bed 100-Year Hydraulics

| Sect. No. | Invert Elev. | HEC-6T | | | | HEC-RAS | | | | DIFFERENCE (%) | | |
|---|---|---|---|---|---|---|---|---|---|---|---|---|
| | | Vel. (fps) | Top Width (ft) | W.S. Elev. | Max. Depth (ft) | Vel. (fps) | Top Width (ft) | W.S. Elev. | Max. Depth (ft) | ΔVEL (%) | ΔTW (%) | ΔDEPTH (%) |
| 11871 | 1463 | 7.73 | 1161.5 | 1469.49 | 6.5 | 7.71 | 1162.7 | 1469.52 | 6.5 | -0.3 | 0.1 | 0.4 |
| 11396 | 1461 | 7.61 | 1187.2 | 1467.85 | 6.9 | 7.66 | 1187.6 | 1467.94 | 6.9 | 0.7 | 0.0 | 1.2 |
| 11003 | 1460 | 7.50 | 1183.3 | 1466.64 | 6.6 | 7.47 | 1183.2 | 1466.72 | 6.7 | -0.4 | 0.0 | 1.2 |
| 10609 | 1459 | 6.95 | 1196.4 | 1465.56 | 6.6 | 6.82 | 1195.0 | 1465.71 | 6.7 | -1.9 | -0.1 | 2.3 |
| 10216 | 1458 | 2.93 | 1192.6 | 1464.48 | 6.5 | 2.96 | 1190.9 | 1464.54 | 6.5 | 0.9 | -0.1 | 0.9 |
| 9717 | 1457 | 2.93 | 1276.7 | 1463.25 | 6.3 | 2.97 | 1276.5 | 1463.34 | 6.3 | 1.2 | 0.0 | 1.4 |
| 9359 | 1455.75 | 2.29 | 1325.4 | 1462.59 | 6.8 | 2.6 | 1292.2 | 1462.67 | 6.9 | 12.1 | -2.6 | 1.1 |
| 8867 | 1454 | 2.20 | 1365.2 | 1461.78 | 7.8 | 2.24 | 1332.9 | 1461.82 | 7.8 | 1.6 | -2.4 | 0.5 |
| 8176 | 1452 | 2.45 | 1396.7 | 1460.38 | 8.4 | 2.49 | 1362.4 | 1460.4 | 8.4 | 1.4 | -2.5 | 0.2 |
| 7758 | 1451 | 2.96 | 1356.4 | 1459.20 | 8.2 | 2.96 | 1304.5 | 1459.21 | 8.2 | 0.1 | -4.0 | 0.1 |
| 7419 | 1450.3 | 3.48 | 1358.4 | 1457.37 | 7.1 | 3.67 | 1285.9 | 1457.67 | 7.4 | 5.1 | -5.6 | 4.0 |
| 6711 | 1448 | 2.22 | 1721.4 | 1454.87 | 6.9 | 2.51 | 3133.8 | 1455.08 | 7.1 | 11.4 | 45.1 | 3.0 |
| 6166 | 1447.43 | 2.05 | 2172.0 | 1453.41 | 6.0 | 2.24 | 2928.9 | 1453.39 | 6.0 | 8.6 | 25.8 | -0.4 |
| 5941 | 1447.24 | 1.63 | 2247.8 | 1452.63 | 5.4 | 1.68 | 2782.5 | 1452.63 | 5.4 | 3.3 | 19.2 | -0.1 |
| 5609 | 1447.06 | 1.96 | 2609.6 | 1451.77 | 4.7 | 1.99 | 2892.7 | 1451.75 | 4.7 | 1.7 | 9.8 | -0.3 |
| 5184 | 1446.88 | 4.19 | 2901.2 | 1451.05 | 4.2 | 4.14 | 2901.3 | 1451.1 | 4.2 | -1.2 | 0.0 | 1.3 |
| 4684 | 1446.7 | 3.34 | 3278.4 | 1450.47 | 3.8 | 3.3 | 3774.0 | 1450.57 | 3.9 | -1.3 | 13.1 | 2.5 |
| 4328 | 1446.7 | 3.05 | 3517.6 | 1450.09 | 3.4 | 2.99 | 4191.2 | 1450.22 | 3.5 | -1.9 | 16.1 | 3.6 |
| 3997 | 1446.7 | 2.71 | 3739.8 | 1449.76 | 3.1 | 2.64 | 4354.2 | 1449.92 | 3.2 | -2.8 | 14.1 | 5.1 |
| 3671 | 1446.7 | 1.96 | 6924.1 | 1449.58 | 2.9 | 2.4 | 6818.9 | 1449.67 | 3.0 | 18.5 | -1.5 | 3.1 |
| 3285 | 1446.2 | 1.45 | 5199.2 | 1449.44 | 3.2 | 1.54 | 6085.1 | 1449.52 | 3.3 | 6.1 | 14.6 | 2.5 |
| 2961 | 1445.7 | 2.81 | 5142.4 | 1449.16 | 3.5 | 3.07 | 6037.4 | 1449.2 | 3.5 | 8.6 | 14.8 | 1.0 |
| 2581 | 1445.2 | 2.87 | 5755.6 | 1448.60 | 3.4 | 2.9 | 5726.0 | 1448.64 | 3.4 | 0.9 | -0.5 | 1.3 |
| 2298 | 1444.7 | 2.58 | 4803.5 | 1448.20 | 3.5 | 2.63 | 5745.0 | 1448.24 | 3.5 | 1.8 | 16.4 | 1.0 |
| 2073 | 1444.2 | 2.32 | 5758.4 | 1447.97 | 3.8 | 2.34 | 5728.9 | 1448 | 3.8 | 0.9 | -0.5 | 0.8 |
| 1677 | 1443.7 | 2.56 | 4747.6 | 1447.34 | 3.6 | 2.59 | 5527.6 | 1447.39 | 3.7 | 1.0 | 14.1 | 1.3 |
| 1285 | 1442.58 | 2.85 | 4238.8 | 1446.50 | 3.9 | 2.92 | 3985.1 | 1446.53 | 4.0 | 2.4 | -6.4 | 0.8 |
| 1000 | 1442.7 | 3.29 | 4461.4 | 1445.85 | 3.1 | 3.35 | 4258.8 | 1445.85 | 3.1 | 1.8 | -4.8 | 0.0 |

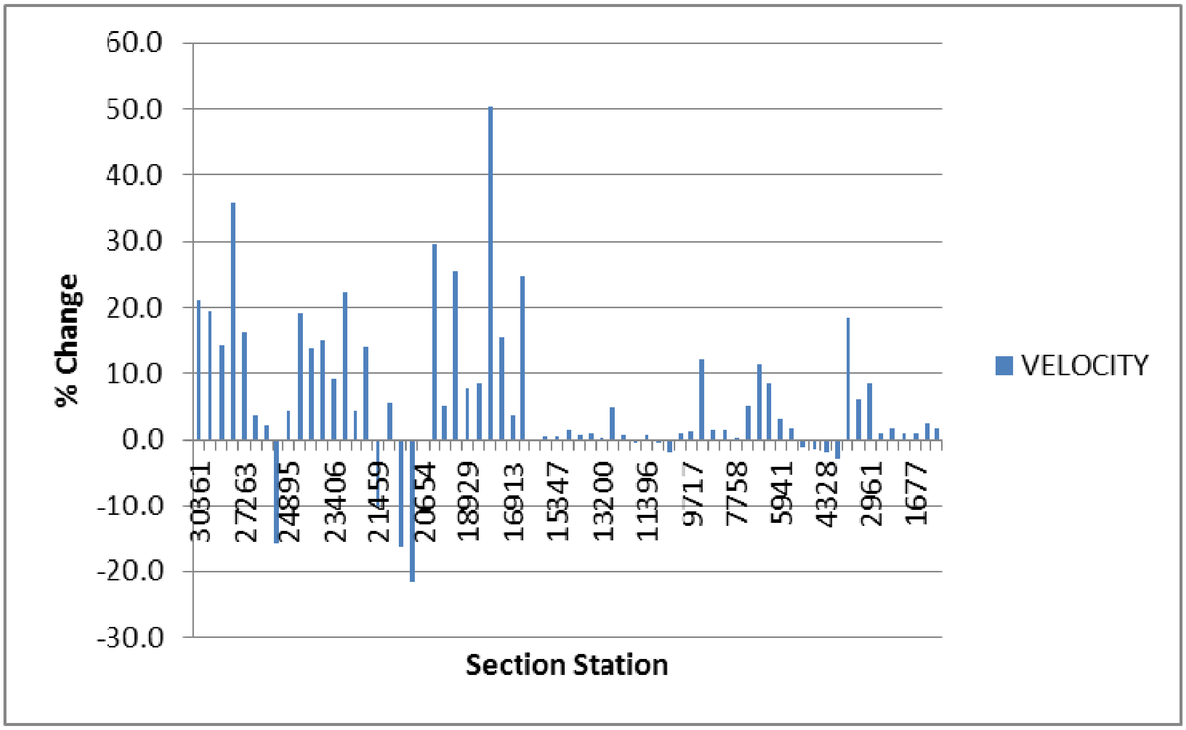


**Figure 9-2 –** Plot illustrating the change in velocity along the study reach of the channel which provides one indicator to expected changes in sediment transport capacity

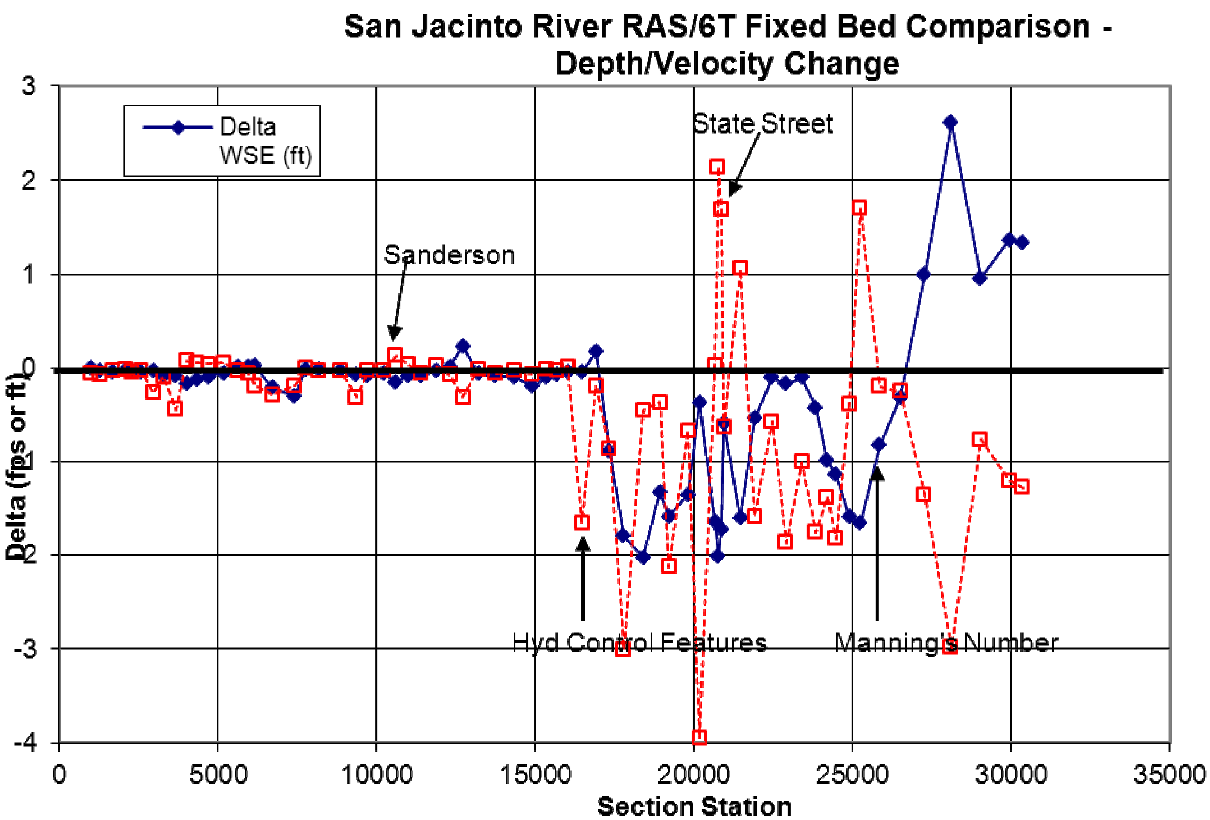


**Figure 9-3 –** Comparison of flow depth and velocity change between HEC-RAS and HEC-6T

### 9.4 Sediment Input Data and Selection of Transport Functions

Representation of sediment grain size distribution in HEC-6T takes the form of percent finer data obtained from sieve analysis of channel sediment grab samples. The two average data curves were input into the model. All sampling and sieve analysis was conducted by CHJ (2008). Sediment data used was described previously in Section 4. HEC-6T gradation classifications use the American Geophysical Union Scale. The same transport function determined in SAM.AID was used. A sensitivity analysis of transport equation is described below. Once the sediment data is compiled the data is then entered on the LT, LF and PF records in HEC-6T model. The model is run with a horizontally varying Manning's value taken from the Webb HEC-RAS model, which reflects differences between the existing and proposed streambed conditions. However, the average Manning's typically used to represent the streambed was n=0.035.

### 9.5 Special Issues of Concern - Quasi-Two-Dimensional Flows

The proposed conditions include the improvement and/or replacement of flood control levees along the study reach. In the existing condition the levees are insufficient to contain events much smaller than the design event. Frequent breaches of the levees have occurred over the period of record and as recently as Winter 2004/2005 (USGS gage 11069500). The HEC-RAS model sections include the north overbank, including some upland terrain, the main channel and levees, and the low-lying south overbank. During flow events water frequently ponds in the south overbank. Overbank flooding is observed in the HEC-RAS modeling in a manner similar to observations, and this presents a problem for HEC-6 modeling. It is important to recall that HEC-6 is a one-dimensional model. Split flows like those observed along the study reach present a problem for the model, however, since they represent two-dimensional flow conditions. While HEC-6T does have mechanisms to deal with divided flows, a divided flow analysis is beyond the current project scope.

To deal with the potential for overbank flows, the present study creates a second low-discharge sediment transport model that assumes all flow only occur in the main channel before the existing levees are overtopped. Levee markers in the HEC-RAS model are retained in the HEC-6T model and a hydrograph with a peak discharge of 15,000 cfs is utilized for the low-flow simulation. This simulation, the narrow simulation, represents both the existing conditions under smaller peak discharges and the proposed condition until the existing conditions levee is scoured away. A second model was created to represent or simulate a "wide condition", where the existing levees are removed (existing condition), or removed and replaced with the proposed conditions levee (proposed condition). These models (wide condition) represent the existing and proposed conditions after the existing levee has been scoured away.

### 9.6 HEC-6 General Streambed Adjustment and Bed Stability

"General" bed adjustment is based on HEC-6T modeling, and presented in Figures 9.1-9.3 and Tables 9.1-9.3 for the low-flow, existing, and proposed conditions, at the initial, peak-of-the-hydrograph, and end-of-the-100-year hydrograph (final) minimum bed elevation. The "narrow" channel reflects a general storm hydrograph of 15,000 cfs while the "wide" channel simulation reflects the 100-year (Q=57,250 cfs) general storm hydrograph. The presentation of these results indicates the bed change for vertical movement of the thalweg and may not necessarily represent the "average bed" elevation change. It is important to note that no pattern of aggradation/degradation is apparent between cross-sections in the figure. Model bed adjustment results for HEC-6T narrow model range from -0.2 to 0.4 feet with an average change of 0.0 ft at the peak of the hydrograph and -0.4 to 2.1 feet with an average change of 0.0 ft at the conclusion of the event. Model bed adjustment results for HEC-6T "wide channel" existing model range from -5.3 to 0.3 feet with an average change of -0.8 ft at the peak of the hydrograph and -5.0 to 0.6 feet with an average change of -0.9 ft at the conclusion of the event. Model bed adjustment results for HEC-6T "wide channel" proposed model range from -1.0 to 0.3 feet with an average change of 0.0 ft at the peak of the hydrograph and -1.1 to 0.8 feet with an average change of 0.0 ft at the conclusion of the event. It is interesting to note from the results that the proposed condition shows less change than the existing condition. All model input and output is included in the Appendix.

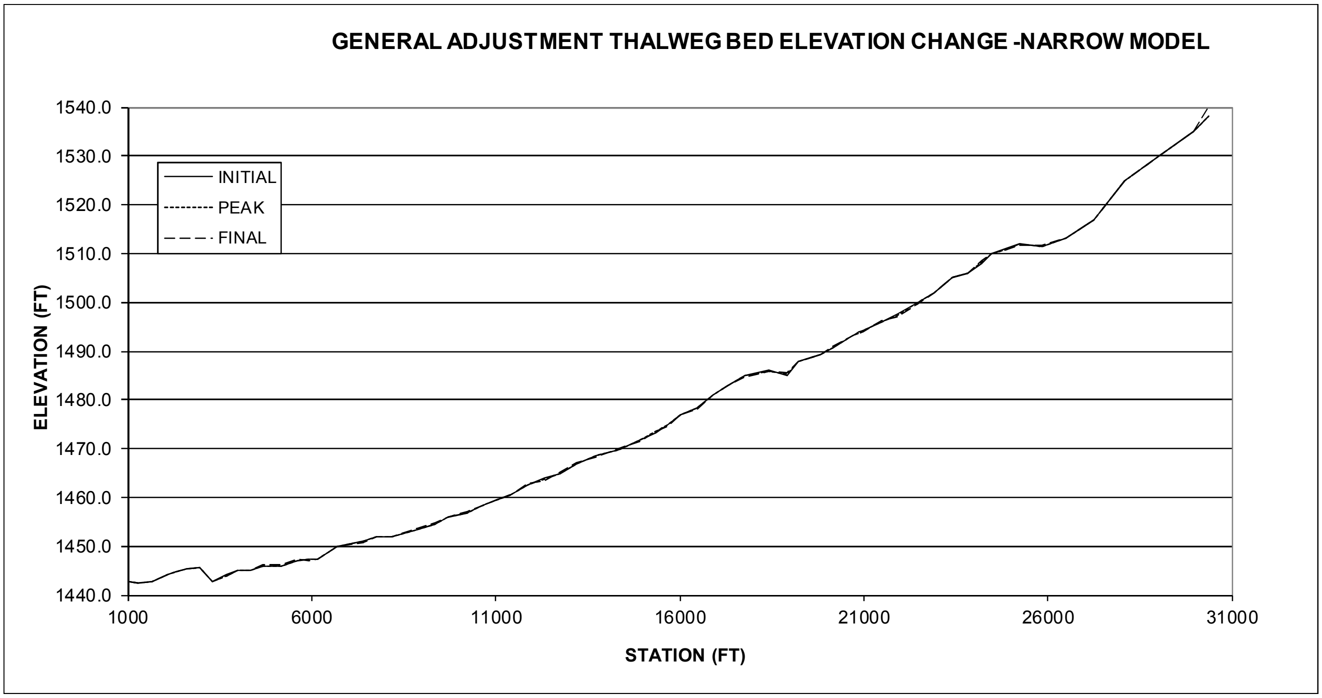


**Figure 9-4 -** General (15,000 cfs) Adjustment Thalweg Bed Elevation Change - Narrow Simulation (Existing & Proposed)

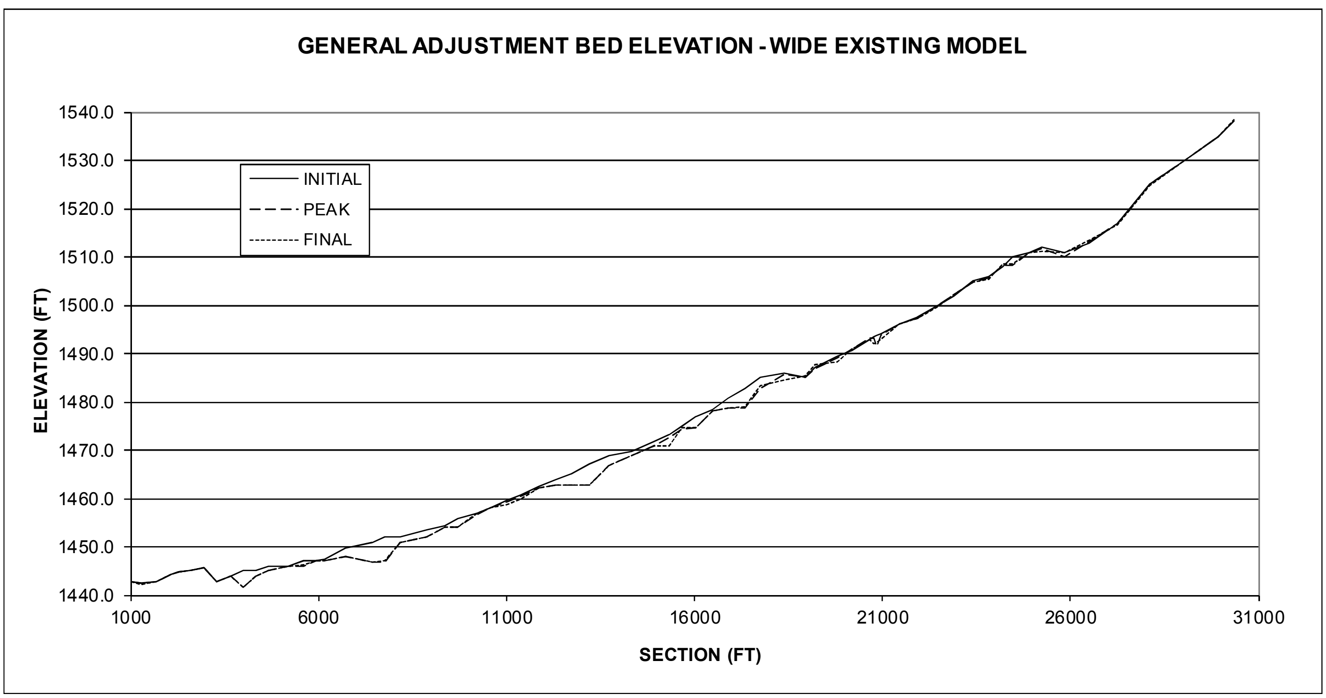


**Figure 9-5 –** 100-year General Adjustment Thalweg Bed Elevation Change - Wide, Existing Condition

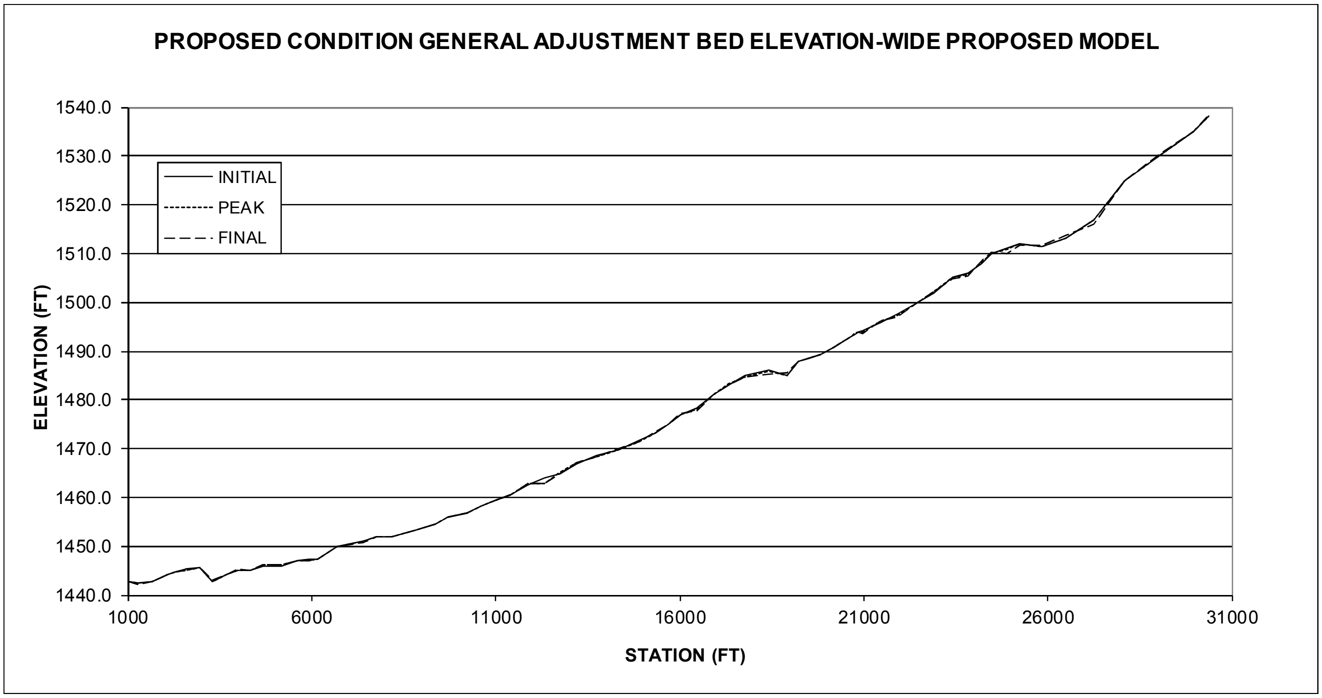


**Figure 9-6 –** 100-year General Adjustment Thalweg Bed Elevation Change - Wide, Proposed Condition

**Table 9-2** - General Adjustment in Bed Elevation – *Narrow Model*

| SECTION | Thalweg Bed Elevation | | | Difference Bed Elevation from Initial | |
|---|---|---|---|---|---|
| | Initial | Peak | Final | Peak (ft) | Final (ft) |
| 1000 | 1442.7 | 1442.7 | 1442.7 | 0.0 | 0.0 |
| 1285 | 1442.6 | 1442.6 | 1442.6 | 0.0 | 0.0 |
| 1677 | 1442.7 | 1442.7 | 1442.8 | 0.0 | 0.1 |
| 2073 | 1444.2 | 1444.2 | 1444.2 | 0.0 | 0.0 |
| 2298 | 1444.7 | 1444.7 | 1444.7 | 0.0 | 0.0 |
| 2581 | 1445.2 | 1445.2 | 1445.2 | 0.0 | 0.0 |
| 2961 | 1445.7 | 1445.7 | 1445.7 | 0.0 | 0.0 |
| 3285 | 1442.7 | 1442.7 | 1442.7 | 0.0 | 0.0 |
| 3671 | 1444.1 | 1444.0 | 1444.0 | 0.0 | 0.0 |
| 3997 | 1445.0 | 1445.0 | 1445.0 | 0.0 | 0.0 |
| 4328 | 1445.0 | 1445.0 | 1445.0 | 0.0 | 0.0 |
| 4684 | 1446.0 | 1446.0 | 1446.0 | 0.0 | 0.0 |
| 5184 | 1446.0 | 1446.0 | 1446.1 | 0.0 | 0.1 |
| 5609 | 1447.0 | 1447.0 | 1447.2 | 0.0 | 0.2 |
| 5941 | 1447.2 | 1447.2 | 1446.9 | 0.0 | -0.3 |
| 6166 | 1447.4 | 1447.4 | 1447.5 | 0.0 | 0.0 |
| 6711 | 1449.8 | 1449.8 | 1449.8 | 0.0 | 0.0 |
| 7419 | 1451.0 | 1451.0 | 1450.9 | 0.0 | -0.1 |

| Table 9-2 - General Adjustment in Bed Elevation – *Narrow Model* | | | | | |
|---|---|---|---|---|---|
| **SECTION** | **Thalweg Bed Elevation** | | | **Difference Bed Elevation from Initial** | |
| | **Initial** | **Peak** | **Final** | **Peak (ft)** | **Final (ft)** |
| 7758 | 1452.0 | 1452.0 | 1452.0 | 0.0 | 0.0 |
| 8176 | 1452.0 | 1452.0 | 1452.0 | 0.0 | 0.0 |
| 8867 | 1453.4 | 1453.4 | 1453.5 | 0.0 | 0.1 |
| 9359 | 1454.5 | 1454.6 | 1454.8 | 0.1 | 0.3 |
| 9717 | 1455.9 | 1455.9 | 1455.9 | 0.0 | 0.0 |
| 10216 | 1456.8 | 1456.9 | 1457.1 | 0.1 | 0.2 |
| 10609 | 1458.2 | 1458.2 | 1458.3 | 0.0 | 0.1 |
| 11003 | 1459.4 | 1459.4 | 1459.4 | 0.0 | 0.0 |
| 11396 | 1460.7 | 1460.7 | 1460.6 | 0.0 | -0.1 |
| 11871 | 1462.6 | 1462.6 | 1462.7 | 0.1 | 0.2 |
| 12317 | 1464.0 | 1463.6 | 1463.6 | -0.4 | -0.4 |
| 12726 | 1465.0 | 1465.0 | 1465.1 | 0.0 | 0.1 |
| 13200 | 1467.0 | 1467.0 | 1467.2 | 0.0 | 0.2 |
| 13733 | 1468.7 | 1468.6 | 1468.3 | -0.1 | -0.4 |
| 14335 | 1469.8 | 1469.9 | 1470.0 | 0.1 | 0.2 |
| 14920 | 1471.8 | 1471.7 | 1471.6 | -0.1 | -0.1 |
| 15347 | 1473.2 | 1473.4 | 1473.5 | 0.2 | 0.3 |
| 15682 | 1475.0 | 1474.8 | 1474.7 | -0.2 | -0.3 |
| 16028 | 1476.9 | 1477.0 | 1477.0 | 0.1 | 0.1 |
| 16476 | 1478.4 | 1478.2 | 1478.0 | -0.1 | -0.3 |
| 16913 | 1480.8 | 1480.9 | 1480.8 | 0.0 | 0.0 |
| 17330 | 1483.0 | 1483.0 | 1482.9 | 0.0 | -0.1 |
| 17768 | 1485.0 | 1484.9 | 1484.6 | -0.1 | -0.4 |
| 18399 | 1486.0 | 1485.9 | 1485.8 | -0.1 | -0.2 |
| 18929 | 1485.0 | 1485.2 | 1485.6 | 0.2 | 0.6 |
| 19200 | 1487.7 | 1487.8 | 1487.8 | 0.1 | 0.1 |
| 19813 | 1489.4 | 1489.4 | 1489.3 | 0.0 | -0.1 |
| 20179 | 1490.7 | 1490.7 | 1491.0 | 0.0 | 0.3 |
| 20654 | 1493.0 | 1493.0 | 1493.1 | 0.0 | 0.1 |
| 20754 | 1493.4 | 1493.3 | 1493.2 | -0.1 | -0.2 |
| 20853 | 1493.8 | 1493.6 | 1493.6 | -0.2 | -0.2 |
| 20953 | 1494.2 | 1494.1 | 1493.9 | 0.0 | -0.3 |
| 21459 | 1496.0 | 1496.0 | 1496.1 | 0.0 | 0.1 |
| 21912 | 1497.5 | 1497.5 | 1497.1 | -0.1 | -0.4 |
| 22448 | 1500.0 | 1500.0 | 1499.7 | 0.0 | -0.3 |
| 22909 | 1502.0 | 1502.0 | 1501.9 | 0.0 | -0.1 |
| 23406 | 1505.0 | 1505.0 | 1505.0 | 0.0 | 0.0 |
| 23817 | 1506.0 | 1505.9 | 1505.9 | -0.1 | -0.1 |
| 24190 | 1508.0 | 1508.1 | 1508.5 | 0.1 | 0.5 |
| 24469 | 1510.0 | 1510.0 | 1510.0 | 0.0 | 0.0 |

| Table 9-2 - General Adjustment in Bed Elevation – *Narrow Model* | | | | | |
|---|---|---|---|---|---|
| **SECTION** | **Thalweg Bed Elevation** | | | **Difference Bed Elevation from Initial** | |
| | **Initial** | **Peak** | **Final** | **Peak (ft)** | **Final (ft)** |
| 24895 | 1511.0 | 1510.9 | 1510.7 | -0.1 | -0.3 |
| 25246 | 1512.0 | 1512.0 | 1511.8 | 0.0 | -0.2 |
| 25846 | 1511.3 | 1511.3 | 1511.6 | 0.1 | 0.3 |
| 26500 | 1513.0 | 1513.1 | 1513.2 | 0.1 | 0.2 |
| 27263 | 1517.0 | 1516.9 | 1516.7 | -0.1 | -0.3 |
| 28104 | 1525.0 | 1525.0 | 1525.0 | 0.0 | 0.0 |
| 29025 | 1530.0 | 1530.0 | 1530.0 | 0.0 | 0.0 |
| 29945 | 1535.0 | 1535.0 | 1535.0 | 0.0 | 0.0 |
| 30361 | 1538.0 | 1538.1 | 1540.1 | 0.1 | 2.1 |

| Table 9-3 – General Adjustment Bed Elevation – *WIDE*, *EXISTING* SIMULATION | | | | | |
|---|---|---|---|---|---|
| **SECTION** | **Thalweg Bed Elevation** | | | **Difference Bed Elevation from Initial** | |
| | **Initial** | **Peak** | **Final** | **Peak (ft)** | **Final (ft)** |
| 1000 | 1442.7 | 1442.7 | 1442.7 | 0.0 | 0.0 |
| 1285 | 1442.6 | 1442.5 | 1442.2 | -0.1 | -0.4 |
| 1677 | 1442.7 | 1442.7 | 1442.8 | 0.0 | 0.1 |
| 2073 | 1444.2 | 1444.2 | 1444.2 | 0.0 | 0.0 |
| 2298 | 1444.7 | 1444.7 | 1444.7 | 0.0 | 0.0 |
| 2581 | 1445.2 | 1445.2 | 1445.0 | 0.0 | -0.2 |
| 2961 | 1445.7 | 1445.7 | 1445.6 | 0.0 | -0.1 |
| 3285 | 1442.7 | 1442.7 | 1442.7 | 0.0 | 0.0 |
| 3671 | 1444.1 | 1444.0 | 1444.0 | 0.0 | 0.0 |
| 3997 | 1445.0 | 1441.6 | 1441.6 | -3.4 | -3.4 |
| 4328 | 1445.0 | 1444.0 | 1444.0 | -1.0 | -1.0 |
| 4684 | 1446.0 | 1445.0 | 1445.1 | -1.0 | -0.9 |
| 5184 | 1446.0 | 1446.0 | 1446.0 | 0.0 | 0.0 |
| 5609 | 1447.0 | 1446.0 | 1446.1 | -1.0 | -0.9 |
| 5941 | 1447.2 | 1447.0 | 1447.1 | -0.2 | -0.1 |
| 6166 | 1447.4 | 1447.0 | 1447.0 | -0.4 | -0.4 |
| 6711 | 1449.8 | 1448.0 | 1448.0 | -1.8 | -1.8 |
| 7419 | 1451.0 | 1446.7 | 1446.7 | -4.3 | -4.3 |
| 7758 | 1452.0 | 1446.7 | 1447.0 | -5.3 | -5.0 |
| 8176 | 1451.9 | 1451.0 | 1451.0 | -0.9 | -0.9 |
| 8867 | 1453.4 | 1452.0 | 1452.0 | -1.4 | -1.4 |
| 9359 | 1454.5 | 1454.0 | 1454.2 | -0.5 | -0.3 |
| 9717 | 1455.8 | 1454.0 | 1454.0 | -1.8 | -1.8 |
| 10216 | 1456.8 | 1456.7 | 1456.8 | -0.1 | 0.0 |

| **Table 9-3 –** General Adjustment Bed Elevation – *WIDE*, *EXISTING* SIMULATION | | | | | |
|---|---|---|---|---|---|
| **SECTION** | **Thalweg Bed Elevation** | | | **Difference Bed Elevation from Initial** | |
| | **Initial** | **Peak** | **Final** | **Peak (ft)** | **Final (ft)** |
| 10609 | 1458.2 | 1458.0 | 1458.1 | -0.2 | 0.0 |
| 11003 | 1459.4 | 1459.3 | 1458.6 | -0.1 | -0.8 |
| 11396 | 1460.7 | 1460.4 | 1459.7 | -0.2 | -0.9 |
| 11871 | 1462.6 | 1462.3 | 1462.3 | -0.3 | -0.3 |
| 12317 | 1464.0 | 1462.7 | 1462.7 | -1.3 | -1.3 |
| 12726 | 1465.0 | 1462.7 | 1462.7 | -2.3 | -2.3 |
| 13200 | 1467.0 | 1462.7 | 1462.7 | -4.3 | -4.3 |
| 13733 | 1468.7 | 1466.7 | 1466.7 | -2.0 | -2.0 |
| 14335 | 1469.8 | 1468.9 | 1468.9 | -0.9 | -0.9 |
| 14920 | 1471.8 | 1470.8 | 1471.0 | -1.0 | -0.8 |
| 15347 | 1473.2 | 1472.7 | 1471.0 | -0.5 | -2.2 |
| 15682 | 1475.0 | 1474.5 | 1474.6 | -0.5 | -0.4 |
| 16028 | 1476.9 | 1474.7 | 1474.7 | -2.2 | -2.2 |
| 16476 | 1478.4 | 1478.0 | 1478.0 | -0.3 | -0.3 |
| 16913 | 1480.8 | 1478.7 | 1478.7 | -2.1 | -2.1 |
| 17330 | 1482.6 | 1478.8 | 1479.0 | -3.8 | -3.6 |
| 17768 | 1485.0 | 1482.8 | 1483.2 | -2.2 | -1.8 |
| 18399 | 1486.0 | 1485.7 | 1484.4 | -0.3 | -1.6 |
| 18929 | 1485.0 | 1485.0 | 1485.2 | 0.0 | 0.2 |
| 19200 | 1487.0 | 1486.7 | 1487.6 | -0.3 | 0.6 |
| 19813 | 1489.4 | 1489.2 | 1488.2 | -0.2 | -1.2 |
| 20179 | 1490.7 | 1491.0 | 1491.0 | 0.3 | 0.3 |
| 20654 | 1493.0 | 1493.1 | 1493.0 | 0.1 | 0.0 |
| 20754 | 1493.4 | 1493.2 | 1492.1 | -0.2 | -1.3 |
| 20853 | 1493.8 | 1491.4 | 1492.2 | -2.4 | -1.6 |
| 20953 | 1494.2 | 1493.8 | 1493.0 | -0.4 | -1.2 |
| 21459 | 1496.0 | 1496.1 | 1496.0 | 0.1 | 0.0 |
| 21912 | 1497.5 | 1497.2 | 1497.1 | -0.3 | -0.4 |
| 22448 | 1500.0 | 1499.9 | 1499.5 | -0.1 | -0.5 |
| 22909 | 1502.0 | 1502.2 | 1502.1 | 0.2 | 0.1 |
| 23406 | 1505.0 | 1504.8 | 1504.8 | -0.2 | -0.2 |
| 23817 | 1506.0 | 1505.7 | 1505.4 | -0.3 | -0.6 |
| 24190 | 1508.0 | 1508.2 | 1508.4 | 0.2 | 0.4 |
| 24469 | 1510.0 | 1508.2 | 1508.7 | -1.8 | -1.3 |
| 24895 | 1511.0 | 1510.8 | 1510.7 | -0.2 | -0.3 |
| 25246 | 1512.0 | 1511.8 | 1511.1 | -0.2 | -0.9 |
| 25846 | 1511.0 | 1510.1 | 1510.8 | -0.9 | -0.2 |
| 26500 | 1513.0 | 1513.2 | 1513.4 | 0.2 | 0.4 |
| 27263 | 1517.0 | 1516.9 | 1516.6 | -0.1 | -0.4 |
| 28104 | 1525.0 | 1525.0 | 1524.9 | 0.0 | -0.1 |
| 29025 | 1530.0 | 1530.0 | 1530.0 | 0.0 | 0.0 |
| 29945 | 1535.0 | 1534.9 | 1534.9 | -0.1 | -0.1 |
| 30361 | 1538.0 | 1538.2 | 1538.3 | 0.2 | 0.3 |

**Table 9-4 –** General Adjustment Bed Elevation – *WIDE*, *PROPOSED* SIMULATION

| SECTION | Streambed Thalweg Elevation | | | Change in Thalweg Elevation | |
|---|---|---|---|---|---|
| | INITIAL | PEAK | FINAL | Peak (ft) | Final (ft) |
| 1000 | 1442.7 | 1442.7 | 1442.7 | 0.0 | 0.0 |
| 1285 | 1442.6 | 1442.5 | 1442.2 | -0.1 | -0.4 |
| 1677 | 1442.7 | 1442.8 | 1442.7 | 0.1 | 0.0 |
| 2073 | 1444.2 | 1444.2 | 1444.2 | 0.0 | 0.0 |
| 2298 | 1444.7 | 1444.7 | 1444.6 | 0.0 | -0.1 |
| 2581 | 1445.2 | 1445.2 | 1445.1 | 0.0 | -0.1 |
| 2961 | 1445.7 | 1445.7 | 1445.6 | 0.0 | -0.1 |
| 3285 | 1442.7 | 1442.8 | 1442.9 | 0.1 | 0.2 |
| 3671 | 1444.1 | 1444.1 | 1444.3 | 0.1 | 0.2 |
| 3997 | 1445.0 | 1445.1 | 1445.2 | 0.1 | 0.2 |
| 4328 | 1445.0 | 1445.1 | 1445.1 | 0.1 | 0.1 |
| 4684 | 1446.0 | 1446.1 | 1446.2 | 0.1 | 0.2 |
| 5184 | 1446.0 | 1446.1 | 1446.1 | 0.1 | 0.1 |
| 5609 | 1447.0 | 1447.0 | 1447.2 | 0.0 | 0.2 |
| 5941 | 1447.2 | 1447.1 | 1447.0 | -0.1 | -0.3 |
| 6166 | 1447.4 | 1447.4 | 1447.5 | 0.0 | 0.0 |
| 6711 | 1449.8 | 1449.8 | 1449.9 | 0.0 | 0.1 |
| 7419 | 1451.0 | 1451.0 | 1450.7 | 0.0 | -0.3 |
| 7758 | 1452.0 | 1452.0 | 1451.9 | 0.0 | 0.0 |
| 8176 | 1452.0 | 1452.0 | 1452.0 | 0.0 | 0.0 |
| 8867 | 1453.4 | 1453.4 | 1453.4 | 0.0 | 0.0 |
| 9359 | 1454.5 | 1454.6 | 1454.6 | 0.1 | 0.1 |
| 9717 | 1455.9 | 1455.9 | 1455.9 | 0.0 | 0.0 |
| 10216 | 1456.8 | 1456.9 | 1456.9 | 0.0 | 0.1 |
| 10609 | 1458.2 | 1458.2 | 1458.2 | 0.0 | 0.0 |
| 11003 | 1459.4 | 1459.4 | 1459.4 | 0.0 | 0.0 |
| 11396 | 1460.7 | 1460.7 | 1460.6 | 0.0 | 0.0 |
| 11871 | 1462.6 | 1462.8 | 1462.9 | 0.3 | 0.4 |
| 12317 | 1464.0 | 1463.0 | 1462.9 | -1.0 | -1.1 |
| 12726 | 1465.0 | 1465.0 | 1465.0 | 0.0 | 0.0 |
| 13200 | 1467.0 | 1467.1 | 1467.1 | 0.1 | 0.1 |
| 13733 | 1468.7 | 1468.4 | 1468.3 | -0.3 | -0.4 |
| 14335 | 1469.8 | 1469.9 | 1470.0 | 0.1 | 0.2 |
| 14920 | 1471.8 | 1471.6 | 1471.4 | -0.2 | -0.3 |
| 15347 | 1473.2 | 1473.2 | 1473.5 | 0.0 | 0.3 |
| 15682 | 1475.0 | 1475.0 | 1475.1 | 0.0 | 0.1 |
| 16028 | 1476.9 | 1477.1 | 1477.2 | 0.1 | 0.2 |
| 16476 | 1478.4 | 1478.0 | 1477.7 | -0.3 | -0.7 |

| Table 9-4 – General Adjustment Bed Elevation – *WIDE*, *PROPOSED* SIMULATION | | | | | |
|---|---|---|---|---|---|
| SECTION | Streambed Thalweg Elevation | | | Change in Thalweg Elevation | |
| | INITIAL | PEAK | FINAL | Peak (ft) | Final (ft) |
| 16913 | 1480.8 | 1480.9 | 1480.8 | 0.0 | 0.0 |
| 17330 | 1483.0 | 1483.2 | 1483.1 | 0.2 | 0.1 |
| 17768 | 1485.0 | 1484.6 | 1484.5 | -0.4 | -0.5 |
| 18399 | 1486.0 | 1485.8 | 1485.3 | -0.2 | -0.7 |
| 18929 | 1485.0 | 1485.1 | 1485.6 | 0.1 | 0.6 |
| 19200 | 1487.7 | 1487.7 | 1487.8 | 0.0 | 0.1 |
| 19813 | 1489.4 | 1489.4 | 1489.4 | 0.0 | 0.0 |
| 20179 | 1490.7 | 1490.7 | 1490.8 | 0.0 | 0.2 |
| 20654 | 1493.0 | 1493.0 | 1493.1 | 0.0 | 0.1 |
| 20754 | 1493.4 | 1493.5 | 1493.4 | 0.1 | 0.0 |
| 20853 | 1493.8 | 1493.8 | 1494.0 | 0.1 | 0.2 |
| 20953 | 1494.2 | 1493.9 | 1493.5 | -0.2 | -0.7 |
| 21459 | 1496.0 | 1496.2 | 1496.2 | 0.2 | 0.2 |
| 21912 | 1497.5 | 1497.4 | 1497.1 | -0.1 | -0.4 |
| 22448 | 1500.0 | 1499.8 | 1500.0 | -0.2 | 0.0 |
| 22909 | 1502.0 | 1502.2 | 1502.3 | 0.2 | 0.3 |
| 23406 | 1505.0 | 1505.0 | 1504.9 | 0.0 | -0.1 |
| 23817 | 1506.0 | 1505.7 | 1505.3 | -0.3 | -0.7 |
| 24190 | 1508.0 | 1508.1 | 1508.6 | 0.1 | 0.6 |
| 24469 | 1510.0 | 1510.1 | 1510.2 | 0.1 | 0.2 |
| 24895 | 1511.0 | 1510.8 | 1510.1 | -0.2 | -0.9 |
| 25246 | 1512.0 | 1511.9 | 1511.6 | -0.1 | -0.4 |
| 25846 | 1511.3 | 1511.3 | 1511.8 | 0.1 | 0.5 |
| 26500 | 1513.0 | 1513.2 | 1513.8 | 0.2 | 0.8 |
| 27263 | 1517.0 | 1516.9 | 1515.9 | -0.1 | -1.1 |
| 28104 | 1525.0 | 1524.9 | 1524.8 | -0.1 | -0.2 |
| 29025 | 1530.0 | 1530.1 | 1530.4 | 0.1 | 0.4 |
| 29945 | 1535.0 | 1535.0 | 1534.9 | 0.0 | -0.1 |
| 30361 | 1538.0 | 1538.2 | 1538.4 | 0.2 | 0.4 |

A comparison of the results of the existing and proposed conditions runs is shown in Table 9.5. The table shows that the difference in bed elevation at the peak of the hydrograph ranges from -0.3 to 5.2 ft with an average difference of 0.8 ft. The table also shows the difference in bed elevation at the end of the run ranges from -0.7 to 5.2 ft, with an average difference of 0.9 ft. Generally, these results suggest that the proposed condition will cause a slight (<1 ft) increase in aggradation in the study reach.

| Table 9-5 – Comparison of Existing and Proposed Conditions General Adjustment Bed Elevation | | | |
|---|---|---|---|
| SECTION | PROPOSED | EXISTING | DIFFERENCE |

| | INITIAL | PEAK | FINAL | INITIAL | PEAK | FINAL | INITIAL | PEAK | FINAL |
|---|---|---|---|---|---|---|---|---|---|
| 1000 | 1442.7 | 1442.7 | 1442.7 | 1442.7 | 1442.7 | 1442.7 | 0.0 | 0.0 | 0.0 |
| 1285 | 1442.6 | 1442.5 | 1442.2 | 1442.6 | 1442.5 | 1442.2 | 0.0 | 0.0 | 0.0 |
| 1677 | 1442.7 | 1442.8 | 1442.7 | 1442.7 | 1442.7 | 1442.8 | 0.0 | 0.0 | -0.1 |
| 2073 | 1444.2 | 1444.2 | 1444.2 | 1444.2 | 1444.2 | 1444.2 | 0.0 | 0.0 | 0.0 |
| 2298 | 1444.7 | 1444.7 | 1444.6 | 1444.7 | 1444.7 | 1444.7 | 0.0 | 0.0 | 0.0 |
| 2581 | 1445.2 | 1445.2 | 1445.1 | 1445.2 | 1445.2 | 1445.0 | 0.0 | 0.0 | 0.1 |
| 2961 | 1445.7 | 1445.7 | 1445.6 | 1445.7 | 1445.7 | 1445.6 | 0.0 | 0.0 | 0.0 |
| 3285 | 1442.7 | 1442.8 | 1442.9 | 1442.7 | 1442.7 | 1442.7 | 0.0 | 0.1 | 0.3 |
| 3671 | 1444.1 | 1444.1 | 1444.3 | 1444.1 | 1444.0 | 1444.0 | 0.0 | 0.1 | 0.3 |
| 3997 | 1445.0 | 1445.1 | 1445.2 | 1445.0 | 1441.6 | 1441.6 | 0.0 | 3.6 | 3.6 |
| 4328 | 1445.0 | 1445.1 | 1445.1 | 1445.0 | 1444.0 | 1444.0 | 0.0 | 1.1 | 1.1 |
| 4684 | 1446.0 | 1446.1 | 1446.2 | 1446.0 | 1445.0 | 1445.1 | 0.0 | 1.1 | 1.1 |
| 5184 | 1446.0 | 1446.1 | 1446.1 | 1446.0 | 1446.0 | 1446.0 | 0.0 | 0.1 | 0.2 |
| 5609 | 1447.0 | 1447.0 | 1447.2 | 1447.0 | 1446.0 | 1446.1 | 0.0 | 1.0 | 1.1 |
| 5941 | 1447.2 | 1447.1 | 1447.0 | 1447.2 | 1447.0 | 1447.1 | 0.0 | 0.1 | -0.1 |
| 6166 | 1447.4 | 1447.4 | 1447.5 | 1447.4 | 1447.0 | 1447.0 | 0.0 | 0.4 | 0.4 |
| 6711 | 1449.8 | 1449.8 | 1449.9 | 1449.8 | 1448.0 | 1448.0 | 0.0 | 1.8 | 1.9 |
| 7419 | 1451.0 | 1451.0 | 1450.7 | 1451.0 | 1446.7 | 1446.7 | 0.0 | 4.3 | 4.0 |
| 7758 | 1452.0 | 1452.0 | 1451.9 | 1452.0 | 1446.7 | 1447.0 | 0.0 | 5.2 | 5.0 |
| 8176 | 1452.0 | 1452.0 | 1452.0 | 1451.9 | 1451.0 | 1451.0 | 0.1 | 1.0 | 1.0 |
| 8867 | 1453.4 | 1453.4 | 1453.4 | 1453.4 | 1452.0 | 1452.0 | 0.0 | 1.4 | 1.4 |
| 9359 | 1454.5 | 1454.6 | 1454.6 | 1454.5 | 1454.0 | 1454.2 | 0.0 | 0.5 | 0.4 |
| 9717 | 1455.9 | 1455.9 | 1455.9 | 1455.8 | 1454.0 | 1454.0 | 0.1 | 1.9 | 1.9 |
| 10216 | 1456.8 | 1456.9 | 1456.9 | 1456.8 | 1456.7 | 1456.8 | 0.0 | 0.2 | 0.1 |
| 10609 | 1458.2 | 1458.2 | 1458.2 | 1458.2 | 1458.0 | 1458.1 | 0.0 | 0.2 | 0.1 |
| 11003 | 1459.4 | 1459.4 | 1459.4 | 1459.4 | 1459.3 | 1458.6 | 0.0 | 0.1 | 0.8 |
| 11396 | 1460.7 | 1460.7 | 1460.6 | 1460.7 | 1460.4 | 1459.7 | 0.0 | 0.2 | 0.9 |
| 11871 | 1462.6 | 1462.8 | 1462.9 | 1462.6 | 1462.3 | 1462.3 | 0.0 | 0.5 | 0.6 |
| 12317 | 1464.0 | 1463.0 | 1462.9 | 1464.0 | 1462.7 | 1462.7 | 0.0 | 0.3 | 0.2 |
| 12726 | 1465.0 | 1465.0 | 1465.0 | 1465.0 | 1462.7 | 1462.7 | 0.0 | 2.3 | 2.2 |
| 13200 | 1467.0 | 1467.1 | 1467.1 | 1467.0 | 1462.7 | 1462.7 | 0.0 | 4.4 | 4.4 |
| 13733 | 1468.7 | 1468.4 | 1468.3 | 1468.7 | 1466.7 | 1466.7 | 0.0 | 1.7 | 1.6 |
| 14335 | 1469.8 | 1469.9 | 1470.0 | 1469.8 | 1468.9 | 1468.9 | 0.0 | 0.9 | 1.0 |
| 14920 | 1471.8 | 1471.6 | 1471.4 | 1471.8 | 1470.8 | 1471.0 | 0.0 | 0.8 | 0.4 |
| 15347 | 1473.2 | 1473.2 | 1473.5 | 1473.2 | 1472.7 | 1471.0 | 0.0 | 0.5 | 2.5 |
| 15682 | 1475.0 | 1475.0 | 1475.1 | 1475.0 | 1474.5 | 1474.6 | 0.0 | 0.5 | 0.4 |
| 16028 | 1476.9 | 1477.1 | 1477.2 | 1476.9 | 1474.7 | 1474.7 | 0.0 | 2.3 | 2.4 |
| 16476 | 1478.4 | 1478.0 | 1477.7 | 1478.4 | 1478.0 | 1478.0 | 0.0 | 0.0 | -0.4 |
| 16913 | 1480.8 | 1480.9 | 1480.8 | 1480.8 | 1478.7 | 1478.7 | 0.0 | 2.2 | 2.1 |
| 17330 | 1483.0 | 1483.2 | 1483.1 | 1482.6 | 1478.8 | 1479.0 | 0.4 | 4.4 | 4.1 |
| 17768 | 1485.0 | 1484.6 | 1484.5 | 1485.0 | 1482.8 | 1483.2 | 0.0 | 1.8 | 1.3 |
| 18399 | 1486.0 | 1485.8 | 1485.3 | 1486.0 | 1485.7 | 1484.4 | 0.0 | 0.1 | 0.8 |
| 18929 | 1485.0 | 1485.1 | 1485.6 | 1485.0 | 1485.0 | 1485.2 | 0.0 | 0.0 | 0.3 |
| 19200 | 1487.7 | 1487.7 | 1487.8 | 1487.0 | 1486.7 | 1487.6 | 0.7 | 1.0 | 0.2 |
| 19813 | 1489.4 | 1489.4 | 1489.4 | 1489.4 | 1489.2 | 1488.2 | 0.0 | 0.2 | 1.2 |
| 20179 | 1490.7 | 1490.7 | 1490.8 | 1490.7 | 1491.0 | 1491.0 | 0.0 | -0.3 | -0.2 |
| 20654 | 1493.0 | 1493.0 | 1493.1 | 1493.0 | 1493.1 | 1493.0 | 0.0 | 0.0 | 0.2 |
| 20754 | 1493.4 | 1493.5 | 1493.4 | 1493.4 | 1493.2 | 1492.1 | 0.0 | 0.3 | 1.3 |

| Table 9-5 – Comparison of Existing and Proposed Conditions General Adjustment Bed Elevation | | | | | | | | | |
|---|---|---|---|---|---|---|---|---|---|
| SECTION | PROPOSED | | | EXISTING | | | DIFFERENCE | | |
| | INITIAL | PEAK | FINAL | INITIAL | PEAK | FINAL | INITIAL | PEAK | FINAL |
| 20853 | 1493.8 | 1493.8 | 1494.0 | 1493.8 | 1491.4 | 1492.2 | 0.0 | 2.4 | 1.8 |
| 20953 | 1494.2 | 1493.9 | 1493.5 | 1494.2 | 1493.8 | 1493.0 | 0.0 | 0.2 | 0.5 |
| 21459 | 1496.0 | 1496.2 | 1496.2 | 1496.0 | 1496.1 | 1496.0 | 0.0 | 0.1 | 0.1 |
| 21912 | 1497.5 | 1497.4 | 1497.1 | 1497.5 | 1497.2 | 1497.1 | 0.0 | 0.2 | 0.0 |
| 22448 | 1500.0 | 1499.8 | 1500.0 | 1500.0 | 1499.9 | 1499.5 | 0.0 | -0.1 | 0.5 |
| 22909 | 1502.0 | 1502.2 | 1502.3 | 1502.0 | 1502.2 | 1502.1 | 0.0 | 0.0 | 0.2 |
| 23406 | 1505.0 | 1505.0 | 1504.9 | 1505.0 | 1504.8 | 1504.8 | 0.0 | 0.2 | 0.1 |
| 23817 | 1506.0 | 1505.7 | 1505.3 | 1506.0 | 1505.7 | 1505.4 | 0.0 | 0.0 | -0.1 |
| 24190 | 1508.0 | 1508.1 | 1508.6 | 1508.0 | 1508.2 | 1508.4 | 0.0 | 0.0 | 0.2 |
| 24469 | 1510.0 | 1510.1 | 1510.2 | 1510.0 | 1508.2 | 1508.7 | 0.0 | 1.9 | 1.6 |
| 24895 | 1511.0 | 1510.8 | 1510.1 | 1511.0 | 1510.8 | 1510.7 | 0.0 | 0.0 | -0.7 |
| 25246 | 1512.0 | 1511.9 | 1511.6 | 1512.0 | 1511.8 | 1511.1 | 0.0 | 0.1 | 0.6 |
| 25846 | 1511.3 | 1511.3 | 1511.8 | 1511.0 | 1510.1 | 1510.8 | 0.3 | 1.2 | 1.0 |
| 26500 | 1513.0 | 1513.2 | 1513.8 | 1513.0 | 1513.2 | 1513.4 | 0.0 | 0.0 | 0.4 |
| 27263 | 1517.0 | 1516.9 | 1515.9 | 1517.0 | 1516.9 | 1516.6 | 0.0 | 0.1 | -0.7 |
| 28104 | 1525.0 | 1524.9 | 1524.8 | 1525.0 | 1525.0 | 1524.9 | 0.0 | 0.0 | -0.1 |
| 29025 | 1530.0 | 1530.1 | 1530.4 | 1530.0 | 1530.0 | 1530.0 | 0.0 | 0.1 | 0.4 |
| 29945 | 1535.0 | 1535.0 | 1534.9 | 1535.0 | 1534.9 | 1534.9 | 0.0 | 0.0 | 0.0 |
| 30361 | 1538.0 | 1538.2 | 1538.4 | 1538.0 | 1538.2 | 1538.3 | 0.0 | 0.0 | 0.1 |

## 9.7 Discussion of Differences in General Scour Results between Existing / Proposed Conditions

The primary influences that affect the sediment transport correspond to changes in sediment continuity balance which determines the change in bed elevation which is directly related to the changes in hydraulic characteristics. A comparison of the hydraulic characteristics for the peak flowrate (Q=57,250 cfs) using velocity and top-width as indicators with the change in streambed assists in evaluating if the general trends related to aggradation and degradation are reasonable and consistent with the floodplain hydraulics. The following table (Table 9-6) lists the hydraulic parameters and the amount of change for both the existing and proposed conditions which illustrates in a side-by-side comparison that the amount of bed variation of each condition and between existing/proposed conditions follows general expected changes. Examining locations where there are extreme shifts in velocity illustrates where there is an expansion or contraction so the sediment balance would make a corresponding change based on changes in the sediment transport capacity.

| **Table 9-6 –** The Hydraulic Parameters and the Amount of Change for Both the Existing and Proposed Conditions | | | | | | | |
|---|---|---|---|---|---|---|---|
| River Sta. / HEC-RAS Section | Q Total (cfs) | Vel. Chnl | | Top Width | | General Adjustment | |
| | | Prop. (ft/s) | Exist (ft/s) | Prop. (ft) | Exist (ft) | Prop. (ft) | Exist (ft) |
| 30361.69 | 57250 | 6.06 | 7.73 | 1717.92 | 1714.54 | 0.2 | 0.2 |

| **Table 9-6 –** The Hydraulic Parameters and the Amount of Change for Both the Existing and Proposed Conditions | | | | | | | |
|---|---|---|---|---|---|---|---|
| **River Sta. / HEC-RAS Section** | **Q Total (cfs)** | **Vel. Chnl** | | **Top Width** | | **General Adjustment** | |
| | | **Prop. (ft/s)** | **Exist (ft/s)** | **Prop. (ft)** | **Exist (ft)** | **Prop. (ft)** | **Exist (ft)** |
| 29945.89 | 57250 | 6.18 | 8.4 | 1619.19 | 1970.01 | 0.0 | -0.1 |
| 29025.39 | 57250 | 5.32 | 6.78 | 1642.74 | 1971.5 | 0.1 | 0.0 |
| 28104.69 | 57250 | 8.34 | 10.61 | 1305.27 | 1427.61 | -0.1 | 0.0 |
| 27263.37 | 57250 | 8.29 | 9.24 | 1077.2 | 1498.41 | -0.1 | -0.1 |
| 26500.53 | 57250 | 6.6 | 6.79 | 831.82 | 1521.52 | 0.2 | 0.2 |
| 25846.05 | 57250 | 9.28 | 7.76 | 688.76 | 2227.99 | 0.1 | -0.9 |
| 25246.64 | 57250 | 10.7 | 10.67 | 815.8 | 995.34 | -0.1 | -0.2 |
| 24895.09 | 57250 | 8.77 | 8.75 | 927.6 | 1170.54 | -0.2 | -0.2 |
| 24469.84 | 57250 | 9.49 | 10.14 | 837.04 | 943.05 | 0.1 | -1.8 |
| 24190.24 | 57250 | 9.94 | 9.56 | 747.33 | 914.46 | 0.1 | 0.2 |
| 23817.09 | 57250 | 11.65 | 11.04 | 790.26 | 811.65 | -0.3 | -0.3 |
| 23406.44 | 57250 | 10.92 | 12.93 | 1027.85 | 1064.78 | 0.0 | -0.2 |
| 22909.46 | 57250 | 8.37 | 6.02 | 1280.17 | 1905.16 | 0.2 | 0.2 |
| 22448.18 | 57250 | 12.62 | 9.44 | 1338.92 | 2621.31 | -0.2 | -0.1 |
| 21912.02 | 57250 | 10.93 | 7.73 | 1336.99 | 2622.68 | -0.1 | -0.3 |
| 21459.26 | 57250 | 9.91 | 6.71 | 1221.47 | 3046.33 | 0.2 | 0.1 |
| 20953.16 | 57250 | 9.59 | 4.94 | 625.56 | 3485.58 | -0.2 | -0.4 |
| 20853.6* | 57250 | 8.77 | 4.21 | 688.73 | 4123.08 | 0.1 | -2.4 |
| 20802.68 | Bridge | | | | | | |
| 20754.2* | 57250 | 9.86 | 12.48 | 749 | 2399.57 | 0.1 | -0.2 |
| 20654.72 | 57250 | 10.3 | 11.25 | 811.44 | 2364.72 | 0.0 | 0.1 |
| 20179.46 | 57250 | 13.4 | 11.2 | 1043.08 | 2053.97 | 0.0 | 0.3 |
| 19813.26 | 57250 | 13.31 | 11.59 | 1128.94 | 2624.15 | 0.0 | -0.2 |
| 19200.76 | 57250 | 8.36 | 6.02 | 1251.09 | 2745.91 | 0.0 | -0.3 |
| 18929.32 | 57250 | 4.72 | 6.54 | 1193.8 | 3537.47 | 0.1 | 0.0 |
| 18399.16 | 57250 | 5.36 | 8.58 | 1205.68 | 4587.94 | -0.2 | -0.3 |
| 17768.32 | 57250 | 5.96 | 7.11 | 1209.36 | 4214.25 | -0.4 | -2.2 |
| 17330.97 | 57250 | 5.56 | 3 | 1211.89 | 6354.63 | 0.2 | -3.8 |
| 16913.42 | 57250 | 5.18 | 6.78 | 1205.58 | 6949.53 | 0.0 | -2.1 |
| 16476.12 | 57250 | 6.7 | 2.27 | 1202.58 | 5797.97 | -0.3 | -0.3 |
| 16028.82 | 57250 | 5.17 | 4.89 | 1196.31 | 6285.66 | 0.1 | -2.2 |
| 15682.82 | 57250 | 4.65 | 1.53 | 1187.48 | 5510.44 | 0.0 | -0.5 |
| 15347.98 | 57250 | 4.12 | 1.35 | 1189.37 | 6460.32 | 0.0 | -0.5 |
| 14920.48 | 57250 | 4.82 | 0.57 | 1188.77 | 5839.47 | -0.2 | -1.0 |

**Table 9-6 –** The Hydraulic Parameters and the Amount of Change for Both the Existing and Proposed Conditions

| River Sta. / HEC-RAS Section | Q Total (cfs) | Vel. Chnl | | Top Width | | General Adjustment | |
|---|---|---|---|---|---|---|---|
| | | Prop. (ft/s) | Exist (ft/s) | Prop. (ft) | Exist (ft) | Prop. (ft) | Exist (ft) |
| 14335.42 | 57250 | 4.77 | 1.75 | 1200.98 | 6619.33 | 0.1 | -0.9 |
| 13733.7 | 57250 | 5.85 | 0.92 | 1215.85 | 5402.46 | -0.3 | -2.0 |
| 13200.36 | 57250 | 6.46 | 2.82 | 1182.31 | 7096.03 | 0.1 | -4.3 |
| 12726.18 | 57250 | 6.33 | 2.82 | 1160.75 | 7146.33 | 0.0 | -2.3 |
| 12317.58 | 57250 | 7.85 | 2.75 | 1174.95 | 6935.44 | -1.0 | -1.3 |
| 11871.18 | 57250 | 7.57 | 2 | 1163.03 | 7237.85 | 0.3 | -0.3 |
| 11396.58 | 57250 | 7.21 | 3.61 | 1188.34 | 7125.82 | 0.0 | -0.2 |
| 11003.2* | 57250 | 6.67 | 3.4 | 1185.58 | 7163.68 | 0.0 | -0.1 |
| 10687.71 | Bridge | | | | | | |
| 10609.8* | 57250 | 6.82 | 5.07 | 1194.44 | 6438.26 | 0.0 | -0.2 |
| 10216.47 | 57250 | 2.96 | 4.29 | 1189.82 | 5752.65 | 0.0 | -0.1 |
| 9716.61 | 57250 | 2.97 | 4.1 | 1274.49 | 7140.59 | 0.0 | -1.8 |
| 9359.16 | 57250 | 2.6 | 5.17 | 1287.93 | 8529.61 | 0.1 | -0.5 |
| 8867.34 | 57250 | 2.24 | 4.19 | 1328.68 | 7002.57 | 0.0 | -1.4 |
| 8175.9 | 57250 | 2.49 | 2.98 | 1358.01 | 8959.4 | 0.0 | -0.9 |
| 7758.4 | 57250 | 2.96 | 4.23 | 1300.99 | 9173.26 | 0.0 | -5.3 |
| 7418.76 | 57250 | 3.67 | 3.96 | 1284.19 | 10251.34 | 0.0 | -4.3 |
| 6710.68 | 57250 | 2.51 | 5.2 | 3129.08 | 5826.56 | 0.0 | -1.8 |
| 6166.06 | 57250 | 2.24 | 3.73 | 2925.72 | 9358.29 | 0.0 | -0.4 |
| 5941.03 | 57250 | 1.68 | 3 | 2782.69 | 8069.71 | -0.1 | -0.2 |
| 5609.07 | 57250 | 1.99 | 3.73 | 2872.02 | 9095.55 | 0.0 | -1.0 |
| 5183.62 | 57250 | 4.14 | 4.18 | 2901.13 | 8694.13 | 0.1 | 0.0 |
| 4684.24 | 57250 | 3.3 | 2.89 | 3765.91 | 6641.47 | 0.1 | -1.0 |
| 4327.64 | 57250 | 2.99 | 2.58 | 4173.5 | 6628.59 | 0.1 | -1.0 |
| 3997.36 | 57250 | 2.64 | 1.38 | 4328.42 | 7089.94 | 0.1 | -3.4 |
| 3670.6 | 57250 | 2.4 | 2.19 | 6808.08 | 6706.78 | 0.1 | 0.0 |
| 3284.55 | 57250 | 1.54 | 1.57 | 6077.32 | 6058.82 | 0.1 | 0.0 |
| 2960.91 | 57250 | 3.07 | 2.82 | 6036.85 | 6037.06 | 0.0 | 0.0 |
| 2580.91 | 57250 | 2.9 | 2.93 | 5724.41 | 5725.74 | 0.0 | 0.0 |
| 2298.35 | 57250 | 2.63 | 2.63 | 5743.78 | 5743.78 | 0.0 | 0.0 |
| 2072.69 | 57250 | 2.34 | 2.34 | 5727.41 | 5727.41 | 0.0 | 0.0 |
| 1677.04 | 57250 | 2.59 | 2.59 | 5526.72 | 5526.68 | 0.1 | 0.0 |
| 1284.64 | 57250 | 2.92 | 2.92 | 3985.09 | 3985.01 | -0.1 | -0.1 |
| 1000 | 57250 | 3.35 | 3.35 | 4258.75 | 4258.75 | 0.0 | 0.0 |

In addition, a comparison of the results of the associated with the "General" adjustment from a single 100-year storm event was compared to the results from the "Long-term" adjustment simulation in order to evaluate if the same general trends related to scour and deposition were occurring. This is illustrated in the following graph that shows that the same trends are occurring, but the amount of change in magnified or increased in the long-term simulation compared to the single storm event. The locations were the greatest amount of scour are occurring are in the locations of the narrowed or contracted section while the largest depositional areas are occurring in the widened areas of the floodplain without the levee, generally upstream or downstream of the proposed project improvements.

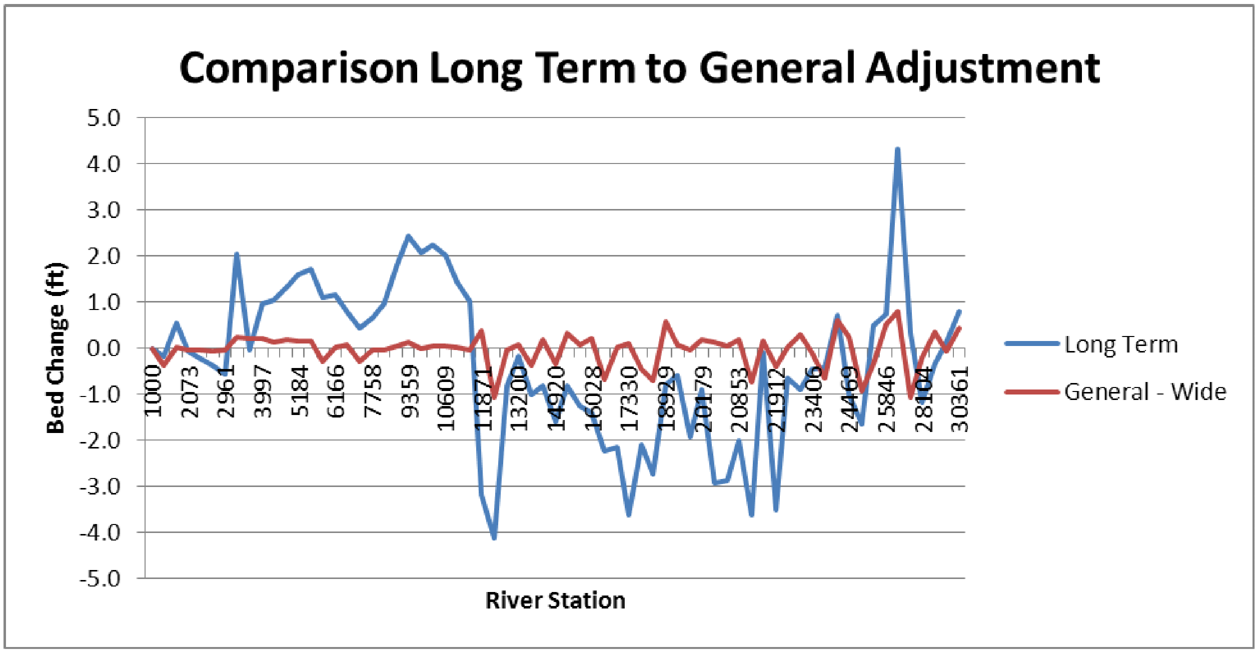


**Figure 9-7 –** Comparison of the "general" single event 100-year thalweg adjustment computed in HEC-6T to the same "long term" model scenario, illustrating that generally there are the same trends regarding locations of aggradation or degradation.

## 9.8 HEC-6 Parameter Sensitivity Analysis

Sensitivity analyses, included in the Appendix, examine the model's bed response with respect to (1) variation in transport function, (2) inflowing sediment load, (3) a combination of inflowing load and sediment transport function, and (4) a "warm-up" discharge. For the sediment transport function analysis the proposed condition model was rerun using the Yang and Ackers-White equations. For the inflowing sediment load analysis the inflowing load is increased and decreased by 50 percent and the proposed condition model is rerun. For the combined transport equation and load sensitivity analysis the Yang equation was run with an inflowing load specific to that transport equation. The final sensitivity analysis, to examine the change in bed response to an initial discharge prior to the main hydrograph, was run. In some instances an initial, small discharge will bring the model into equilibrium with respect to sediment gradation in the bed, the inflowing sediment load, and the channel hydraulics. For this analysis a discharge of Q=7500 cfs was run for three hours prior to the general adjustment hydrograph.

Table 9.7 shows the differences in bed elevation resulting from different sediment transport equations. The differences for both the Yang and Ackers-White equations ranges from -2.1 to 1.2 ft, with an average change of -0.1 ft. The Yang equation shows slightly more aggradation than Ackers-White based on the difference between the peaks.

Table 9.8 shows the differences in bed elevation resulting from different sediment inflowing load. The differences for both the 50% change ranges from -1.0 to 0.8 ft, with an average change of 0.0 ft. The average change value suggests that the study reach as a whole is stable relative to inflowing load.

| **Table 9-7 –** Sensitivity Analysis for General Adjustment Sediment Transport Equation on Bed Elevation: TOFFALETI (T), YANG (Y) AND ACKERS-WHITE (AW) | | | | | | | | | | |
|---|---|---|---|---|---|---|---|---|---|---|
| **SECTION** | **PEAK-T** | **FINAL-T** | **PEAK-Y** | **FINAL-Y** | **PEAK-AW** | **FINAL-AW** | **ΔPEAK-TY** | **ΔFINAL-TY** | **ΔPEAK-TAW** | **ΔFINAL-TAW** |
| 1000 | 1442.7 | 1442.7 | 1442.7 | 1442.7 | 1442.7 | 1442.7 | 0.0 | 0.0 | 0.0 | 0.0 |
| 1285 | 1442.5 | 1442.2 | 1442.4 | 1442.3 | 1442.4 | 1442.3 | -0.2 | 0.1 | -0.1 | 0.1 |
| 1677 | 1442.8 | 1442.7 | 1442.8 | 1443.0 | 1442.8 | 1442.9 | 0.0 | 0.2 | 0.0 | 0.2 |
| 2073 | 1444.2 | 1444.2 | 1444.2 | 1444.2 | 1444.2 | 1444.2 | 0.0 | 0.0 | 0.0 | 0.0 |
| 2298 | 1444.7 | 1444.6 | 1444.6 | 1444.5 | 1444.6 | 1444.5 | 0.0 | -0.1 | 0.0 | -0.2 |
| 2581 | 1445.2 | 1445.1 | 1445.1 | 1444.9 | 1445.1 | 1444.9 | -0.1 | -0.2 | 0.0 | -0.3 |
| 2961 | 1445.7 | 1445.6 | 1445.6 | 1445.3 | 1445.6 | 1445.5 | -0.1 | -0.3 | -0.1 | -0.2 |
| 3285 | 1442.8 | 1442.9 | 1442.8 | 1443.1 | 1442.8 | 1443.0 | 0.0 | 0.2 | 0.1 | 0.0 |
| 3671 | 1444.1 | 1444.3 | 1444.2 | 1444.4 | 1444.2 | 1444.4 | 0.1 | 0.1 | 0.1 | 0.2 |
| 3997 | 1445.1 | 1445.2 | 1445.2 | 1445.4 | 1445.1 | 1445.3 | 0.0 | 0.2 | 0.0 | 0.1 |
| 4328 | 1445.1 | 1445.1 | 1445.2 | 1445.5 | 1445.1 | 1445.4 | 0.1 | 0.3 | 0.0 | 0.3 |
| 4684 | 1446.1 | 1446.2 | 1446.3 | 1446.7 | 1446.2 | 1446.6 | 0.2 | 0.5 | 0.1 | 0.4 |
| 5184 | 1446.1 | 1446.1 | 1446.4 | 1446.9 | 1446.3 | 1446.6 | 0.4 | 0.7 | 0.2 | 0.5 |
| 5609 | 1447.0 | 1447.2 | 1447.6 | 1448.0 | 1447.4 | 1447.7 | 0.6 | 0.8 | 0.4 | 0.5 |
| 5941 | 1447.1 | 1447.0 | 1447.3 | 1447.5 | 1447.1 | 1447.3 | 0.2 | 0.5 | 0.0 | 0.4 |
| 6166 | 1447.4 | 1447.5 | 1447.6 | 1447.7 | 1447.4 | 1447.6 | 0.2 | 0.3 | 0.0 | 0.1 |
| 6711 | 1449.8 | 1449.9 | 1449.6 | 1449.6 | 1449.8 | 1449.5 | -0.2 | -0.3 | 0.0 | -0.4 |
| 7419 | 1451.0 | 1450.7 | 1450.4 | 1450.2 | 1450.4 | 1450.4 | -0.6 | -0.5 | -0.6 | -0.3 |
| 7758 | 1452.0 | 1451.9 | 1451.8 | 1451.6 | 1451.9 | 1451.7 | -0.2 | -0.3 | -0.1 | -0.2 |
| 8176 | 1452.0 | 1452.0 | 1452.0 | 1451.9 | 1452.0 | 1451.9 | 0.0 | 0.0 | 0.0 | 0.0 |
| 8867 | 1453.4 | 1453.4 | 1453.6 | 1453.7 | 1453.6 | 1453.7 | 0.1 | 0.3 | 0.1 | 0.2 |
| 9359 | 1454.6 | 1454.6 | 1454.9 | 1455.2 | 1454.8 | 1454.9 | 0.3 | 0.5 | 0.2 | 0.3 |
| 9717 | 1455.9 | 1455.9 | 1456.0 | 1456.3 | 1456.1 | 1456.1 | 0.1 | 0.4 | 0.2 | 0.2 |
| 10216 | 1456.9 | 1456.9 | 1457.1 | 1457.6 | 1457.2 | 1457.3 | 0.3 | 0.7 | 0.3 | 0.4 |
| 10609 | 1458.2 | 1458.2 | 1458.9 | 1459.1 | 1458.8 | 1458.6 | 0.7 | 0.9 | 0.6 | 0.4 |
| 11003 | 1459.4 | 1459.4 | 1459.8 | 1460.0 | 1459.7 | 1459.6 | 0.4 | 0.5 | 0.3 | 0.2 |
| 11396 | 1460.7 | 1460.6 | 1460.8 | 1460.8 | 1460.8 | 1460.7 | 0.2 | 0.2 | 0.1 | 0.1 |
| 11871 | 1462.8 | 1462.9 | 1462.6 | 1462.7 | 1462.6 | 1461.8 | -0.2 | -0.2 | -0.3 | -1.2 |
| 12317 | 1463.0 | 1462.9 | 1462.6 | 1462.7 | 1462.5 | 1461.8 | -0.4 | -0.2 | -0.5 | -1.1 |
| 12726 | 1465.0 | 1465.0 | 1464.8 | 1464.9 | 1465.0 | 1465.0 | -0.2 | 0.0 | 0.0 | 0.0 |
| 13200 | 1467.1 | 1467.1 | 1467.5 | 1467.5 | 1467.5 | 1467.2 | 0.5 | 0.4 | 0.4 | 0.1 |
| 13733 | 1468.4 | 1468.3 | 1468.2 | 1468.4 | 1467.7 | 1467.6 | -0.2 | 0.1 | -0.8 | -0.7 |
| 14335 | 1469.9 | 1470.0 | 1469.9 | 1470.0 | 1470.0 | 1469.4 | 0.1 | 0.0 | 0.1 | -0.6 |
| 14920 | 1471.6 | 1471.4 | 1471.6 | 1471.8 | 1471.4 | 1471.5 | 0.1 | 0.4 | -0.2 | 0.1 |
| 15347 | 1473.2 | 1473.5 | 1473.5 | 1473.9 | 1473.5 | 1473.5 | 0.3 | 0.4 | 0.3 | 0.0 |
| 15682 | 1475.0 | 1475.1 | 1475.5 | 1475.4 | 1475.2 | 1475.0 | 0.5 | 0.3 | 0.2 | 0.0 |
| 16028 | 1477.1 | 1477.2 | 1477.3 | 1477.3 | 1477.1 | 1477.0 | 0.2 | 0.2 | 0.0 | -0.1 |

| **Table 9-7 –** Sensitivity Analysis for General Adjustment Sediment Transport Equation on Bed Elevation: TOFFALETI (T), YANG (Y) AND ACKERS-WHITE (AW) | | | | | | | | | | |
|---|---|---|---|---|---|---|---|---|---|---|
| **SECTION** | **PEAK-T** | **FINAL-T** | **PEAK-Y** | **FINAL-Y** | **PEAK-AW** | **FINAL-AW** | **ΔPEAK-TY** | **ΔFINAL-TY** | **ΔPEAK-TAW** | **ΔFINAL-TAW** |
| 16476 | 1478.0 | 1477.7 | 1478.4 | 1478.3 | 1478.1 | 1478.1 | 0.4 | 0.6 | 0.1 | 0.4 |
| 16913 | 1480.9 | 1480.8 | 1481.2 | 1480.8 | 1480.9 | 1480.8 | 0.3 | 0.0 | 0.0 | 0.0 |
| 17330 | 1483.2 | 1483.1 | 1483.0 | 1482.6 | 1482.6 | 1482.0 | -0.3 | -0.5 | -0.6 | -1.1 |
| 17768 | 1484.6 | 1484.5 | 1483.4 | 1483.2 | 1483.6 | 1482.9 | -1.2 | -1.3 | -1.0 | -1.7 |
| 18399 | 1485.8 | 1485.3 | 1484.0 | 1483.4 | 1484.6 | 1483.7 | -1.8 | -1.9 | -1.2 | -1.5 |
| 18929 | 1485.1 | 1485.6 | 1484.8 | 1485.8 | 1485.2 | 1486.4 | -0.2 | 0.2 | 0.1 | 0.9 |
| 19200 | 1487.7 | 1487.8 | 1488.9 | 1487.7 | 1488.5 | 1488.1 | 1.2 | -0.1 | 0.8 | 0.3 |
| 19813 | 1489.4 | 1489.4 | 1489.5 | 1489.1 | 1489.4 | 1489.1 | 0.2 | -0.3 | 0.0 | -0.2 |
| 20179 | 1490.7 | 1490.8 | 1490.7 | 1490.9 | 1491.1 | 1490.8 | 0.0 | 0.1 | 0.4 | 0.0 |
| 20654 | 1493.0 | 1493.1 | 1492.8 | 1492.2 | 1492.5 | 1491.0 | -0.2 | -0.9 | -0.6 | -2.1 |
| 20754 | 1493.5 | 1493.4 | 1493.2 | 1492.8 | 1493.0 | 1492.2 | -0.3 | -0.6 | -0.5 | -1.2 |
| 20853 | 1493.8 | 1494.0 | 1492.9 | 1493.1 | 1493.2 | 1492.4 | -0.9 | -0.8 | -0.7 | -1.6 |
| 20953 | 1493.9 | 1493.5 | 1493.2 | 1493.6 | 1492.1 | 1492.8 | -0.8 | 0.1 | -1.9 | -0.7 |
| 21459 | 1496.2 | 1496.2 | 1495.8 | 1495.1 | 1495.9 | 1495.2 | -0.3 | -1.0 | -0.3 | -1.0 |
| 21912 | 1497.4 | 1497.1 | 1497.2 | 1496.9 | 1496.6 | 1496.7 | -0.2 | -0.3 | -0.9 | -0.4 |
| 22448 | 1499.8 | 1500.0 | 1500.0 | 1499.5 | 1500.0 | 1498.9 | 0.2 | -0.6 | 0.2 | -1.1 |
| 22909 | 1502.2 | 1502.3 | 1502.2 | 1501.9 | 1502.0 | 1501.8 | 0.1 | -0.4 | -0.2 | -0.5 |
| 23406 | 1505.0 | 1504.9 | 1504.6 | 1504.7 | 1505.0 | 1505.0 | -0.4 | -0.2 | 0.1 | 0.1 |
| 23817 | 1505.7 | 1505.3 | 1505.5 | 1505.7 | 1505.0 | 1505.2 | -0.2 | 0.4 | -0.7 | -0.1 |
| 24190 | 1508.1 | 1508.6 | 1507.4 | 1507.8 | 1508.2 | 1508.3 | -0.8 | -0.8 | 0.1 | -0.3 |
| 24469 | 1510.1 | 1510.2 | 1509.8 | 1509.5 | 1510.1 | 1510.0 | -0.4 | -0.8 | 0.0 | -0.3 |
| 24895 | 1510.8 | 1510.1 | 1510.8 | 1510.3 | 1510.5 | 1510.4 | 0.0 | 0.2 | -0.3 | 0.3 |
| 25246 | 1511.9 | 1511.6 | 1511.2 | 1511.4 | 1511.3 | 1511.3 | -0.7 | -0.3 | -0.6 | -0.3 |
| 25846 | 1511.3 | 1511.8 | 1512.1 | 1512.8 | 1511.5 | 1511.8 | 0.7 | 1.0 | 0.1 | 0.0 |
| 26500 | 1513.2 | 1513.8 | 1514.4 | 1514.5 | 1513.7 | 1513.6 | 1.1 | 0.7 | 0.5 | -0.2 |
| 27263 | 1516.9 | 1515.9 | 1516.5 | 1516.5 | 1515.8 | 1515.5 | -0.4 | 0.6 | -1.1 | -0.4 |
| 28104 | 1524.9 | 1524.8 | 1524.4 | 1523.5 | 1525.0 | 1524.9 | -0.6 | -1.2 | 0.0 | 0.2 |
| 29025 | 1530.1 | 1530.4 | 1529.9 | 1529.4 | 1530.0 | 1530.1 | -0.2 | -1.0 | -0.1 | -0.3 |
| 29945 | 1535.0 | 1534.9 | 1534.5 | 1533.5 | 1535.0 | 1535.0 | -0.4 | -1.4 | 0.0 | 0.1 |
| 30361 | 1538.2 | 1538.4 | 1537.3 | 1537.3 | 1538.0 | 1538.2 | -0.9 | -1.1 | -0.2 | -0.2 |

| Table 9-8 – Sensitivity Analysis for General Adjustment Inflowing Sediment Load on Bed Elevation | | | | | | | | | | |
|---|---|---|---|---|---|---|---|---|---|---|
| **SECTION** | **PEAK** | **FINAL** | **PEAK+ 50%** | **FINAL+ 50%** | **PEAK- 50%** | **FINAL- 50%** | **ΔPEAK+ 50 (ft)** | **ΔFINAL+ 50 (ft)** | **ΔPEAK- 50 (ft)** | **ΔFINAL -50 (ft)** |
| 1000 | 1442.7 | 1442.7 | 1442.7 | 1442.7 | 1442.7 | 1442.7 | 0.0 | 0.0 | 0.0 | 0.0 |
| 1285 | 1442.5 | 1442.2 | 1442.5 | 1442.2 | 1442.5 | 1442.2 | 0.0 | 0.0 | 0.0 | 0.0 |
| 1677 | 1442.8 | 1442.7 | 1442.8 | 1442.7 | 1442.8 | 1442.7 | 0.0 | 0.0 | 0.0 | 0.0 |
| 2073 | 1444.2 | 1444.2 | 1444.2 | 1444.2 | 1444.2 | 1444.2 | 0.0 | 0.0 | 0.0 | 0.0 |
| 2298 | 1444.7 | 1444.6 | 1444.7 | 1444.6 | 1444.7 | 1444.6 | 0.0 | 0.0 | 0.0 | 0.0 |
| 2581 | 1445.2 | 1445.1 | 1445.2 | 1445.1 | 1445.2 | 1445.1 | 0.0 | 0.0 | 0.0 | 0.0 |
| 2961 | 1445.7 | 1445.6 | 1445.7 | 1445.6 | 1445.7 | 1445.6 | 0.0 | 0.0 | 0.0 | 0.0 |
| 3285 | 1442.8 | 1442.9 | 1442.8 | 1442.9 | 1442.8 | 1442.9 | 0.0 | 0.0 | 0.0 | 0.0 |
| 3671 | 1444.1 | 1444.3 | 1444.1 | 1444.3 | 1444.1 | 1444.3 | 0.0 | 0.0 | 0.0 | 0.0 |
| 3997 | 1445.1 | 1445.2 | 1445.1 | 1445.2 | 1445.1 | 1445.2 | 0.0 | 0.0 | 0.0 | 0.0 |
| 4328 | 1445.1 | 1445.1 | 1445.1 | 1445.1 | 1445.1 | 1445.1 | 0.0 | 0.0 | 0.0 | 0.0 |
| 4684 | 1446.1 | 1446.2 | 1446.1 | 1446.2 | 1446.1 | 1446.2 | 0.0 | 0.0 | 0.0 | 0.0 |
| 5184 | 1446.1 | 1446.1 | 1446.1 | 1446.2 | 1446.1 | 1446.2 | 0.0 | 0.0 | 0.0 | 0.0 |
| 5609 | 1447.0 | 1447.2 | 1447.0 | 1447.2 | 1447.0 | 1447.2 | 0.0 | 0.1 | 0.0 | 0.0 |
| 5941 | 1447.1 | 1447.0 | 1447.1 | 1446.8 | 1447.1 | 1447.0 | 0.0 | -0.2 | 0.0 | 0.0 |
| 6166 | 1447.4 | 1447.5 | 1447.4 | 1447.4 | 1447.4 | 1447.7 | 0.0 | 0.0 | 0.0 | 0.2 |
| 6711 | 1449.8 | 1449.9 | 1449.8 | 1449.9 | 1449.8 | 1449.8 | 0.0 | 0.0 | 0.0 | -0.1 |
| 7419 | 1451.0 | 1450.7 | 1451.0 | 1450.7 | 1451.0 | 1450.8 | 0.0 | 0.0 | 0.0 | 0.1 |
| 7758 | 1452.0 | 1451.9 | 1452.0 | 1451.9 | 1452.0 | 1451.7 | 0.0 | 0.0 | 0.0 | -0.3 |
| 8176 | 1452.0 | 1452.0 | 1452.0 | 1452.0 | 1452.0 | 1452.0 | 0.0 | 0.0 | 0.0 | 0.0 |
| 8867 | 1453.4 | 1453.4 | 1453.4 | 1453.4 | 1453.4 | 1453.5 | 0.0 | 0.0 | 0.0 | 0.0 |
| 9359 | 1454.6 | 1454.6 | 1454.5 | 1454.6 | 1454.6 | 1454.6 | 0.0 | 0.0 | 0.0 | 0.0 |
| 9717 | 1455.9 | 1455.9 | 1455.9 | 1455.9 | 1455.9 | 1455.9 | 0.0 | 0.0 | 0.0 | 0.0 |
| 10216 | 1456.9 | 1456.9 | 1456.9 | 1456.9 | 1456.9 | 1456.9 | 0.0 | 0.0 | 0.0 | 0.0 |
| 10609 | 1458.2 | 1458.2 | 1458.2 | 1458.2 | 1458.2 | 1458.2 | 0.0 | 0.0 | 0.0 | 0.0 |
| 11003 | 1459.4 | 1459.4 | 1459.4 | 1459.4 | 1459.4 | 1459.4 | 0.0 | 0.0 | 0.0 | 0.0 |
| 11396 | 1460.7 | 1460.6 | 1460.7 | 1460.6 | 1460.7 | 1460.6 | 0.0 | 0.0 | 0.0 | 0.0 |
| 11871 | 1462.8 | 1462.9 | 1462.8 | 1462.9 | 1462.8 | 1462.9 | 0.0 | 0.0 | 0.0 | 0.0 |
| 12317 | 1463.0 | 1462.9 | 1463.0 | 1462.9 | 1463.0 | 1462.9 | 0.0 | 0.0 | 0.0 | 0.0 |
| 12726 | 1465.0 | 1465.0 | 1465.0 | 1464.9 | 1465.0 | 1465.0 | 0.0 | 0.0 | 0.0 | 0.0 |
| 13200 | 1467.1 | 1467.1 | 1467.1 | 1467.0 | 1467.1 | 1467.1 | 0.0 | 0.0 | 0.0 | 0.0 |
| 13733 | 1468.4 | 1468.3 | 1468.5 | 1468.4 | 1468.4 | 1468.3 | 0.1 | 0.1 | 0.0 | 0.0 |
| 14335 | 1469.9 | 1470.0 | 1469.9 | 1470.0 | 1469.9 | 1470.0 | 0.0 | 0.0 | 0.0 | 0.0 |
| 14920 | 1471.6 | 1471.4 | 1471.6 | 1471.4 | 1471.6 | 1471.4 | 0.0 | 0.0 | 0.0 | 0.0 |
| 15347 | 1473.2 | 1473.5 | 1473.2 | 1473.5 | 1473.2 | 1473.5 | 0.0 | 0.0 | 0.0 | 0.0 |
| 15682 | 1475.0 | 1475.1 | 1475.0 | 1475.1 | 1475.0 | 1475.1 | 0.0 | 0.0 | 0.0 | 0.0 |
| 16028 | 1477.1 | 1477.2 | 1477.1 | 1477.2 | 1477.1 | 1477.2 | 0.0 | 0.0 | 0.0 | 0.0 |
| 16476 | 1478.0 | 1477.7 | 1478.0 | 1477.6 | 1478.0 | 1477.6 | 0.0 | -0.1 | 0.0 | 0.0 |
| 16913 | 1480.9 | 1480.8 | 1480.9 | 1480.9 | 1480.9 | 1480.8 | 0.0 | 0.0 | 0.0 | 0.0 |
| 17330 | 1483.2 | 1483.1 | 1483.2 | 1483.1 | 1483.2 | 1483.1 | 0.0 | 0.0 | 0.0 | 0.0 |

| Table 9-8 – Sensitivity Analysis for General Adjustment Inflowing Sediment Load on Bed Elevation | | | | | | | | | | |
|---|---|---|---|---|---|---|---|---|---|---|
| **SECTION** | **PEAK** | **FINAL** | **PEAK+ 50%** | **FINAL+ 50%** | **PEAK- 50%** | **FINAL- 50%** | **ΔPEAK+ 50 (ft)** | **ΔFINAL+ 50 (ft)** | **ΔPEAK- 50 (ft)** | **ΔFINAL -50 (ft)** |
| 17768 | 1484.6 | 1484.5 | 1484.6 | 1484.5 | 1484.6 | 1484.6 | 0.0 | 0.0 | 0.0 | 0.0 |
| 18399 | 1485.8 | 1485.3 | 1485.8 | 1485.2 | 1485.8 | 1485.3 | 0.0 | -0.1 | 0.0 | 0.0 |
| 18929 | 1485.1 | 1485.6 | 1485.1 | 1485.6 | 1485.1 | 1485.6 | 0.0 | 0.0 | 0.0 | 0.0 |
| 19200 | 1487.7 | 1487.8 | 1487.7 | 1487.8 | 1487.7 | 1487.7 | 0.0 | 0.0 | 0.0 | 0.0 |
| 19813 | 1489.4 | 1489.4 | 1489.4 | 1489.4 | 1489.4 | 1489.4 | 0.0 | 0.0 | 0.0 | 0.0 |
| 20179 | 1490.7 | 1490.8 | 1490.7 | 1490.9 | 1490.7 | 1490.8 | 0.0 | 0.0 | 0.0 | 0.0 |
| 20654 | 1493.0 | 1493.1 | 1493.0 | 1493.1 | 1493.1 | 1493.1 | 0.0 | 0.0 | 0.0 | 0.0 |
| 20754 | 1493.5 | 1493.4 | 1493.5 | 1493.5 | 1493.5 | 1493.4 | 0.0 | 0.0 | 0.0 | 0.0 |
| 20853 | 1493.8 | 1494.0 | 1493.8 | 1493.9 | 1493.9 | 1493.9 | 0.0 | 0.0 | 0.0 | -0.1 |
| 20953 | 1493.9 | 1493.5 | 1494.0 | 1493.6 | 1493.9 | 1493.6 | 0.0 | 0.1 | 0.0 | 0.1 |
| 21459 | 1496.2 | 1496.2 | 1496.2 | 1496.1 | 1496.2 | 1496.2 | 0.0 | -0.1 | 0.0 | 0.0 |
| 21912 | 1497.4 | 1497.1 | 1497.4 | 1497.9 | 1497.5 | 1497.2 | 0.0 | 0.8 | 0.0 | 0.0 |
| 22448 | 1499.8 | 1500.0 | 1499.8 | 1499.5 | 1499.8 | 1500.0 | 0.0 | -0.5 | 0.0 | -0.1 |
| 22909 | 1502.2 | 1502.3 | 1502.1 | 1502.1 | 1502.2 | 1502.1 | 0.0 | -0.2 | 0.0 | -0.2 |
| 23406 | 1505.0 | 1504.9 | 1505.0 | 1504.9 | 1505.0 | 1505.4 | 0.0 | 0.0 | 0.0 | 0.5 |
| 23817 | 1505.7 | 1505.3 | 1505.8 | 1505.2 | 1505.7 | 1505.4 | 0.0 | -0.1 | 0.0 | 0.1 |
| 24190 | 1508.1 | 1508.6 | 1508.1 | 1508.5 | 1508.2 | 1508.6 | 0.0 | -0.1 | 0.0 | 0.0 |
| 24469 | 1510.1 | 1510.2 | 1510.1 | 1510.2 | 1510.1 | 1510.2 | 0.0 | 0.0 | 0.0 | 0.0 |
| 24895 | 1510.8 | 1510.1 | 1510.8 | 1510.0 | 1510.8 | 1510.2 | 0.0 | -0.1 | 0.0 | 0.1 |
| 25246 | 1511.9 | 1511.6 | 1511.9 | 1511.8 | 1511.9 | 1511.6 | 0.0 | 0.2 | 0.0 | -0.1 |
| 25846 | 1511.3 | 1511.8 | 1511.3 | 1511.7 | 1511.4 | 1511.7 | 0.0 | -0.1 | 0.0 | -0.1 |
| 26500 | 1513.2 | 1513.8 | 1513.2 | 1513.7 | 1513.3 | 1513.8 | 0.0 | -0.1 | 0.0 | 0.0 |
| 27263 | 1516.9 | 1515.9 | 1517.0 | 1516.4 | 1516.9 | 1516.1 | 0.0 | 0.5 | 0.0 | 0.1 |
| 28104 | 1524.9 | 1524.8 | 1525.0 | 1524.9 | 1524.9 | 1524.8 | 0.0 | 0.1 | 0.0 | 0.0 |
| 29025 | 1530.1 | 1530.4 | 1530.0 | 1530.0 | 1530.1 | 1530.4 | -0.1 | -0.4 | 0.0 | 0.0 |
| 29945 | 1535.0 | 1534.9 | 1535.0 | 1534.9 | 1534.9 | 1535.2 | 0.0 | 0.0 | -0.1 | 0.3 |
| 30361 | 1538.2 | 1538.4 | 1537.8 | 1537.5 | 1538.9 | 1539.2 | -0.4 | -1.0 | 0.7 | 0.8 |

Table 9.9 shows the difference in bed elevation for the combined inflowing load and sediment transport equation sensitivity test. For this sensitivity analysis an additional inflowing load was developed for Yang's equation. The differences between the Yang and Toffaleti equations ranges from -2.0 to 1.0 ft, with an average change of -0.2 ft. The Yang equation shows slightly more degradation than Toffaleti based on the difference between the final bed elevation. Overall, however, this difference is not significant.

| Table 9-9 – Sensitivity Analysis for combined Transport Equation and Inflowing Load on Bed Change: (T - TOFFALETI, Y- YANG) | | | | | | |
|---|---|---|---|---|---|---|
| **SECTION** | **Toffaleti Thalweg Elevation** | | **Yang Thalweg Elevation** | | **ΔPEAK-TY (ft)** | **ΔFINAL-TY (ft)** |
| | **Thalweg at Peak** | **Tahlweg at Final** | **Thalweg at Peak** | **Tahlweg at Final** | | |
| 1000 | 1442.7 | 1442.7 | 1442.7 | 1442.7 | 0.0 | 0.0 |

| **Table 9-9 –** Sensitivity Analysis for combined Transport Equation and Inflowing Load on Bed Change: (T - TOFFALETI, Y- YANG) | | | | | | |
|---|---|---|---|---|---|---|
| **SECTION** | **Toffaleti Thalweg Elevation** | | **Yang Thalweg Elevation** | | **ΔPEAK-TY** | **ΔFINAL-TY** |
| | **Thalweg at Peak** | **Tahlweg at Final** | **Thalweg at Peak** | **Tahlweg at Final** | **(ft)** | **(ft)** |
| 1285 | 1442.5 | 1442.2 | 1442.4 | 1442.4 | -0.1 | 0.2 |
| 1677 | 1442.8 | 1442.7 | 1442.8 | 1442.9 | 0.0 | 0.2 |
| 2073 | 1444.2 | 1444.2 | 1444.2 | 1444.2 | 0.0 | 0.0 |
| 2298 | 1444.7 | 1444.6 | 1444.6 | 1444.5 | 0.0 | -0.1 |
| 2581 | 1445.2 | 1445.1 | 1445.1 | 1445.1 | 0.0 | -0.1 |
| 2961 | 1445.7 | 1445.6 | 1445.6 | 1445.4 | 0.0 | -0.3 |
| 3285 | 1442.8 | 1442.9 | 1443.0 | 1443.3 | 0.3 | 0.4 |
| 3671 | 1444.1 | 1444.3 | 1444.4 | 1444.5 | 0.2 | 0.3 |
| 3997 | 1445.1 | 1445.2 | 1445.1 | 1445.4 | 0.0 | 0.2 |
| 4328 | 1445.1 | 1445.1 | 1445.1 | 1445.4 | 0.0 | 0.3 |
| 4684 | 1446.1 | 1446.2 | 1446.2 | 1446.6 | 0.1 | 0.4 |
| 5184 | 1446.1 | 1446.1 | 1446.3 | 1446.6 | 0.2 | 0.5 |
| 5609 | 1447.0 | 1447.2 | 1447.4 | 1447.7 | 0.4 | 0.6 |
| 5941 | 1447.1 | 1447.0 | 1447.1 | 1447.4 | 0.0 | 0.4 |
| 6166 | 1447.4 | 1447.5 | 1447.4 | 1447.6 | 0.0 | 0.1 |
| 6711 | 1449.8 | 1449.9 | 1449.8 | 1449.5 | 0.0 | -0.4 |
| 7419 | 1451.0 | 1450.7 | 1450.4 | 1450.5 | -0.6 | -0.2 |
| 7758 | 1452.0 | 1451.9 | 1451.9 | 1451.7 | -0.1 | -0.2 |
| 8176 | 1452.0 | 1452.0 | 1452.0 | 1452.0 | 0.0 | 0.0 |
| 8867 | 1453.4 | 1453.4 | 1453.6 | 1453.8 | 0.1 | 0.4 |
| 9359 | 1454.6 | 1454.6 | 1454.8 | 1455.1 | 0.2 | 0.5 |
| 9717 | 1455.9 | 1455.9 | 1456.1 | 1456.2 | 0.2 | 0.3 |
| 10216 | 1456.9 | 1456.9 | 1457.2 | 1457.4 | 0.3 | 0.5 |
| 10609 | 1458.2 | 1458.2 | 1458.7 | 1458.7 | 0.5 | 0.5 |
| 11003 | 1459.4 | 1459.4 | 1459.7 | 1459.7 | 0.2 | 0.2 |
| 11396 | 1460.7 | 1460.6 | 1460.7 | 1460.7 | 0.0 | 0.1 |
| 11871 | 1462.8 | 1462.9 | 1462.6 | 1461.7 | -0.3 | -1.3 |
| 12317 | 1463.0 | 1462.9 | 1462.8 | 1461.6 | -0.1 | -1.4 |
| 12726 | 1465.0 | 1465.0 | 1465.0 | 1464.9 | 0.0 | 0.0 |
| 13200 | 1467.1 | 1467.1 | 1467.5 | 1467.2 | 0.4 | 0.1 |
| 13733 | 1468.4 | 1468.3 | 1467.6 | 1467.6 | -0.8 | -0.7 |
| 14335 | 1469.9 | 1470.0 | 1470.0 | 1469.4 | 0.1 | -0.6 |
| 14920 | 1471.6 | 1471.4 | 1471.4 | 1471.5 | -0.1 | 0.1 |
| 15347 | 1473.2 | 1473.5 | 1473.5 | 1473.5 | 0.3 | 0.0 |
| 15682 | 1475.0 | 1475.1 | 1475.2 | 1475.0 | 0.2 | 0.0 |
| 16028 | 1477.1 | 1477.2 | 1477.1 | 1477.0 | 0.1 | -0.1 |
| 16476 | 1478.0 | 1477.7 | 1478.1 | 1478.1 | 0.1 | 0.4 |
| 16913 | 1480.9 | 1480.8 | 1480.9 | 1480.8 | 0.1 | 0.0 |
| 17330 | 1483.2 | 1483.1 | 1482.6 | 1482.1 | -0.6 | -1.0 |

| **Table 9-9 –** Sensitivity Analysis for combined Transport Equation and Inflowing Load on Bed Change: (T - TOFFALETI, Y- YANG) | | | | | | |
|---|---|---|---|---|---|---|
| **SECTION** | **Toffaleti Thalweg Elevation** | | **Yang Thalweg Elevation** | | **$\Delta_{PEAK}$-TY** | **$\Delta_{FINAL}$-TY** |
| | **Thalweg at Peak** | **Tahlweg at Final** | **Thalweg at Peak** | **Tahlweg at Final** | **(ft)** | **(ft)** |
| 17768 | 1484.6 | 1484.5 | 1483.7 | 1483.0 | -0.9 | -1.5 |
| 18399 | 1485.8 | 1485.3 | 1484.5 | 1484.1 | -1.3 | -1.2 |
| 18929 | 1485.1 | 1485.6 | 1485.2 | 1486.5 | 0.2 | 1.0 |
| 19200 | 1487.7 | 1487.8 | 1488.6 | 1488.2 | 0.9 | 0.4 |
| 19813 | 1489.4 | 1489.4 | 1489.4 | 1489.1 | 0.0 | -0.2 |
| 20179 | 1490.7 | 1490.8 | 1491.0 | 1490.9 | 0.3 | 0.0 |
| 20654 | 1493.0 | 1493.1 | 1492.5 | 1491.1 | -0.5 | -2.0 |
| 20754 | 1493.5 | 1493.4 | 1493.0 | 1492.2 | -0.5 | -1.2 |
| 20853 | 1493.8 | 1494.0 | 1493.2 | 1492.4 | -0.6 | -1.5 |
| 20953 | 1493.9 | 1493.5 | 1492.4 | 1492.8 | -1.6 | -0.6 |
| 21459 | 1496.2 | 1496.2 | 1495.9 | 1495.0 | -0.3 | -1.2 |
| 21912 | 1497.4 | 1497.1 | 1496.6 | 1496.7 | -0.8 | -0.4 |
| 22448 | 1499.8 | 1500.0 | 1500.0 | 1498.9 | 0.2 | -1.1 |
| 22909 | 1502.2 | 1502.3 | 1502.0 | 1501.8 | -0.2 | -0.5 |
| 23406 | 1505.0 | 1504.9 | 1505.0 | 1505.0 | 0.1 | 0.1 |
| 23817 | 1505.7 | 1505.3 | 1505.1 | 1505.4 | -0.6 | 0.0 |
| 24190 | 1508.1 | 1508.6 | 1508.2 | 1508.3 | 0.1 | -0.3 |
| 24469 | 1510.1 | 1510.2 | 1510.1 | 1510.0 | 0.0 | -0.3 |
| 24895 | 1510.8 | 1510.1 | 1510.5 | 1510.4 | -0.3 | 0.3 |
| 25246 | 1511.9 | 1511.6 | 1511.3 | 1511.3 | -0.6 | -0.3 |
| 25846 | 1511.3 | 1511.8 | 1511.5 | 1511.9 | 0.2 | 0.1 |
| 26500 | 1513.2 | 1513.8 | 1513.7 | 1513.6 | 0.5 | -0.2 |
| 27263 | 1516.9 | 1515.9 | 1515.8 | 1515.5 | -1.1 | -0.4 |
| 28104 | 1524.9 | 1524.8 | 1525.0 | 1524.9 | 0.0 | 0.1 |
| 29025 | 1530.1 | 1530.4 | 1530.1 | 1530.1 | 0.0 | -0.3 |
| 29945 | 1535.0 | 1534.9 | 1535.0 | 1535.0 | 0.1 | 0.1 |
| 30361 | 1538.2 | 1538.4 | 1538.2 | 1538.0 | -0.1 | -0.4 |

The final sensitivity analysis, the results of which are shown in Table 9.10, was performed in order to examine the change in bed response to an initial discharge prior to the main hydrograph. As noted above, in some instances an initial, small discharge will bring the model into equilibrium with respect to sediment gradation in the bed, the inflowing sediment load, and the channel hydraulics. The results of the analysis indicate that the difference in predicted bed change ranges from -2.0 to 0.8 ft with an average bed change of 0.0 ft.

| Table 9-10 – Sensitivity Analysis for General Adjustment Initial Warm-up on Bed Elevation | | | | | | | |
|---|---|---|---|---|---|---|---|
| SECTION | Initial Thalweg Elevation | General Storm Adjustment | | General Storm with Warm-up Flow | | Difference in Calculated Thalweg Elevation | |
| | | Thalweg at Peak | Thalweg at Final | Thalweg at Peak | Thalweg at Final | $\Delta_{PEAK}$-WU (ft) | $\Delta_{FINAL}$-WU (ft) |
| 1000 | 1442.7 | 1442.7 | 1442.7 | 1442.7 | 1442.7 | 0.0 | 0.0 |
| 1285 | 1442.6 | 1442.5 | 1442.2 | 1442.5 | 1442.2 | 0.0 | 0.0 |
| 1677 | 1442.7 | 1442.8 | 1442.7 | 1442.8 | 1442.7 | 0.0 | 0.0 |
| 2073 | 1444.2 | 1444.2 | 1444.2 | 1444.2 | 1444.2 | 0.0 | 0.0 |
| 2298 | 1444.7 | 1444.7 | 1444.6 | 1444.7 | 1444.6 | 0.0 | 0.0 |
| 2581 | 1445.2 | 1445.2 | 1445.1 | 1445.2 | 1445.1 | 0.0 | 0.0 |
| 2961 | 1445.7 | 1445.7 | 1445.6 | 1445.7 | 1445.6 | 0.0 | 0.0 |
| 3285 | 1442.7 | 1442.8 | 1442.9 | 1442.8 | 1442.9 | 0.0 | 0.0 |
| 3671 | 1444.1 | 1444.1 | 1444.3 | 1444.1 | 1444.3 | 0.0 | 0.0 |
| 3997 | 1445.0 | 1445.1 | 1445.2 | 1445.1 | 1445.2 | 0.0 | 0.0 |
| 4328 | 1445.0 | 1445.1 | 1445.1 | 1445.1 | 1445.2 | 0.0 | 0.0 |
| 4684 | 1446.0 | 1446.1 | 1446.2 | 1446.1 | 1446.2 | 0.0 | 0.0 |
| 5184 | 1446.0 | 1446.1 | 1446.1 | 1446.1 | 1446.2 | 0.0 | 0.0 |
| 5609 | 1447.0 | 1447.0 | 1447.2 | 1447.0 | 1447.1 | 0.0 | 0.0 |
| 5941 | 1447.2 | 1447.1 | 1447.0 | 1447.0 | 1447.0 | -0.1 | 0.1 |
| 6166 | 1447.4 | 1447.4 | 1447.5 | 1447.4 | 1447.5 | 0.0 | 0.0 |
| 6711 | 1449.8 | 1449.8 | 1449.9 | 1449.8 | 1449.9 | 0.0 | 0.0 |
| 7419 | 1451.0 | 1451.0 | 1450.7 | 1451.0 | 1450.7 | 0.0 | 0.0 |
| 7758 | 1452.0 | 1452.0 | 1451.9 | 1452.0 | 1451.9 | 0.0 | 0.0 |
| 8176 | 1452.0 | 1452.0 | 1452.0 | 1452.0 | 1452.0 | 0.0 | 0.0 |
| 8867 | 1453.4 | 1453.4 | 1453.4 | 1453.5 | 1453.5 | 0.0 | 0.1 |
| 9359 | 1454.5 | 1454.6 | 1454.6 | 1454.6 | 1454.8 | 0.0 | 0.2 |
| 9717 | 1455.9 | 1455.9 | 1455.9 | 1455.9 | 1455.9 | 0.0 | 0.0 |
| 10216 | 1456.8 | 1456.9 | 1456.9 | 1456.9 | 1457.0 | 0.0 | 0.1 |
| 10609 | 1458.2 | 1458.2 | 1458.2 | 1458.3 | 1458.3 | 0.1 | 0.1 |
| 11003 | 1459.4 | 1459.4 | 1459.4 | 1459.2 | 1459.3 | -0.2 | -0.2 |
| 11396 | 1460.7 | 1460.7 | 1460.6 | 1460.7 | 1460.6 | 0.0 | 0.0 |
| 11871 | 1462.6 | 1462.8 | 1462.9 | 1462.7 | 1462.8 | -0.1 | -0.1 |
| 12317 | 1464.0 | 1463.0 | 1462.9 | 1463.3 | 1463.0 | 0.3 | 0.1 |
| 12726 | 1465.0 | 1465.0 | 1465.0 | 1465.0 | 1465.0 | 0.0 | 0.1 |
| 13200 | 1467.0 | 1467.1 | 1467.1 | 1467.1 | 1467.3 | 0.1 | 0.2 |
| 13733 | 1468.7 | 1468.4 | 1468.3 | 1468.3 | 1468.0 | -0.1 | -0.4 |
| 14335 | 1469.8 | 1469.9 | 1470.0 | 1469.9 | 1469.9 | 0.0 | -0.1 |
| 14920 | 1471.8 | 1471.6 | 1471.4 | 1471.5 | 1471.4 | -0.1 | -0.1 |
| 15347 | 1473.2 | 1473.2 | 1473.5 | 1473.3 | 1473.4 | 0.1 | -0.1 |
| 15682 | 1475.0 | 1475.0 | 1475.1 | 1475.0 | 1475.0 | 0.0 | 0.0 |
| 16028 | 1476.9 | 1477.1 | 1477.2 | 1477.1 | 1477.2 | 0.0 | 0.0 |
| 16476 | 1478.4 | 1478.0 | 1477.7 | 1478.0 | 1477.5 | 0.0 | -0.2 |
| 16913 | 1480.8 | 1480.9 | 1480.8 | 1480.9 | 1480.8 | 0.0 | 0.0 |
| 17330 | 1483.0 | 1483.2 | 1483.1 | 1483.2 | 1483.0 | 0.0 | -0.1 |
| 17768 | 1485.0 | 1484.6 | 1484.5 | 1484.6 | 1484.5 | 0.0 | 0.0 |
| 18399 | 1486.0 | 1485.8 | 1485.3 | 1485.6 | 1485.3 | -0.2 | 0.0 |
| 18929 | 1485.0 | 1485.1 | 1485.6 | 1485.2 | 1485.7 | 0.1 | 0.1 |

| **Table 9-10 –** Sensitivity Analysis for General Adjustment Initial Warm-up on Bed Elevation | | | | | | | |
|---|---|---|---|---|---|---|---|
| **SECTION** | **Initial Thalweg Elevation** | **General Storm Adjustment** | | **General Storm with Warm-up Flow** | | **Difference in Calculated Thalweg Elevation** | |
| | | **Thalweg at Peak** | **Thalweg at Final** | **Thalweg at Peak** | **Thalweg at Final** | **$\Delta_{PEAK}$-WU (ft)** | **$\Delta_{FINAL}$-WU (ft)** |
| 19200 | 1487.7 | 1487.7 | 1487.8 | 1487.8 | 1487.7 | 0.0 | 0.0 |
| 19813 | 1489.4 | 1489.4 | 1489.4 | 1489.4 | 1489.4 | 0.0 | 0.0 |
| 20179 | 1490.7 | 1490.7 | 1490.8 | 1490.7 | 1490.7 | 0.0 | -0.1 |
| 20654 | 1493.0 | 1493.0 | 1493.1 | 1493.4 | 1493.3 | 0.4 | 0.2 |
| 20754 | 1493.4 | 1493.5 | 1493.4 | 1491.5 | 1492.4 | -2.0 | -1.1 |
| 20853 | 1493.8 | 1493.8 | 1494.0 | 1494.4 | 1493.9 | 0.5 | 0.0 |
| 20953 | 1494.2 | 1493.9 | 1493.5 | 1493.6 | 1493.6 | -0.3 | 0.2 |
| 21459 | 1496.0 | 1496.2 | 1496.2 | 1496.3 | 1496.5 | 0.1 | 0.3 |
| 21912 | 1497.5 | 1497.4 | 1497.1 | 1497.2 | 1496.8 | -0.3 | -0.3 |
| 22448 | 1500.0 | 1499.8 | 1500.0 | 1500.0 | 1499.7 | 0.2 | -0.4 |
| 22909 | 1502.0 | 1502.2 | 1502.3 | 1502.1 | 1502.0 | 0.0 | -0.3 |
| 23406 | 1505.0 | 1505.0 | 1504.9 | 1505.0 | 1505.5 | 0.1 | 0.6 |
| 23817 | 1506.0 | 1505.7 | 1505.3 | 1505.5 | 1505.5 | -0.2 | 0.1 |
| 24190 | 1508.0 | 1508.1 | 1508.6 | 1508.3 | 1508.7 | 0.1 | 0.1 |
| 24469 | 1510.0 | 1510.1 | 1510.2 | 1510.2 | 1510.2 | 0.1 | 0.0 |
| 24895 | 1511.0 | 1510.8 | 1510.1 | 1510.6 | 1510.2 | -0.2 | 0.1 |
| 25246 | 1512.0 | 1511.9 | 1511.6 | 1511.9 | 1511.5 | -0.1 | -0.1 |
| 25846 | 1511.3 | 1511.3 | 1511.8 | 1511.4 | 1511.6 | 0.1 | -0.2 |
| 26500 | 1513.0 | 1513.2 | 1513.8 | 1513.3 | 1513.5 | 0.1 | -0.3 |
| 27263 | 1517.0 | 1516.9 | 1515.9 | 1516.8 | 1516.7 | -0.2 | 0.8 |
| 28104 | 1525.0 | 1524.9 | 1524.8 | 1525.0 | 1524.9 | 0.0 | 0.1 |
| 29025 | 1530.0 | 1530.1 | 1530.4 | 1530.0 | 1530.2 | 0.0 | -0.2 |
| 29945 | 1535.0 | 1535.0 | 1534.9 | 1534.9 | 1535.0 | -0.1 | 0.1 |
| 30361 | 1538.0 | 1538.2 | 1538.4 | 1538.5 | 1538.5 | 0.2 | 0.0 |

The results of these tests indicate that the model is relatively insensitive ($\Delta z<1$ ft) to variations of considered parameters. Some sections in the model will exhibit greater erosion or deposition as a result of these variations depending on local channel parameters; however, they are not significant to the total scour of the model on average. However, in order to compensate for these variations a residual safety factor has been incorporated in the selection of the appropriate maximum levee slope lining cutoff depths.

### 9.9 Maximum Design General Adjustment Values for Proposed Conditions

A comparison of the calculated adjustments in the streambed for the General Single 100-year flood hydrograph was performed to evaluate the maximum change from the different simulations. This comparison was performed for both the “wide” and “narrow” cross-section simulations. The maximum aggradation or degradation is illustrated in the following table and will be used in evaluating to maximum total bed adjustment with the other streambed adjustment components that are calculated in the sections of this report. The table illustrates the maximum change in the streambed thalweg elevation either at the peak of the flood hydrograph or at the final end of the simulation. The largest positive value at each section was selected as the maximum aggradation and if the values were negative then a zero value was assigned. The largest negative value was used to define the maximum general scour and if there were only positive values then a zero value was assigned. The highlighted values in the table reflect the maximum or minimum value used for aggradation or degradation respectively, and a non-highlighted cell would reflect a value of zero.

**Table 9-11 –** Maximum Change in the Streambed Thalweg Elevation Either at the Peak of the Flood Hydrograph or at the Final End of the Simulation

| SECTION | General - Narrow | | General - Wide | | Max Gen (ft) | Min Gen (ft) |
|---|---|---|---|---|---|---|
| | Peak (ft) | Final (ft) | Peak (ft) | Final (ft) | | |
| 1000 | 0.0 | 0.0 | 0.0 | 0.0 | 0.0 | 0.0 |
| 1285 | 0.0 | 0.0 | -0.1 | -0.4 | 0.0 | -0.4 |
| 1677 | 0.0 | 0.1 | 0.1 | 0.0 | 0.1 | 0.0 |
| 2073 | 0.0 | 0.0 | 0.0 | 0.0 | 0.0 | 0.0 |
| 2298 | 0.0 | 0.0 | 0.0 | -0.1 | 0.0 | -0.1 |
| 2581 | 0.0 | 0.0 | 0.0 | -0.1 | 0.0 | -0.1 |
| 2961 | 0.0 | 0.0 | 0.0 | -0.1 | 0.0 | -0.1 |
| 3285 | 0.0 | 0.0 | 0.1 | 0.2 | 0.2 | 0.0 |
| 3671 | 0.0 | 0.0 | 0.1 | 0.2 | 0.2 | 0.0 |
| 3997 | 0.0 | 0.0 | 0.1 | 0.2 | 0.2 | 0.0 |
| 4328 | 0.0 | 0.0 | 0.1 | 0.1 | 0.1 | 0.0 |
| 4684 | 0.0 | 0.0 | 0.1 | 0.2 | 0.2 | 0.0 |
| 5184 | 0.0 | 0.1 | 0.1 | 0.1 | 0.1 | 0.0 |
| 5609 | 0.0 | 0.2 | 0.0 | 0.2 | 0.2 | 0.0 |
| 5941 | 0.0 | -0.3 | -0.1 | -0.3 | 0.0 | -0.3 |
| 6166 | 0.0 | 0.0 | 0.0 | 0.0 | 0.0 | 0.0 |
| 6711 | 0.0 | 0.0 | 0.0 | 0.1 | 0.1 | 0.0 |
| 7419 | 0.0 | -0.1 | 0.0 | -0.3 | 0.0 | -0.3 |
| 7758 | 0.0 | 0.0 | 0.0 | 0.0 | 0.0 | 0.0 |
| 8176 | 0.0 | 0.0 | 0.0 | 0.0 | 0.0 | 0.0 |
| 8867 | 0.0 | 0.1 | 0.0 | 0.0 | 0.1 | 0.0 |
| 9359 | 0.1 | 0.3 | 0.1 | 0.1 | 0.3 | 0.1 |
| 9717 | 0.0 | 0.0 | 0.0 | 0.0 | 0.0 | 0.0 |
| 10216 | 0.1 | 0.2 | 0.0 | 0.1 | 0.2 | 0.0 |
| 10609 | 0.0 | 0.1 | 0.0 | 0.0 | 0.1 | 0.0 |
| 11003 | 0.0 | 0.0 | 0.0 | 0.0 | 0.0 | 0.0 |
| 11396 | 0.0 | -0.1 | 0.0 | 0.0 | 0.0 | -0.1 |
| 11871 | 0.1 | 0.2 | 0.3 | 0.4 | 0.4 | 0.1 |
| 12317 | -0.4 | -0.4 | -1.0 | -1.1 | -0.4 | -1.1 |
| 12726 | 0.0 | 0.1 | 0.0 | 0.0 | 0.1 | 0.0 |
| 13200 | 0.0 | 0.2 | 0.1 | 0.1 | 0.2 | 0.0 |
| 13733 | -0.1 | -0.4 | -0.3 | -0.4 | -0.1 | -0.4 |
| 14335 | 0.1 | 0.2 | 0.1 | 0.2 | 0.2 | 0.1 |
| 14920 | -0.1 | -0.1 | -0.2 | -0.3 | -0.1 | -0.3 |
| 15347 | 0.2 | 0.3 | 0.0 | 0.3 | 0.3 | 0.0 |

**Table 9-11 –** Maximum Change in the Streambed Thalweg Elevation Either at the Peak of the Flood Hydrograph or at the Final End of the Simulation

| SECTION | General - Narrow | | General - Wide | | Max Gen (ft) | Min Gen (ft) |
|---|---|---|---|---|---|---|
| | Peak (ft) | Final (ft) | Peak (ft) | Final (ft) | | |
| 15682 | -0.2 | -0.3 | 0.0 | 0.1 | 0.1 | -0.3 |
| 16028 | 0.1 | 0.1 | 0.1 | 0.2 | 0.2 | 0.1 |
| 16476 | -0.1 | -0.3 | -0.3 | -0.7 | -0.1 | -0.7 |
| 16913 | 0.0 | 0.0 | 0.0 | 0.0 | 0.0 | 0.0 |
| 17330 | 0.0 | -0.1 | 0.2 | 0.1 | 0.2 | -0.1 |
| 17768 | -0.1 | -0.4 | -0.4 | -0.5 | -0.1 | -0.5 |
| 18399 | -0.1 | -0.2 | -0.2 | -0.7 | -0.1 | -0.7 |
| 18929 | 0.2 | 0.6 | 0.1 | 0.6 | 0.6 | 0.1 |
| 19200 | 0.1 | 0.1 | 0.0 | 0.1 | 0.1 | 0.0 |
| 19813 | 0.0 | -0.1 | 0.0 | 0.0 | 0.0 | -0.1 |
| 20179 | 0.0 | 0.3 | 0.0 | 0.2 | 0.3 | 0.0 |
| 20654 | 0.0 | 0.1 | 0.0 | 0.1 | 0.1 | 0.0 |
| 20754 | -0.1 | -0.2 | 0.1 | 0.0 | 0.1 | -0.2 |
| 20853 | -0.2 | -0.2 | 0.1 | 0.2 | 0.2 | -0.2 |
| 20953 | 0.0 | -0.3 | -0.2 | -0.7 | 0.0 | -0.7 |
| 21459 | 0.0 | 0.1 | 0.2 | 0.2 | 0.2 | 0.0 |
| 21912 | -0.1 | -0.4 | -0.1 | -0.4 | -0.1 | -0.4 |
| 22448 | 0.0 | -0.3 | -0.2 | 0.0 | 0.0 | -0.3 |
| 22909 | 0.0 | -0.1 | 0.2 | 0.3 | 0.3 | -0.1 |
| 23406 | 0.0 | 0.0 | 0.0 | -0.1 | 0.0 | -0.1 |
| 23817 | -0.1 | -0.1 | -0.3 | -0.7 | -0.1 | -0.7 |
| 24190 | 0.1 | 0.5 | 0.1 | 0.6 | 0.6 | 0.1 |
| 24469 | 0.0 | 0.0 | 0.1 | 0.2 | 0.2 | 0.0 |
| 24895 | -0.1 | -0.3 | -0.2 | -0.9 | -0.1 | -0.9 |
| 25246 | 0.0 | -0.2 | -0.1 | -0.4 | 0.0 | -0.4 |
| 25846 | 0.1 | 0.3 | 0.1 | 0.5 | 0.5 | 0.1 |
| 26500 | 0.1 | 0.2 | 0.2 | 0.8 | 0.8 | 0.1 |
| 27263 | -0.1 | -0.3 | -0.1 | -1.1 | -0.1 | -1.1 |
| 28104 | 0.0 | 0.0 | -0.1 | -0.2 | 0.0 | -0.2 |
| 29025 | 0.0 | 0.0 | 0.1 | 0.4 | 0.4 | 0.0 |
| 29945 | 0.0 | 0.0 | 0.0 | -0.1 | 0.0 | -0.1 |
| 30361 | 0.1 | 2.1 | 0.2 | 0.4 | 2.1 | 0.1 |

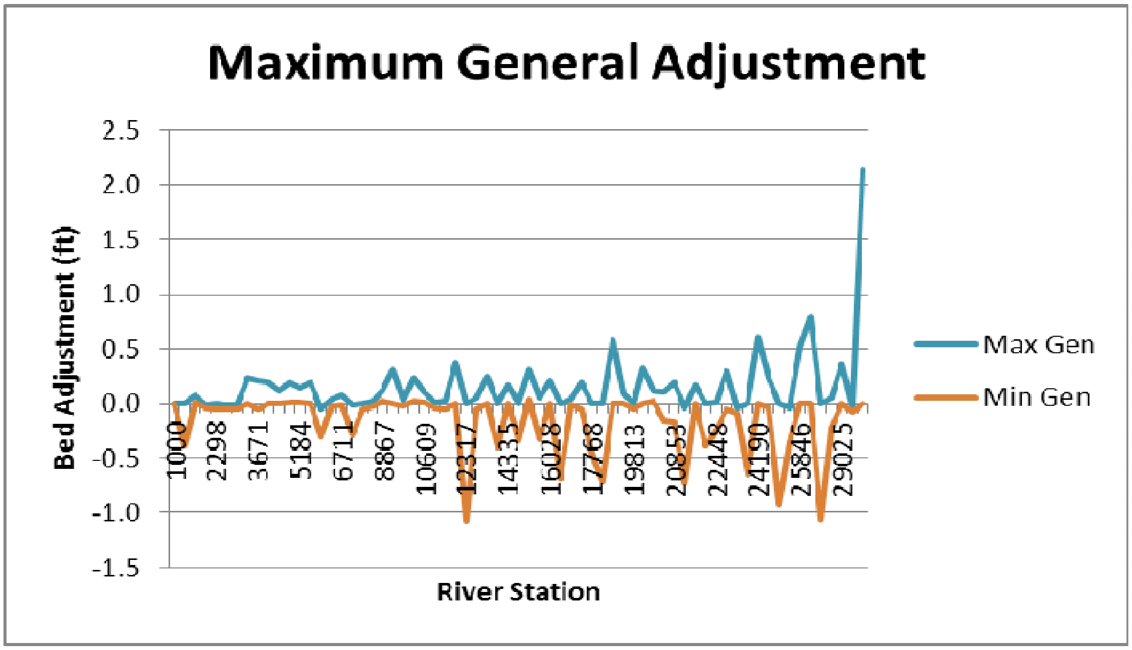


**Figure 9-8** – Comparison of the "maximum" degradation and aggradation computed from the difference scenario HEC-6T models

# 10 Long-Term Adjustment

## 10.1 HEC-6T Long-Term Adjustment Modeling

FEMA's *Riverine Erosion Hazard Areas Mapping Feasibility Study* (FEMA, September 199) recommends a time scale of decades for delineation of scour activities. The document notes that a 60-year has been chosen as suitable based on assessment of coastal erosion. Continuous simulation modeling is one recommended approach to long-term analysis because the method is systematic and repeatable. In this study the HEC-6T model is used in a continuous simulation mode to assess possible long-term temporal variation in stream geometry.

The long-term hydrograph for hydraulic input is developed from Gage 11069500 data, as described above. The mean daily averaged gage data covers a period of 87 years (1920 to 2007). The hydrograph was plotted such that only discharges greater than 5000 cfs were considered since flows less than this value fail to produce discharges in the HEC-RAS models from along the entire study reach. This filtering resulted in a hydrograph lasting 16 days, and represents the complete 87 years of long-term hydrology. An additional day was added to the hydrograph to bring the discharge in the model close to 5000 cfs, otherwise the events in the scaled linearized occur in the same sequence as presented in the original data. The linearized hydrograph is presented in Figure 10.1.

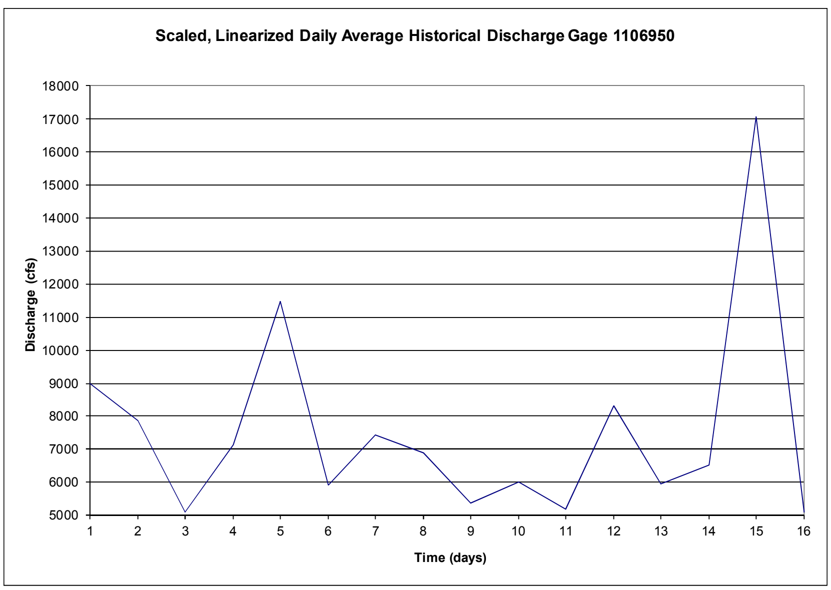


**Figure 10-1 -** Mean Daily and Linearized Hydrograph

This hydrograph, along with the sediment data detailed above in Section 4, are entered into the HEC-6T model and run in the manner previously described in Section 9. Iterative model runs are not required in for long-term analysis in this system since so little significant flow occurs in the River. The present study methodology assumes that the future hydrology and grain size distribution remain as in the present and the past. Also, only the proposed conditions wide model is used for long-term simulation, which assumes that the existing levee has been completely scoured away.

Figures 10.2A and B, and Tables 10.1A and B present the results of the long-term simulation. The figure shows that over the long-term the bed in the study reach has degrading and aggrading sections. Generally, aggradation is expected for the study reach as a whole based on site visits and gravel mining operations upstream, however, degradational pockets may be reasonable in an aggrading condition. It is presently unclear if gravel mining operations will continue. As of the time of writing, mining operations have ceased (personal communication, L. Whitehorn, Director, Sobaba Public Works, 9-15-2008); however, it is unclear if future in-stream mining operations are planned. The Tables 10.1 A and 10.1 B indicate that the long-term bed change is expected to range from -4.1 to 4.2 ft, with an average change of -0.2ft in the existing condition, and from -3.3 to 2.9 ft, with an average change of -0.2 ft in the proposed condition.

### *10.1.1 Discussion of Long-Term Adjustment Results*

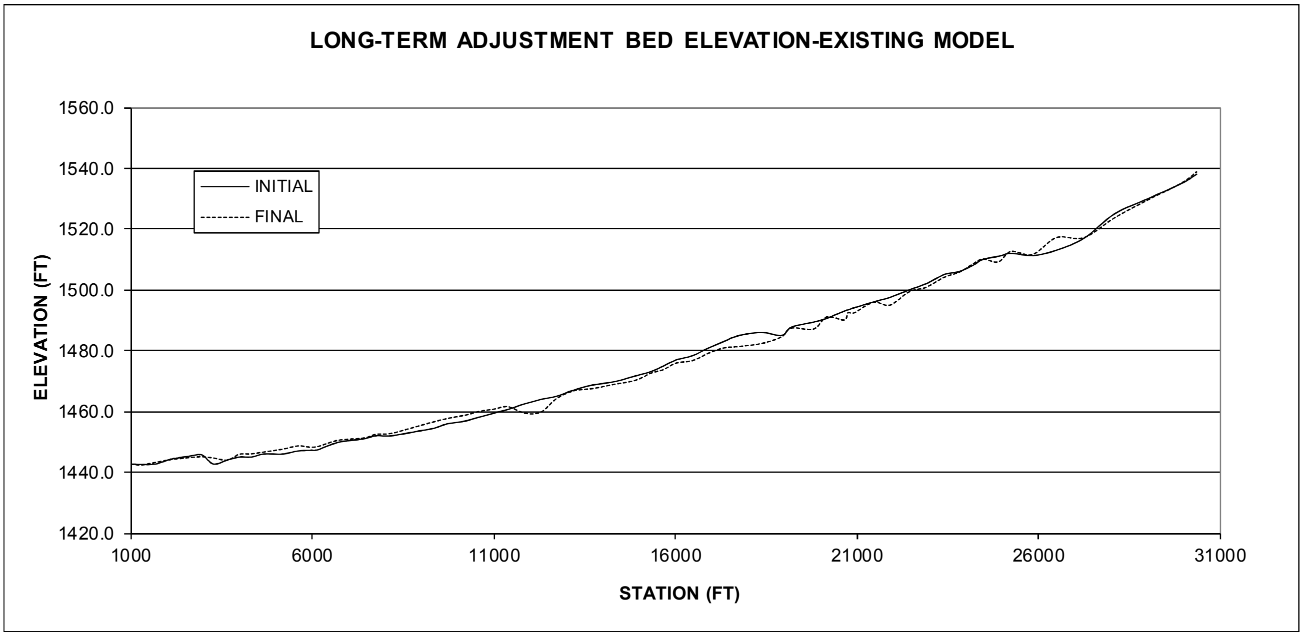


**Figure 10-2A -** Long-Term Adjustment Bed Elevation

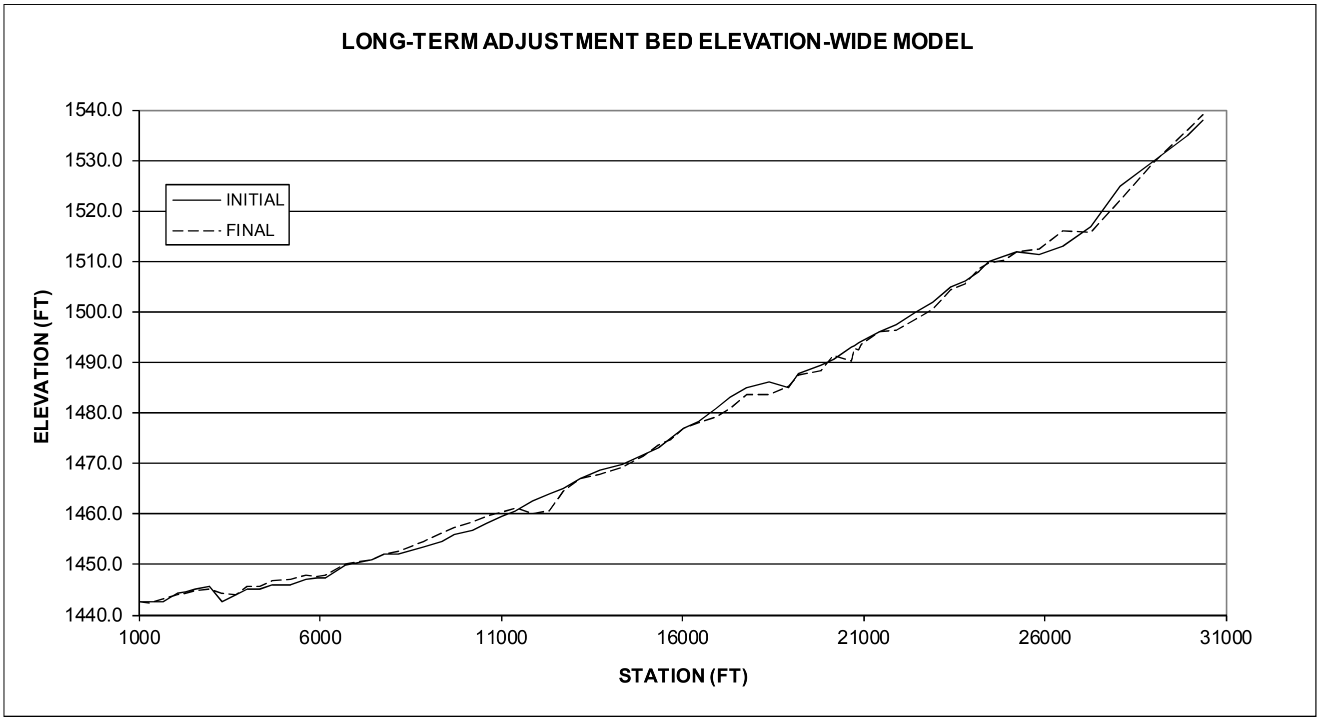


**Figure 10-2B -** Long-Term Adjustment Bed Elevation

| **Table 10-1A –** Long-Term Adjustment Bed Elevation-Existing Model | | | |
|---|---|---|---|
| **SECTION** | **Thalweg Elevation** | | **Change in Thalweg Elevation (ft)** |
| | **Initial Streambed Elevation** | **Final Streambed Elevation** | |
| 1000 | 1442.7 | 1442.7 | 0.0 |
| 1284.6 | 1442.6 | 1442.4 | -0.2 |
| 1677 | 1442.7 | 1443.2 | 0.5 |
| 2072.6 | 1444.2 | 1444.1 | -0.1 |
| 2298.3 | 1444.7 | 1444.4 | -0.3 |
| 2580.9 | 1445.2 | 1444.8 | -0.4 |
| 2960.9 | 1445.7 | 1445.1 | -0.6 |
| 3284.5 | 1442.7 | 1444.7 | 2.0 |
| 3670.6 | 1444.1 | 1444.0 | 0.0 |
| 3997.3 | 1445.0 | 1445.9 | 0.9 |
| 4327.6 | 1445.0 | 1446.0 | 1.0 |
| 4684.2 | 1446.0 | 1446.7 | 0.7 |
| 5183.6 | 1446.0 | 1447.6 | 1.6 |
| 5609 | 1447.0 | 1448.7 | 1.7 |
| 5941 | 1447.2 | 1448.3 | 1.0 |
| 6166 | 1447.4 | 1448.5 | 1.1 |
| 6710.6 | 1449.8 | 1450.5 | 0.7 |
| 7418.7 | 1451.0 | 1451.2 | 0.2 |
| 7758.4 | 1452.0 | 1452.5 | 0.5 |
| 8175.9 | 1452.0 | 1452.8 | 0.8 |
| 8867.3 | 1453.4 | 1455.0 | 1.6 |
| 9359.1 | 1454.5 | 1456.6 | 2.1 |
| 9716.6 | 1455.9 | 1457.7 | 1.8 |
| 10216 | 1456.8 | 1458.8 | 2.0 |
| 10609 | 1458.2 | 1460.0 | 1.8 |
| 11003 | 1459.4 | 1460.8 | 1.3 |
| 11396 | 1460.7 | 1461.6 | 0.9 |
| 11871 | 1462.6 | 1459.4 | -3.2 |
| 12317 | 1464.0 | 1459.9 | -4.1 |
| 12726 | 1465.0 | 1464.2 | -0.8 |
| 13200 | 1467.0 | 1466.8 | -0.2 |
| 13733 | 1468.7 | 1467.5 | -1.2 |
| 14335 | 1469.8 | 1468.9 | -0.8 |
| 14920 | 1471.8 | 1470.3 | -1.5 |
| 15347 | 1473.2 | 1472.7 | -0.5 |
| 15682 | 1475.0 | 1473.8 | -1.2 |
| 16028 | 1476.9 | 1475.9 | -1.0 |
| 16476 | 1478.4 | 1476.7 | -1.6 |
| 16913 | 1480.8 | 1479.1 | -1.7 |

| **Table 10-1A –** Long-Term Adjustment Bed Elevation-Existing Model | | | |
|---|---|---|---|
| **SECTION** | **Thalweg Elevation** | | **Change in Thalweg Elevation (ft)** |
| | **Initial Streambed Elevation** | **Final Streambed Elevation** | |
| 17330 | 1483.0 | 1480.9 | -2.1 |
| 17768 | 1485.0 | 1481.4 | -3.6 |
| 18399 | 1486.0 | 1482.4 | -3.6 |
| 18929 | 1485.0 | 1484.6 | -0.4 |
| 19200 | 1487.7 | 1487.4 | -0.3 |
| 19813 | 1489.4 | 1487.1 | -2.3 |
| 20179 | 1490.7 | 1491.1 | 0.5 |
| 20654 | 1493.0 | 1490.1 | -2.9 |
| 20754 | 1493.4 | 1492.4 | -1.0 |
| 20853 | 1493.8 | 1492.3 | -1.5 |
| 20953 | 1494.2 | 1492.5 | -1.7 |
| 21459 | 1496.0 | 1495.9 | -0.1 |
| 21912 | 1497.5 | 1495.0 | -2.5 |
| 22448 | 1500.0 | 1499.4 | -0.6 |
| 22909 | 1502.0 | 1500.8 | -1.2 |
| 23406 | 1505.0 | 1504.1 | -0.9 |
| 23817 | 1506.0 | 1505.8 | -0.2 |
| 24190 | 1508.0 | 1508.4 | 0.4 |
| 24469 | 1510.0 | 1510.1 | 0.1 |
| 24895 | 1511.0 | 1509.2 | -1.8 |
| 25246 | 1512.0 | 1512.6 | 0.6 |
| 25846 | 1511.3 | 1511.6 | 0.4 |
| 26500 | 1513.0 | 1517.2 | 4.2 |
| 27263 | 1517.0 | 1517.2 | 0.2 |
| 28104 | 1525.0 | 1523.7 | -1.3 |
| 29025 | 1530.0 | 1529.6 | -0.4 |
| 29945 | 1535.0 | 1535.1 | 0.1 |
| 30361 | 1538.0 | 1538.8 | 0.8 |

| **Table 10-1B –** Long-Term Adjustment Bed Elevation-Wide Model | | | |
|---|---|---|---|
| **SECTION** | **Thalweg Elevation** | | **Change in Thalweg Elevation / Adjustment (ft)** |
| | **Initial Streambed Elevation** | **Final Streambed Elevation** | |
| 1000 | 1442.7 | 1442.7 | 0.0 |
| 1284.6 | 1442.6 | 1442.4 | -0.2 |
| 1677 | 1442.7 | 1443.2 | 0.5 |

**Table 10-1B –** Long-Term Adjustment Bed Elevation-Wide Model

| SECTION | Thalweg Elevation | | Change in Thalweg Elevation / Adjustment (ft) |
|---|---|---|---|
| | Initial Streambed Elevation | Final Streambed Elevation | |
| 2072.6 | 1444.2 | 1444.0 | -0.2 |
| 2298.3 | 1444.7 | 1444.4 | -0.3 |
| 2580.9 | 1445.2 | 1444.7 | -0.5 |
| 2960.9 | 1445.7 | 1445.0 | -0.7 |
| 3284.5 | 1442.7 | 1444.4 | 1.7 |
| 3670.6 | 1444.1 | 1444.0 | 0.0 |
| 3997.3 | 1445.0 | 1445.6 | 0.6 |
| 4327.6 | 1445.0 | 1445.7 | 0.6 |
| 4684.2 | 1446.0 | 1446.8 | 0.8 |
| 5183.6 | 1446.0 | 1446.9 | 0.9 |
| 5609 | 1447.0 | 1447.9 | 0.9 |
| 5941 | 1447.2 | 1447.6 | 0.3 |
| 6166 | 1447.4 | 1447.9 | 0.4 |
| 6710.6 | 1449.8 | 1450.0 | 0.2 |
| 7418.7 | 1451.0 | 1450.8 | -0.2 |
| 7758.4 | 1452.0 | 1452.1 | 0.1 |
| 8175.9 | 1452.0 | 1452.5 | 0.5 |
| 8867.3 | 1453.4 | 1454.6 | 1.2 |
| 9359.1 | 1454.5 | 1456.2 | 1.7 |
| 9716.6 | 1455.9 | 1457.3 | 1.4 |
| 10216 | 1456.8 | 1458.4 | 1.6 |
| 10609 | 1458.2 | 1459.5 | 1.4 |
| 11003 | 1459.4 | 1460.3 | 0.9 |
| 11396 | 1460.7 | 1461.3 | 0.6 |
| 11871 | 1462.6 | 1460.1 | -2.4 |
| 12317 | 1464.0 | 1460.7 | -3.3 |
| 12726 | 1465.0 | 1464.5 | -0.5 |
| 13200 | 1467.0 | 1467.0 | 0.0 |
| 13733 | 1468.7 | 1467.9 | -0.8 |
| 14335 | 1469.8 | 1469.2 | -0.6 |
| 14920 | 1471.8 | 1471.4 | -0.4 |
| 15347 | 1473.2 | 1473.8 | 0.6 |
| 15682 | 1475.0 | 1474.8 | -0.2 |
| 16028 | 1476.9 | 1476.9 | 0.0 |
| 16476 | 1478.4 | 1478.2 | -0.1 |
| 16913 | 1480.8 | 1479.3 | -1.6 |
| 17330 | 1483.0 | 1481.0 | -2.0 |
| 17768 | 1485.0 | 1483.7 | -1.3 |

| Table 10-1B – Long-Term Adjustment Bed Elevation-Wide Model | | | |
|---|---|---|---|
| SECTION | Thalweg Elevation | | Change in Thalweg Elevation / Adjustment (ft) |
| | Initial Streambed Elevation | Final Streambed Elevation | |
| 18399 | 1486.0 | 1483.6 | -2.4 |
| 18929 | 1485.0 | 1485.3 | 0.3 |
| 19200 | 1487.7 | 1487.5 | -0.2 |
| 19813 | 1489.4 | 1488.3 | -1.1 |
| 20179 | 1490.7 | 1491.3 | 0.7 |
| 20654 | 1493.0 | 1490.4 | -2.6 |
| 20754 | 1493.4 | 1492.9 | -0.5 |
| 20853 | 1493.8 | 1492.6 | -1.2 |
| 20953 | 1494.2 | 1493.7 | -0.5 |
| 21459 | 1496.0 | 1496.0 | 0.0 |
| 21912 | 1497.5 | 1496.5 | -1.1 |
| 22448 | 1500.0 | 1498.6 | -1.4 |
| 22909 | 1502.0 | 1500.6 | -1.4 |
| 23406 | 1505.0 | 1504.3 | -0.7 |
| 23817 | 1506.0 | 1505.5 | -0.5 |
| 24190 | 1508.0 | 1508.7 | 0.7 |
| 24469 | 1510.0 | 1509.7 | -0.3 |
| 24895 | 1511.0 | 1510.2 | -0.8 |
| 25246 | 1512.0 | 1511.8 | -0.2 |
| 25846 | 1511.3 | 1512.3 | 1.1 |
| 26500 | 1513.0 | 1515.9 | 2.9 |
| 27263 | 1517.0 | 1515.8 | -1.2 |
| 28104 | 1525.0 | 1522.2 | -2.8 |
| 29025 | 1530.0 | 1529.5 | -0.5 |
| 29945 | 1535.0 | 1535.9 | 0.9 |
| 30361 | 1538.0 | 1539.0 | 1.0 |

## 10.2 Long-Term Bed Adjustment with General Adjustment Interspersed in Time

The HEC-18 criteria for evaluating total design bed elevation change combines the general adjustment, long-term adjustment and local scour components of bed change to arrive at a single. The criteria do not indicate special methods for combining these parameters. There is debate in the literature and among sediment transport specialists and modelers as to the impact model results may realize based on where the general adjustment 100-year event may occur in time with respect to the long-term hydrograph. That is, it is possible that the design event occurring prior, following or within the long-term hydrograph may result in significantly different total bed responses. To address this concern, three additional long-term models were run: (1) a model with the design event preceding the long-term hydrograph, (2) a model with the design event in the middle of the long-term hydrograph, and (3) a model with the design event following the design event. The results of these long-term simulations with the design event interspersed within the long-term hydrograph are shown in Table 10.2. The results of the simulations indicated that in the present system, the average difference in bed change for all sections is approximately -0.3 ft. When comparing the maximum changes between models (shown in Table 10.2 in bold) no one model has significantly more maximum or minimum bed change results for all sections. Therefore, no one method is preferable to the others. However, for evaluating the levee design toe-down requirements then a comparison of all the long-term adjustment simulations will be used to determine the "maximum" adjustment at each river section.

**Table 10-2 –** Comparison of Combined General and Long-Term Bed Adjustment Varied by Interspersing the General Hydrograph at the Beginning, Centered and Following the Long-Term Hydrograph

| SECTION | Initial Thalweg Elevation | Adjusted Thalweg Elevation | | | Thalweg Elevation Change from Initial | | |
|---|---|---|---|---|---|---|---|
| | | General Storm Proceeding | General Storm Centered | General Storm Following | Proceeding (ft) | Centered (ft) | Following (ft) |
| 1000 | 1442.7 | 1442.7 | 1442.7 | 1442.7 | 0.0 | 0.0 | 0.0 |
| 1285 | 1442.6 | 1442.4 | 1442.3 | 1442.3 | -0.2 | -0.2 | -0.2 |
| 1677 | 1442.7 | 1443.2 | 1443.2 | 1443.2 | 0.5 | 0.5 | 0.5 |
| 2073 | 1444.2 | 1444.1 | 1444.1 | 1444.1 | -0.1 | -0.1 | -0.1 |
| 2298 | 1444.7 | 1444.4 | 1444.4 | 1444.5 | -0.3 | -0.3 | -0.2 |
| 2581 | 1445.2 | 1444.8 | 1444.8 | 1444.8 | -0.4 | -0.4 | -0.4 |
| 2961 | 1445.7 | 1445.1 | 1445.1 | 1445.1 | -0.6 | -0.6 | -0.6 |
| 3285 | 1442.7 | 1444.8 | 1444.7 | 1444.9 | 2.1 | 2.0 | 2.2 |
| 3671 | 1444.1 | 1444.2 | 1444.7 | 1444.7 | 0.2 | 0.7 | 0.6 |
| 3997 | 1445.0 | 1446.0 | 1445.9 | 1446.1 | 1.0 | 0.9 | 1.1 |
| 4328 | 1445.0 | 1446.1 | 1446.1 | 1446.2 | 1.1 | 1.1 | 1.2 |
| 4684 | 1446.0 | 1447.3 | 1447.4 | 1447.5 | 1.3 | 1.4 | 1.5 |
| 5184 | 1446.0 | 1447.6 | 1447.6 | 1447.7 | 1.6 | 1.6 | 1.7 |
| 5609 | 1447.0 | 1448.7 | 1448.7 | 1448.7 | 1.7 | 1.7 | 1.7 |
| 5941 | 1447.2 | 1448.3 | 1448.3 | 1448.1 | 1.0 | 1.1 | 0.9 |
| 6166 | 1447.4 | 1448.5 | 1448.5 | 1448.4 | 1.0 | 1.1 | 0.9 |
| 6711 | 1449.8 | 1450.5 | 1450.5 | 1450.3 | 0.7 | 0.7 | 0.5 |
| 7419 | 1451.0 | 1451.2 | 1451.3 | 1451.2 | 0.2 | 0.3 | 0.2 |
| 7758 | 1452.0 | 1452.5 | 1452.5 | 1452.4 | 0.5 | 0.5 | 0.4 |
| 8176 | 1452.0 | 1452.8 | 1452.8 | 1452.8 | 0.8 | 0.8 | 0.8 |
| 8867 | 1453.4 | 1455.0 | 1455.0 | 1455.0 | 1.6 | 1.6 | 1.6 |
| 9359 | 1454.5 | 1456.7 | 1456.6 | 1456.7 | 2.2 | 2.1 | 2.2 |
| 9717 | 1455.9 | 1457.7 | 1457.6 | 1457.8 | 1.8 | 1.7 | 1.9 |
| 10216 | 1456.8 | 1458.8 | 1458.6 | 1458.9 | 2.0 | 1.8 | 2.1 |
| 10609 | 1458.2 | 1460.0 | 1459.8 | 1460.1 | 1.8 | 1.6 | 1.9 |
| 11003 | 1459.4 | 1460.7 | 1460.5 | 1460.6 | 1.2 | 1.1 | 1.1 |
| 11396 | 1460.7 | 1461.5 | 1461.5 | 1461.3 | 0.8 | 0.8 | 0.6 |
| 11871 | 1462.6 | 1459.4 | 1459.3 | 1459.0 | -3.1 | -3.3 | -3.6 |
| 12317 | 1464.0 | 1459.9 | 1459.9 | 1460.7 | -4.1 | -4.1 | -3.3 |
| 12726 | 1465.0 | 1464.1 | 1464.3 | 1464.0 | -0.9 | -0.7 | -1.0 |
| 13200 | 1467.0 | 1466.8 | 1467.0 | 1466.9 | -0.2 | 0.0 | -0.1 |
| 13733 | 1468.7 | 1467.5 | 1467.7 | 1467.6 | -1.2 | -1.0 | -1.1 |

**Table 10-2 –** Comparison of Combined General and Long-Term Bed Adjustment Varied by Interspersing the General Hydrograph at the Beginning, Centered and Following the Long-Term Hydrograph

| SECTION | Initial Thalweg Elevation | Adjusted Thalweg Elevation | | | Thalweg Elevation Change from Initial | | |
|---|---|---|---|---|---|---|---|
| | | General Storm Proceeding | General Storm Centered | General Storm Following | Proceeding (ft) | Centered (ft) | Following (ft) |
| 14335 | 1469.8 | 1469.1 | 1468.7 | 1469.6 | -0.7 | -1.1 | -0.2 |
| 14920 | 1471.8 | 1470.6 | 1470.2 | 1469.3 | -1.2 | -1.6 | -2.4 |
| 15347 | 1473.2 | 1472.1 | 1472.2 | 1471.9 | -1.1 | -0.9 | -1.2 |
| 15682 | 1475.0 | 1473.2 | 1474.0 | 1473.4 | -1.8 | -1.0 | -1.6 |
| 16028 | 1476.9 | 1475.6 | 1475.8 | 1475.3 | -1.3 | -1.1 | -1.6 |
| 16476 | 1478.4 | 1476.2 | 1476.5 | 1476.0 | -2.1 | -1.9 | -2.3 |
| 16913 | 1480.8 | 1479.0 | 1479.0 | 1478.8 | -1.9 | -1.8 | -2.0 |
| 17330 | 1482.6 | 1480.2 | 1480.4 | 1479.4 | -2.4 | -2.3 | -3.2 |
| 17768 | 1485.0 | 1482.9 | 1482.7 | 1482.9 | -2.1 | -2.3 | -2.1 |
| 18399 | 1486.0 | 1483.4 | 1483.3 | 1483.1 | -2.6 | -2.7 | -2.9 |
| 18929 | 1485.0 | 1484.4 | 1484.1 | 1484.3 | -0.6 | -0.9 | -0.7 |
| 19200 | 1487.0 | 1487.3 | 1487.1 | 1487.1 | 0.3 | 0.1 | 0.1 |
| 19813 | 1489.4 | 1487.4 | 1486.9 | 1487.6 | -2.0 | -2.5 | -1.8 |
| 20179 | 1490.7 | 1489.3 | 1489.6 | 1489.1 | -1.4 | -1.1 | -1.6 |
| 20654 | 1493.0 | 1491.0 | 1490.7 | 1490.1 | -2.0 | -2.3 | -2.9 |
| 20754 | 1493.4 | 1492.0 | 1491.4 | 1490.5 | -1.4 | -2.0 | -2.9 |
| 20853 | 1493.8 | 1491.4 | 1492.1 | 1491.6 | -2.4 | -1.7 | -2.1 |
| 20953 | 1494.2 | 1493.8 | 1491.4 | 1490.8 | -0.4 | -2.7 | -3.4 |
| 21459 | 1496.0 | 1494.0 | 1495.7 | 1495.7 | -2.0 | -0.3 | -0.3 |
| 21912 | 1497.5 | 1496.4 | 1493.6 | 1494.2 | -1.1 | -3.9 | -3.3 |
| 22448 | 1500.0 | 1498.4 | 1499.7 | 1499.2 | -1.6 | -0.3 | -0.8 |
| 22909 | 1502.0 | 1500.8 | 1500.6 | 1501.1 | -1.2 | -1.4 | -0.9 |
| 23406 | 1505.0 | 1504.2 | 1504.2 | 1504.5 | -0.8 | -0.8 | -0.5 |
| 23817 | 1506.0 | 1505.7 | 1505.6 | 1505.7 | -0.3 | -0.4 | -0.3 |
| 24190 | 1508.0 | 1508.3 | 1508.8 | 1508.4 | 0.3 | 0.8 | 0.4 |
| 24469 | 1510.0 | 1509.7 | 1509.0 | 1509.2 | -0.3 | -1.0 | -0.8 |
| 24895 | 1511.0 | 1509.7 | 1509.8 | 1509.6 | -1.3 | -1.2 | -1.4 |
| 25246 | 1512.0 | 1512.7 | 1512.3 | 1512.5 | 0.7 | 0.3 | 0.5 |
| 25846 | 1511.2 | 1512.4 | 1512.2 | 1512.1 | 1.2 | 1.0 | 0.9 |
| 26500 | 1513.0 | 1517.6 | 1517.3 | 1517.4 | 4.6 | 4.3 | 4.4 |
| 27263 | 1517.0 | 1517.7 | 1517.7 | 1517.6 | 0.7 | 0.7 | 0.6 |
| 28104 | 1525.0 | 1524.0 | 1524.1 | 1523.7 | -1.0 | -0.9 | -1.3 |
| 29025 | 1530.0 | 1529.8 | 1529.6 | 1529.9 | -0.2 | -0.4 | -0.1 |
| 29945 | 1535.0 | 1535.0 | 1534.9 | 1535.3 | 0.0 | -0.1 | 0.3 |
| 30361 | 1538.0 | 1538.8 | 1538.8 | 1538.5 | 0.8 | 0.8 | 0.5 |

### 10.3 Long-Term Bed Adjustment Utilizing Annual Peak and Daily Average Data

The work of Jaffe (2009) suggests that the total volume of stream flows over time is the primary factor for determining long-term bed adjustment in channels of the arid west. It is not clear, however, how peaks in the present system's long-term hydrograph may influence long-term bed change. To test the present model system's sensitivity to flow peaks on long-term bed change, a hydrograph was generated utilizing the available annual peak and daily average stream gage data. This analysis only used the mean daily flows above 5,000 cfs. An examination of yearly peak and daily average data for the same event indicates that the system is very flashy. Since no other information is available peaks are assumed to last 45 minutes based on engineering judgment. Daily averages have been taken and scaled for the full data set as described in *Section 3-Hydrology*. Peak discharges are scaled from the daily averages. The resulting long-term hydrograph, with these peaks, is shown in Figure 10-3. The hydrograph is inserted into the long-term model and the model is rerun.

A comparison of the model output for the long-term model run based on daily averages and the long-term run based on daily averages with peaks is shown in Table 10-3. The table shows that differences in bed elevation at the conclusion of the model runs range from -2.6 to 0.6 feet, with an average difference of -0.1 feet. Hence, the daily average hydrograph produces slightly more degradation than the daily average plus peaks hydrograph. A comparison of the total volume for each hydrograph was determined. The daily average hydrograph, as modeled, has a total volume of 120,353 cfs-days, while the average plus peaks hydrograph, as modeled, has a total volume of 99,685 cfs-days. While there is a slightly larger total volume in the daily average hydrograph, the highest values of the average plus peaks hydrograph is several times higher than the daily average hydrograph.

The results of the procedures were compared for the toedown design and top of levee. The maximum amount of aggradation and maximum amount of degradation was determined for each cross-section. The maximum values were compared for all simulations and the maximum value was incorporated for the design recommendation for the levee design.

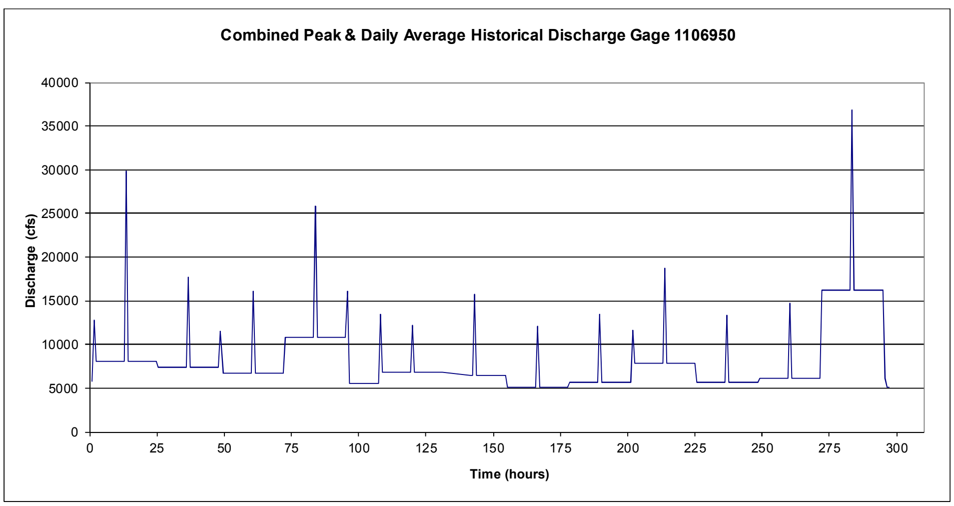


**Figure 10-3 -** Mean Daily Long-Term Hydrograph with Peaks

| **Table 10-3** – Comparison of Daily Average Long-Term Bed Change and Daily Average with Peak Long-Term Bed Change (FT) | | | | | | |
|---|---|---|---|---|---|---|
| **SECTION** | **INITIAL (Thalweg Elevation)** | **AVERAGE ONLY** | | **PEAK & AVERAGE** | | **Difference between Average vs. Peak and Average (ft)** |
| | | **FINAL BED (Thalweg Elevation)** | **BED CHANGE (ft)** | **FINAL BED (Thalweg Elevation)** | **BED CHANGE (ft)** | |
| 1000 | 1442.7 | 1442.7 | 0.0 | 1442.7 | 0.0 | 0.0 |
| 1284.6 | 1442.6 | 1442.4 | -0.2 | 1442.4 | -0.2 | 0.0 |
| 1677 | 1442.7 | 1443.2 | 0.5 | 1443.1 | 0.4 | -0.1 |
| 2072.6 | 1444.2 | 1444.0 | -0.2 | 1444.2 | 0.0 | 0.1 |
| 2298.3 | 1444.7 | 1444.4 | -0.3 | 1444.3 | -0.4 | -0.1 |
| 2580.9 | 1445.2 | 1444.7 | -0.5 | 1444.6 | -0.6 | -0.1 |
| 2960.9 | 1445.7 | 1445.0 | -0.7 | 1445.1 | -0.6 | 0.1 |
| 3284.5 | 1442.7 | 1444.4 | 1.7 | 1444.3 | 1.6 | -0.1 |
| 3670.6 | 1444.1 | 1444.0 | 0.0 | 1444.0 | 0.0 | 0.0 |
| 3997.3 | 1445.0 | 1445.6 | 0.6 | 1445.6 | 0.6 | 0.0 |
| 4327.6 | 1445.0 | 1445.7 | 0.6 | 1445.6 | 0.6 | 0.0 |
| 4684.2 | 1446.0 | 1446.8 | 0.8 | 1446.8 | 0.8 | -0.1 |
| 5183.6 | 1446.0 | 1446.9 | 0.9 | 1446.9 | 0.9 | -0.1 |
| 5609 | 1447.0 | 1447.9 | 0.9 | 1447.9 | 0.9 | -0.1 |
| 5941 | 1447.2 | 1447.6 | 0.3 | 1447.5 | 0.2 | -0.1 |
| 6166 | 1447.4 | 1447.9 | 0.4 | 1447.7 | 0.3 | -0.1 |
| 6710.6 | 1449.8 | 1450.0 | 0.2 | 1449.9 | 0.1 | -0.1 |
| 7418.7 | 1451.0 | 1450.8 | -0.2 | 1450.8 | -0.2 | 0.0 |
| 7758.4 | 1452.0 | 1452.1 | 0.1 | 1452.1 | 0.1 | 0.0 |
| 8175.9 | 1452.0 | 1452.5 | 0.5 | 1452.4 | 0.4 | 0.0 |
| 8867.3 | 1453.4 | 1454.6 | 1.2 | 1454.6 | 1.2 | 0.0 |
| 9359.1 | 1454.5 | 1456.2 | 1.7 | 1456.0 | 1.5 | -0.2 |
| 9716.6 | 1455.9 | 1457.3 | 1.4 | 1457.1 | 1.2 | -0.2 |
| 10216 | 1456.8 | 1458.4 | 1.6 | 1458.3 | 1.5 | -0.1 |
| 10609 | 1458.2 | 1459.5 | 1.4 | 1459.5 | 1.3 | -0.1 |
| 11003 | 1459.4 | 1460.3 | 0.9 | 1460.2 | 0.8 | -0.1 |
| 11396 | 1460.7 | 1461.3 | 0.6 | 1461.2 | 0.5 | -0.1 |
| 11871 | 1462.6 | 1460.1 | -2.4 | 1460.1 | -2.5 | -0.1 |
| 12317 | 1464.0 | 1460.7 | -3.3 | 1460.2 | -3.8 | -0.4 |
| 12726 | 1465.0 | 1464.5 | -0.5 | 1464.6 | -0.4 | 0.1 |
| 13200 | 1467.0 | 1467.0 | 0.0 | 1467.1 | 0.1 | 0.0 |
| 13733 | 1468.7 | 1467.9 | -0.8 | 1467.9 | -0.8 | 0.1 |
| 14335 | 1469.8 | 1469.2 | -0.6 | 1469.4 | -0.4 | 0.2 |
| 14920 | 1471.8 | 1471.4 | -0.4 | 1471.3 | -0.4 | -0.1 |
| 15347 | 1473.2 | 1473.8 | 0.6 | 1473.4 | 0.2 | -0.4 |
| 15682 | 1475.0 | 1474.8 | -0.2 | 1475.0 | 0.0 | 0.2 |
| 16028 | 1476.9 | 1476.9 | 0.0 | 1477.0 | 0.1 | 0.1 |

| **Table 10-3** – Comparison of Daily Average Long-Term Bed Change and Daily Average with Peak Long-Term Bed Change (FT) | | | | | | |
|---|---|---|---|---|---|---|
| **SECTION** | **INITIAL (Thalweg Elevation)** | **AVERAGE ONLY** | | **PEAK & AVERAGE** | | **Difference between Average vs. Peak and Average (ft)** |
| | | **FINAL BED (Thalweg Elevation)** | **BED CHANGE (ft)** | **FINAL BED (Thalweg Elevation)** | **BED CHANGE (ft)** | |
| 16476 | 1478.4 | 1478.2 | -0.1 | 1478.1 | -0.3 | -0.1 |
| 16913 | 1480.8 | 1479.3 | -1.6 | 1479.5 | -1.3 | 0.2 |
| 17330 | 1482.6 | 1481.0 | -1.6 | 1481.2 | -1.4 | 0.2 |
| 17768 | 1485.0 | 1483.7 | -1.3 | 1483.4 | -1.6 | -0.2 |
| 18399 | 1486.0 | 1483.6 | -2.4 | 1483.8 | -2.2 | 0.2 |
| 18929 | 1485.0 | 1485.3 | 0.3 | 1485.9 | 0.9 | 0.6 |
| 19200 | 1487.0 | 1487.5 | 0.5 | 1488.0 | 1.0 | 0.5 |
| 19813 | 1489.4 | 1488.3 | -1.1 | 1488.2 | -1.2 | -0.1 |
| 20179 | 1490.7 | 1491.3 | 0.7 | 1490.0 | -0.7 | -1.4 |
| 20654 | 1493.0 | 1490.4 | -2.6 | 1490.8 | -2.2 | 0.4 |
| 20754 | 1493.4 | 1492.9 | -0.5 | 1490.3 | -3.1 | -2.6 |
| 20853 | 1493.8 | 1492.6 | -1.2 | 1492.9 | -0.9 | 0.3 |
| 20953 | 1494.2 | 1493.7 | -0.5 | 1491.9 | -2.2 | -1.8 |
| 21459 | 1496.0 | 1496.0 | 0.0 | 1496.1 | 0.1 | 0.0 |
| 21912 | 1497.5 | 1496.5 | -1.1 | 1495.5 | -2.0 | -0.9 |
| 22448 | 1500.0 | 1498.6 | -1.4 | 1499.1 | -0.9 | 0.6 |
| 22909 | 1502.0 | 1500.6 | -1.4 | 1500.9 | -1.1 | 0.3 |
| 23406 | 1505.0 | 1504.3 | -0.7 | 1504.6 | -0.4 | 0.2 |
| 23817 | 1506.0 | 1505.5 | -0.5 | 1506.1 | 0.1 | 0.6 |
| 24190 | 1508.0 | 1508.7 | 0.7 | 1509.2 | 1.2 | 0.5 |
| 24469 | 1510.0 | 1509.7 | -0.3 | 1509.9 | -0.1 | 0.2 |
| 24895 | 1511.0 | 1510.2 | -0.8 | 1510.3 | -0.7 | 0.0 |
| 25246 | 1512.0 | 1511.8 | -0.2 | 1511.7 | -0.3 | -0.1 |
| 25846 | 1511.2 | 1512.3 | 1.1 | 1512.3 | 1.1 | 0.0 |
| 26500 | 1513.0 | 1515.9 | 2.9 | 1515.8 | 2.8 | -0.1 |
| 27263 | 1517.0 | 1515.8 | -1.2 | 1515.3 | -1.7 | -0.5 |
| 28104 | 1525.0 | 1522.2 | -2.8 | 1522.4 | -2.6 | 0.2 |
| 29025 | 1530.0 | 1529.5 | -0.5 | 1529.5 | -0.5 | 0.0 |
| 29945 | 1535.0 | 1535.9 | 0.9 | 1535.8 | 0.8 | -0.1 |
| 30361 | 1538.0 | 1539.0 | 1.0 | 1539.0 | 1.0 | 0.0 |

## 10.4 Maximum Long-Term Bed Adjustment Comparison of Different Simulation Conditions

The results of the different long-term simulations were compared in order to evaluate the maximum streambed adjustment. This comparison is illustrated in the following table and graph. The table illustrates the controlling simulation condition for the maximum value using the following abbreviations: LT – Wide Long-Term Simulation, DA – Daily Average Flow, or DP – Daily average plus peak. The table comparison illustrates that the Long-Term Wide model simulation was the controlling condition for a majority. In addition, the maximum values from the simulations which integrated both the long-term hydrograph with the general 100-year storm hydrograph were compared to sum of the maximum values for the individual long-term and general storm simulations. The maximum value between either the combined or the summed individual values was utilized for the design of the levee. Graphically it illustrates trends that you would expect in that (1) the maximum deposition occurs generally upstream and downstream of the levee area where there is a widened floodplain, (2) locations of scour generally occur in the narrowed or confined floodplain width of the levee system, (3) maximum scour occurs at the locations where there is a bridge contraction.

**Table 10-4** – Comparison of Different Long-Term Simulations to Evaluate Max Streambed Adjustment

| SECTION | Proposed Long-Term Adjustment (Thalweg Change) | | | Comparison | | | |
|---|---|---|---|---|---|---|---|
| | | | | Aggradation | | Degradation | |
| | LT-Wide (ft) | Daily Avg Q (ft) | Daily +Peak Q (ft) | Max Agrad (ft) | Control Cond. | Max Scour (ft) | Control Cond. |
| 1000 | 0.00 | 0.00 | 0.00 | **0.00** | | **0.00** | |
| 1285 | -0.19 | -0.19 | -0.20 | **0.00** | | **-0.20** | DP |
| 1677 | 0.54 | 0.53 | 0.43 | **0.54** | LT | **0.00** | LT |
| 2073 | -0.08 | -0.17 | -0.03 | **0.00** | | **-0.17** | DA |
| 2298 | -0.23 | -0.29 | -0.38 | **0.00** | | **-0.38** | DP |
| 2581 | -0.38 | -0.46 | -0.57 | **0.00** | | **-0.57** | DP |
| 2961 | -0.58 | -0.69 | -0.58 | **0.00** | | **-0.69** | DA |
| 3285 | 2.04 | 1.66 | 1.59 | **2.04** | LT | **0.00** | |
| 3671 | -0.05 | -0.05 | -0.02 | **0.00** | | **-0.05** | DA |
| 3997 | 0.96 | 0.61 | 0.57 | **0.96** | LT | **0.00** | |
| 4328 | 1.05 | 0.64 | 0.60 | **1.05** | LT | **0.00** | |
| 4684 | 1.33 | 0.82 | 0.75 | **1.33** | LT | **0.00** | |
| 5184 | 1.60 | 0.93 | 0.86 | **1.60** | LT | **0.00** | |
| 5609 | 1.71 | 0.94 | 0.86 | **1.71** | LT | **0.00** | |
| 5941 | 1.10 | 0.34 | 0.24 | **1.10** | LT | **0.00** | |
| 6166 | 1.15 | 0.42 | 0.32 | **1.15** | LT | **0.00** | |
| 6711 | 0.80 | 0.17 | 0.05 | **0.80** | LT | **0.00** | |
| 7419 | 0.42 | -0.17 | -0.21 | **0.42** | LT | **-0.21** | DP |
| 7758 | 0.66 | 0.10 | 0.08 | **0.66** | LT | **0.00** | |
| 8176 | 0.96 | 0.47 | 0.44 | **0.96** | LT | **0.00** | |
| 8867 | 1.80 | 1.18 | 1.17 | **1.80** | LT | **0.00** | |
| 9359 | 2.43 | 1.71 | 1.55 | **2.43** | LT | **0.00** | |
| 9717 | 2.07 | 1.35 | 1.19 | **2.07** | LT | **0.00** | |
| 10216 | 2.24 | 1.57 | 1.46 | **2.24** | LT | **0.00** | |
| 10609 | 2.01 | 1.35 | 1.29 | **2.01** | LT | **0.00** | |
| 11003 | 1.44 | 0.92 | 0.82 | **1.44** | LT | **0.00** | |
| 11396 | 1.01 | 0.64 | 0.53 | **1.01** | LT | **0.00** | |
| 11871 | -3.18 | -2.45 | -2.51 | **0.00** | | **-3.18** | LT |

| Table 10-4 – Comparison of Different Long-Term Simulations to Evaluate Max Streambed Adjustment | | | | | | | |
|---|---|---|---|---|---|---|---|
| **SECTION** | **Proposed Long-Term Adjustment (Thalweg Change)** | | | **Comparison** | | | |
| | | | | **Aggradation** | | **Degradation** | |
| | **LT-Wide (ft)** | **Daily Avg Q (ft)** | **Daily +Peak Q (ft)** | **Max Agrad (ft)** | **Control Cond.** | **Max Scour (ft)** | **Control Cond.** |
| 12317 | -4.14 | -3.35 | -3.79 | **0.00** | | **-4.14** | LT |
| 12726 | -0.81 | -0.51 | -0.43 | **0.00** | | **-0.81** | LT |
| 13200 | -0.19 | 0.04 | 0.06 | **0.06** | DP | **-0.19** | LT |
| 13733 | -1.02 | -0.84 | -0.78 | **0.00** | | **-1.02** | LT |
| 14335 | -0.82 | -0.62 | -0.41 | **0.00** | | **-0.82** | LT |
| 14920 | -1.60 | -0.36 | -0.44 | **0.00** | | **-1.60** | LT |
| 15347 | -0.83 | 0.60 | 0.20 | **0.60** | DA | **-0.83** | LT |
| 15682 | -1.25 | -0.17 | 0.01 | **0.01** | DP | **-1.25** | LT |
| 16028 | -1.41 | 0.00 | 0.05 | **0.05** | DP | **-1.41** | LT |
| 16476 | -2.24 | -0.14 | -0.28 | **0.00** | | **-2.24** | LT |
| 16913 | -2.16 | -1.56 | -1.33 | **0.00** | | **-2.16** | LT |
| 17330 | -3.62 | -1.65 | -1.40 | **0.00** | | **-3.62** | LT |
| 17768 | -2.11 | -1.32 | -1.56 | **0.00** | | **-2.11** | LT |
| 18399 | -2.74 | -2.40 | -2.18 | **0.00** | | **-2.74** | LT |
| 18929 | -0.78 | 0.27 | 0.91 | **0.91** | DP | **-0.78** | LT |
| 19200 | -0.59 | 0.53 | 1.00 | **1.00** | DP | **-0.59** | LT |
| 19813 | -1.94 | -1.05 | -1.20 | **0.00** | | **-1.94** | LT |
| 20179 | -0.89 | 0.67 | -0.70 | **0.67** | DA | **-0.89** | LT |
| 20654 | -2.93 | -2.62 | -2.17 | **0.00** | | **-2.93** | LT |
| 20754 | -2.89 | -0.52 | -3.09 | **0.00** | | **-3.09** | DP |
| 20853 | -2.01 | -1.20 | -0.87 | **0.00** | | **-2.01** | LT |
| 20953 | -3.63 | -0.46 | -2.25 | **0.00** | | **-3.63** | LT |
| 21459 | -0.11 | 0.01 | 0.06 | **0.06** | DP | **-0.11** | LT |
| 21912 | -3.52 | -1.05 | -1.96 | **0.00** | | **-3.52** | LT |
| 22448 | -0.65 | -1.43 | -0.86 | **0.00** | | **-1.43** | LT |
| 22909 | -0.89 | -1.40 | -1.10 | **0.00** | | **-1.40** | DA |
| 23406 | -0.46 | -0.66 | -0.45 | **0.00** | | **-0.66** | DA |
| 23817 | -0.43 | -0.50 | 0.12 | **0.12** | DP | **-0.50** | DA |
| 24190 | 0.70 | 0.66 | 1.17 | **1.17** | DP | **0.00** | |
| 24469 | -1.02 | -0.30 | -0.06 | **0.00** | | **-1.02** | LT |
| 24895 | -1.65 | -0.76 | -0.73 | **0.00** | | **-1.65** | LT |
| 25246 | 0.50 | -0.19 | -0.32 | **0.50** | LT | **-0.32** | DP |
| 25846 | 0.73 | 1.13 | 1.12 | **1.13** | DA | **0.00** | |
| 26500 | 4.32 | 2.92 | 2.84 | **4.32** | LT | **0.00** | |
| 27263 | 0.33 | -1.24 | -1.70 | **0.33** | DP | **-1.70** | DP |
| 28104 | -1.18 | -2.81 | -2.60 | **0.00** | | **-2.81** | DA |

| Table 10-4 – Comparison of Different Long-Term Simulations to Evaluate Max Streambed Adjustment | | | | | | | |
|---|---|---|---|---|---|---|---|
| SECTION | Proposed Long-Term Adjustment (Thalweg Change) | | | Comparison | | | |
| | | | | Aggradation | | Degradation | |
| | LT-Wide (ft) | Daily Avg Q (ft) | Daily +Peak Q (ft) | Max Agrad (ft) | Control Cond. | Max Scour (ft) | Control Cond. |
| 29025 | -0.36 | -0.51 | -0.46 | **0.00** | | **-0.51** | DA |
| 29945 | 0.13 | 0.87 | 0.79 | **0.87** | DA | **0.00** | |
| 30361 | 0.80 | 1.03 | 0.98 | **1.03** | DA | **0.00** | |

The following table presents the evaluation of the combined Long-term and General adjustment components for use in the design of the levee system. The maximum adjustment of the individual simulations for Long-term and General adjustment were summed and then compared to the simulation which combined the long-term and general hydrographs. The maximum of the combined long-term/general adjustment is used for both the levee design toe down and top elevation profile.

**Table 10-5 –** Evaluation of Combined Long-Term and General Adjustment Components for Use in Design of the Levee System

| River Sta. SECTION | Max LT (ft) | Max Gen (ft) | Sum Max (ft) | Min LT (ft) | Min Gen (ft) | Sum Min (ft) | Combined LT and General | | | Max | Min | Max Aggrad | Max Scour |
|---|---|---|---|---|---|---|---|---|---|---|---|---|---|
| | | | | | | | DP-lo | DC-lo | DF-lo | | | | |
| 1000 | 0.0 | 0.0 | 0.0 | 0.0 | 0.0 | | 0.00 | 0.00 | 0.00 | 0.00 | 0.00 | 0.0 | 0.0 |
| 1285 | -0.2 | 0.0 | 0.0 | -0.2 | -0.4 | -0.6 | -0.20 | -0.23 | -0.25 | -0.20 | -0.25 | 0.00 | -0.58 |
| 1677 | 0.5 | 0.1 | 0.6 | 0.4 | 0.0 | | 0.55 | 0.48 | 0.53 | 0.55 | 0.48 | 0.60 | 0.00 |
| 2073 | 0.0 | 0.0 | 0.0 | -0.2 | 0.0 | -0.2 | -0.11 | -0.12 | -0.06 | -0.06 | -0.12 | 0.00 | -0.22 |
| 2298 | -0.2 | 0.0 | 0.0 | -0.4 | -0.1 | -0.4 | -0.26 | -0.28 | -0.23 | -0.23 | -0.28 | 0.00 | -0.43 |
| 2581 | -0.4 | 0.0 | 0.0 | -0.6 | -0.1 | -0.6 | -0.39 | -0.43 | -0.41 | -0.39 | -0.43 | 0.00 | -0.63 |
| 2961 | -0.6 | 0.0 | 0.0 | -0.7 | -0.1 | -0.7 | -0.60 | -0.62 | -0.57 | -0.57 | -0.62 | 0.00 | -0.75 |
| 3285 | 2.0 | 0.2 | 2.3 | 1.6 | 0.0 | | 2.06 | 2.00 | 2.16 | 2.16 | 2.00 | 2.27 | 0.00 |
| 3671 | 0.0 | 0.2 | 0.2 | 0.0 | 0.0 | | 0.20 | 0.69 | 0.63 | 0.69 | 0.20 | 0.69 | 0.00 |
| 3997 | 1.0 | 0.2 | 1.2 | 0.6 | 0.0 | | 0.98 | 0.91 | 1.08 | 1.08 | 0.91 | 1.16 | 0.00 |
| 4328 | 1.0 | 0.1 | 1.2 | 0.6 | 0.0 | | 1.06 | 1.07 | 1.23 | 1.23 | 1.06 | 1.23 | 0.00 |
| 4684 | 1.3 | 0.2 | 1.5 | 0.8 | 0.0 | | 1.33 | 1.39 | 1.50 | 1.50 | 1.33 | 1.52 | 0.00 |
| 5184 | 1.6 | 0.1 | 1.8 | 0.9 | 0.0 | | 1.58 | 1.65 | 1.67 | 1.67 | 1.58 | 1.75 | 0.00 |
| 5609 | 1.7 | 0.2 | 1.9 | 0.9 | 0.0 | | 1.66 | 1.71 | 1.66 | 1.71 | 1.66 | 1.90 | 0.00 |
| 5941 | 1.1 | 0.0 | 1.0 | 0.2 | -0.3 | -0.3 | 1.01 | 1.05 | 0.90 | 1.05 | 0.90 | 1.05 | -0.30 |
| 6166 | 1.1 | 0.0 | 1.2 | 0.3 | 0.0 | | 1.04 | 1.08 | 0.94 | 1.08 | 0.94 | 1.18 | 0.00 |
| 6711 | 0.8 | 0.1 | 0.9 | 0.1 | 0.0 | | 0.68 | 0.69 | 0.52 | 0.69 | 0.52 | 0.88 | 0.00 |
| 7419 | 0.4 | 0.0 | 0.4 | -0.2 | -0.3 | -0.5 | 0.23 | 0.27 | 0.19 | 0.27 | 0.19 | 0.42 | -0.49 |
| 7758 | 0.7 | 0.0 | 0.7 | 0.1 | 0.0 | | 0.47 | 0.51 | 0.44 | 0.51 | 0.44 | 0.67 | 0.00 |

**Table 10-5 –** Evaluation of Combined Long-Term and General Adjustment Components for Use in Design of the Levee System

| River Sta. SECTION | Max LT (ft) | Max Gen (ft) | Sum Max (ft) | Min LT (ft) | Min Gen (ft) | Sum Min (ft) | Combined LT and General | | | Max | Min | Max Aggrad | Max Scour |
|---|---|---|---|---|---|---|---|---|---|---|---|---|---|
| | | | | | | | DP-lo | DC-lo | DF-lo | | | | |
| 8176 | 1.0 | 0.0 | 1.0 | 0.4 | 0.0 | | 0.79 | 0.81 | 0.79 | 0.81 | 0.79 | 0.98 | 0.00 |
| 8867 | 1.8 | 0.1 | 1.9 | 1.2 | 0.0 | | 1.64 | 1.61 | 1.60 | 1.64 | 1.60 | 1.92 | 0.00 |
| 9359 | 2.4 | 0.3 | 2.7 | 1.5 | 0.1 | | 2.19 | 2.12 | 2.25 | 2.25 | 2.12 | 2.74 | 0.00 |
| 9717 | 2.1 | 0.0 | 2.1 | 1.2 | 0.0 | | 1.82 | 1.67 | 1.93 | 1.93 | 1.67 | 2.10 | 0.00 |
| 10216 | 2.2 | 0.2 | 2.5 | 1.5 | 0.0 | | 1.98 | 1.81 | 2.05 | 2.05 | 1.81 | 2.48 | 0.00 |
| 10609 | 2.0 | 0.1 | 2.1 | 1.3 | 0.0 | | 1.78 | 1.62 | 1.94 | 1.94 | 1.62 | 2.12 | 0.00 |
| 11003 | 1.4 | 0.0 | 1.5 | 0.8 | 0.0 | | 1.24 | 1.09 | 1.13 | 1.24 | 1.09 | 1.46 | 0.00 |
| 11396 | 1.0 | 0.0 | 1.0 | 0.5 | -0.1 | -0.1 | 0.84 | 0.80 | 0.64 | 0.84 | 0.64 | 1.03 | -0.10 |
| 11871 | -2.4 | 0.4 | 0.4 | -3.2 | 0.1 | -3.2 | -3.12 | -3.26 | -3.56 | -3.12 | -3.56 | 0.40 | -3.56 |
| 12317 | -3.3 | -0.4 | 0.0 | -4.1 | -1.1 | -5.2 | -4.14 | -4.11 | -3.35 | -3.35 | -4.14 | 0.00 | -5.22 |
| 12726 | -0.4 | 0.1 | 0.1 | -0.8 | 0.0 | -0.9 | -0.93 | -0.73 | -0.98 | -0.73 | -0.98 | 0.10 | -0.98 |
| 13200 | 0.1 | 0.2 | 0.3 | -0.2 | 0.0 | -0.2 | -0.21 | -0.04 | -0.13 | -0.04 | -0.21 | 0.30 | -0.21 |
| 13733 | -0.8 | -0.1 | 0.0 | -1.0 | -0.4 | -1.4 | -1.22 | -0.98 | -1.09 | -0.98 | -1.22 | 0.00 | -1.42 |
| 14335 | -0.4 | 0.2 | 0.2 | -0.8 | 0.1 | -0.8 | -0.66 | -1.08 | -0.18 | -0.18 | -1.08 | 0.20 | -1.08 |
| 14920 | -0.4 | -0.1 | 0.0 | -1.6 | -0.3 | -1.9 | -1.20 | -1.55 | -2.41 | -1.20 | -2.41 | 0.00 | -2.41 |
| 15347 | 0.6 | 0.3 | 0.9 | -0.8 | 0.0 | -0.8 | -1.09 | -0.95 | -1.22 | -0.95 | -1.22 | 0.90 | -1.22 |
| 15682 | 0.0 | 0.1 | 0.1 | -1.3 | -0.3 | -1.6 | -1.77 | -0.99 | -1.63 | -0.99 | -1.77 | 0.10 | -1.77 |
| 16028 | 0.1 | 0.2 | 0.3 | -1.4 | 0.1 | | -1.30 | -1.11 | -1.63 | -1.11 | -1.63 | 0.30 | -1.63 |
| 16476 | -0.1 | -0.1 | 0.0 | -2.2 | -0.7 | -2.9 | -2.10 | -1.87 | -2.34 | -1.87 | -2.34 | 0.00 | -2.92 |
| 16913 | -1.3 | 0.0 | 0.0 | -2.2 | 0.0 | -2.2 | -1.88 | -1.83 | -2.03 | -1.83 | -2.03 | 0.00 | -2.18 |
| 17330 | -1.4 | 0.2 | 0.2 | -3.6 | -0.1 | -3.7 | -2.41 | -2.26 | -3.18 | -2.26 | -3.18 | 0.20 | -3.67 |
| 17768 | -1.3 | -0.1 | | -2.1 | -0.5 | -2.6 | -2.13 | -2.32 | -2.06 | -2.06 | -2.32 | 0.00 | -2.56 |
| 18399 | -2.2 | -0.1 | | -2.7 | -0.7 | -3.5 | -2.57 | -2.73 | -2.87 | -2.57 | -2.87 | 0.00 | -3.45 |
| 18929 | 0.9 | 0.6 | 1.5 | -0.8 | 0.1 | | -0.64 | -0.89 | -0.67 | -0.64 | -0.89 | 1.50 | -0.89 |
| 19200 | 1.0 | 0.1 | 1.1 | -0.6 | 0.0 | -0.6 | 0.25 | 0.07 | 0.08 | 0.25 | 0.07 | 1.10 | -0.59 |
| 19813 | -1.1 | 0.0 | 0.0 | -1.9 | -0.1 | -2.0 | -2.05 | -2.49 | -1.81 | -1.81 | -2.49 | 0.00 | -2.49 |
| 20179 | 0.7 | 0.3 | 1.0 | -0.9 | 0.0 | -0.9 | -1.40 | -1.06 | -1.57 | -1.06 | -1.57 | 1.00 | -1.57 |
| 20654 | -2.2 | 0.1 | 0.1 | -2.9 | 0.0 | -2.9 | -2.01 | -2.29 | -2.91 | -2.01 | -2.91 | 0.10 | -2.91 |
| 20754 | -0.5 | 0.1 | 0.1 | -3.1 | -0.2 | -3.2 | -1.38 | -1.97 | -2.86 | -1.38 | -2.86 | 0.10 | -3.25 |

**Table 10-5 –** Evaluation of Combined Long-Term and General Adjustment Components for Use in Design of the Levee System

| River Sta. SECTION | Max LT (ft) | Max Gen (ft) | Sum Max (ft) | Min LT (ft) | Min Gen (ft) | Sum Min (ft) | Combined LT and General | | | Max | Min | Max Aggrad | Max Scour |
|---|---|---|---|---|---|---|---|---|---|---|---|---|---|
| | | | | | | | DP-lo | DC-lo | DF-lo | | | | |
| 20853 | -0.9 | 0.2 | 0.2 | -2.0 | -0.2 | -2.2 | -2.39 | -1.70 | -2.14 | -1.70 | -2.39 | 0.20 | -2.39 |
| 20953 | -0.5 | 0.0 | 0.0 | -3.6 | -0.7 | -4.4 | -0.43 | -2.74 | -3.40 | -0.43 | -3.40 | 0.00 | -4.36 |
| 21459 | 0.1 | 0.2 | 0.3 | -0.1 | 0.0 | -0.1 | -2.00 | -0.32 | -0.29 | -0.29 | -2.00 | 0.30 | -2.00 |
| 21912 | -1.1 | -0.1 | 0.0 | -3.5 | -0.4 | -3.9 | -1.11 | -3.91 | -3.34 | -1.11 | -3.91 | 0.00 | -3.91 |
| 22448 | -0.7 | 0.0 | 0.0 | -1.4 | -0.3 | -1.7 | -1.58 | -0.34 | -0.81 | -0.34 | -1.58 | 0.00 | -1.68 |
| 22909 | -0.9 | 0.3 | 0.3 | -1.4 | -0.1 | -1.4 | -1.17 | -1.38 | -0.91 | -0.91 | -1.38 | 0.30 | -1.45 |
| 23406 | -0.4 | 0.0 | 0.0 | -0.7 | -0.1 | -0.8 | -0.78 | -0.77 | -0.46 | -0.46 | -0.78 | 0.00 | -0.78 |
| 23817 | 0.1 | -0.1 | 0.1 | -0.5 | -0.7 | -1.2 | -0.30 | -0.45 | -0.30 | -0.30 | -0.45 | 0.10 | -1.15 |
| 24190 | 1.2 | 0.6 | 1.8 | 0.7 | 0.1 | | 0.33 | 0.82 | 0.38 | 0.82 | 0.33 | 1.80 | 0.00 |
| 24469 | -0.1 | 0.2 | 0.2 | -1.0 | 0.0 | -1.1 | -0.28 | -0.98 | -0.81 | -0.28 | -0.98 | 0.20 | -1.06 |
| 24895 | -0.7 | -0.1 | 0.0 | -1.7 | -0.9 | -2.6 | -1.34 | -1.17 | -1.43 | -1.17 | -1.43 | 0.00 | -2.57 |
| 25246 | 0.5 | 0.0 | 0.5 | -0.3 | -0.4 | -0.7 | 0.72 | 0.28 | 0.45 | 0.72 | 0.28 | 0.72 | -0.67 |
| 25846 | 1.1 | 0.5 | 1.6 | 0.7 | 0.1 | | 1.16 | 0.96 | 0.88 | 1.16 | 0.88 | 1.60 | 0.00 |
| 26500 | 4.3 | 0.8 | 5.1 | 2.8 | 0.1 | | 4.57 | 4.27 | 4.38 | 4.57 | 4.27 | 5.10 | 0.00 |
| 27263 | 0.3 | -0.1 | 0.3 | -1.7 | -1.1 | -2.8 | 0.75 | 0.69 | 0.61 | 0.75 | 0.61 | 0.75 | -2.77 |
| 28104 | -1.2 | 0.0 | 0.0 | -2.8 | -0.2 | -3.0 | -0.99 | -0.91 | -1.34 | -0.91 | -1.34 | 0.00 | -3.03 |
| 29025 | -0.4 | 0.4 | 0.4 | -0.5 | 0.0 | -0.5 | -0.19 | -0.41 | -0.07 | -0.07 | -0.41 | 0.40 | -0.51 |
| 29945 | 0.9 | 0.0 | 0.9 | 0.1 | -0.1 | -0.1 | -0.01 | -0.07 | 0.33 | 0.33 | -0.07 | 0.90 | -0.10 |
| 30361 | 1.0 | 2.1 | 3.1 | 0.8 | 0.1 | | 0.83 | 0.78 | 0.51 | 0.83 | 0.51 | 3.10 | 0.00 |

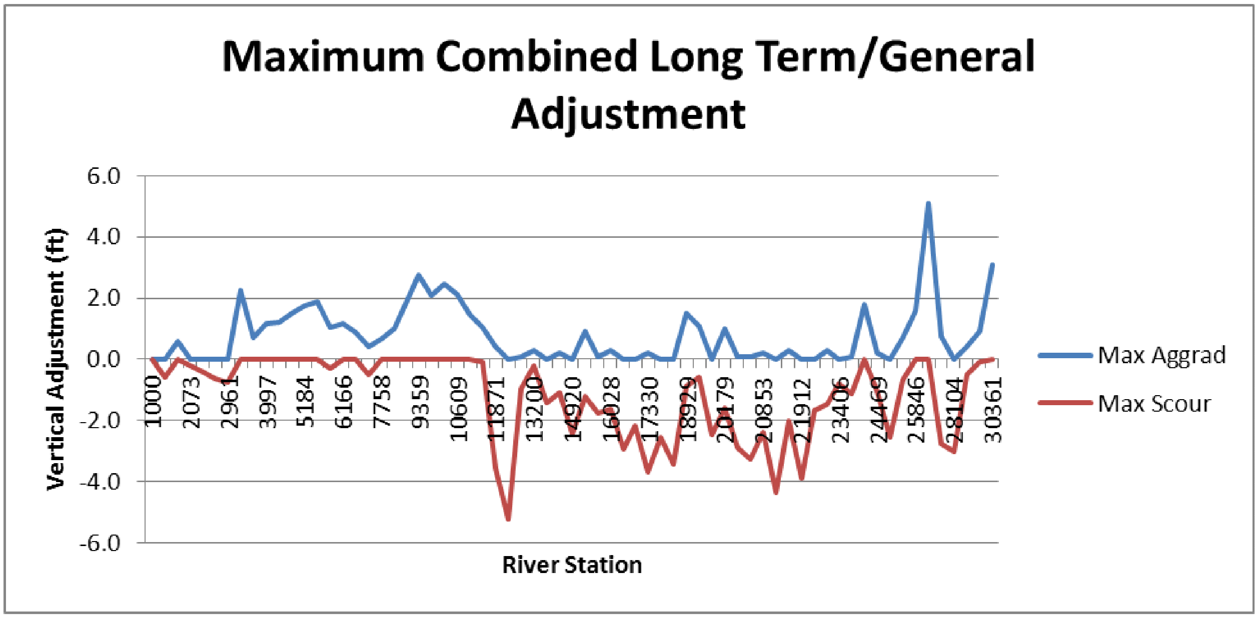


**Figure 10-4 –** Comparison of the maximum aggradation or degradation from the different scenarios of HEC-6T model with the combined Long Term and General Storm streambed adjustment

# 11 Other Adjustment

## 11.1 Overview

Other scour comprises the local scour components. For this study, these components are those that occur as a result of the presence of a bridge. The impacts of the other scour components are generally limited the vicinity of the bridge that causes them; however, they are significant because they are frequently many times larger than the long-term or general adjustment components of scour. In this study, the other scour components considered are contraction scour, pier scour and abutment scour. All three are calculated using the HEC number 18 procedures in HEC-RAS.

### *11.1.1 Contraction Scour*

Contraction scour occurs when the flow area of a stream is reduced by a natural contraction in the channel, a bridge or another structure that restricts the flow. At a contraction, several different factors can contribute to the occurrence of contraction scour. These factors may include natural channel contraction; the presence of road embankments at the approach to the bridge; bridge abutments projecting into the main channel; bridge piers are blocking a significant portion of the flow area; or a drop in the downstream tailwater, which causes increased velocities inside the bridge. There are two forms of contraction scour that can occur and are a function of the quantity of bed material being transported upstream of the contraction reach: live-bed contraction scour and clear-water contraction scour. Live-bed contraction scour occurs when sediment-laden water flows into the contracted section, while clear-water contraction scour occurs when sediment transport in upstream of the contraction is negligible. Local scour from contraction at bridges is taken from HEC-RAS HEC-18 output presented in Section 8. Bridge contraction is also accounted for in HEC-6 modeling and not removed to be conservative.

### *11.1.2 Local Scour at Piers*

Pier scour is a function of the acceleration of flow around the pier and the formation of flow vortices. The vortices remove material from the base of the pier, forming a scour depression. As the depth of scour increases, the magnitude of the vortex decreases reducing the rate of scour. The factors that control the depth of local scour at a pier are: velocity of the flow; depth of flow; width of the pier; length of the pier in the flow; gradation of bed material; angle of attack of flow; shape of the pier; and debris. Local scour from piers is taken from HEC-RAS HEC-18 output presented in Section 8.

### *11.1.3 Local Scour at Abutments*

Local scour at abutments occurs when an abutment obstructs the flow. The obstruction of the flow forms a vortex at the upstream end of the abutment and running along the toe of the abutment, and also at the downstream end of the abutment. Local scour from abutments is taken from HEC-RAS HEC-18 output presented in Section 8.

## 11.2 Modeling

### *11.2.1 Bedform Height*

Supercritical flow conditions can result in the formation of anti-dunes in a sand bed channel. The trough of the anti-dune can result in bedform height, which can estimated using Kennedy's equation of the form:

$$H=0.027V^2$$

where H is the bedform height and V is the velocity. Since bedforms have both positive and negative components like sine waves, for example, only half of the value of the bedform (H/2) is used to account for aggradation or degradation.

Equations for (1) pier, (2) abutment, and (3) contraction scour are presented in *Section 8*.

## 11.3 Results

Other scour is determined by calculating the sum HEC-18 bridge scour (LS), low-flow incisement (I), which is assumed to be 2 ft based on site visits, bend scour (BS), which was found to be zero for all sections, and bed from height (H/2). The results of the local are shown in Table 11-1. Detailed calculations are included in the Appendix.

**Table 11-1** – Other Scour Components (FT): Local Scour (LS, Bedform Height (H/2), Low-Flow Incisement (I)

| SECTION | LS | H/2 | I | TOTAL |
|---|---|---|---|---|
| 1000 | 0.0 | 0.5 | 2.0 | 2.5 |
| 1285 | 0.0 | 0.5 | 2.0 | 2.5 |
| 1677 | 0.0 | 0.4 | 2.0 | 2.4 |
| 2073 | 0.0 | 0.9 | 2.0 | 2.9 |
| 2298 | 0.0 | 0.9 | 2.0 | 2.9 |
| 2581 | 0.0 | 0.6 | 2.0 | 2.6 |
| 2961 | 0.0 | 0.7 | 2.0 | 2.7 |
| 3285 | 0.0 | 0.9 | 2.0 | 2.9 |
| 3671 | 0.0 | 0.8 | 2.0 | 2.8 |
| 3997 | 0.0 | 0.9 | 2.0 | 2.9 |
| 4328 | 0.0 | 0.8 | 2.0 | 2.8 |
| 4684 | 0.0 | 1.0 | 2.0 | 3.0 |
| 5184 | 0.0 | 0.7 | 2.0 | 2.7 |
| 5609 | 0.0 | 0.6 | 2.0 | 2.6 |
| 5941 | 0.0 | 0.8 | 2.0 | 2.8 |
| 6166 | 0.0 | 0.6 | 2.0 | 2.6 |
| 6711 | 0.0 | 0.8 | 2.0 | 2.8 |
| 7419 | 0.0 | 2.1 | 2.0 | 4.1 |
| 7758 | 0.0 | 1.9 | 2.0 | 3.9 |
| 8176 | 0.0 | 1.8 | 2.0 | 3.8 |
| 8867 | 0.0 | 2.4 | 2.0 | 4.4 |
| 9359 | 0.0 | 1.4 | 2.0 | 3.4 |
| 9717 | 0.0 | 1.7 | 2.0 | 3.7 |
| 10216 | 0.0 | 0.6 | 2.0 | 2.6 |
| 10609 | 3.4 | 0.4 | 2.0 | 5.8 |
| 11003 | 0.0 | 0.5 | 2.0 | 2.5 |
| 11396 | 0.0 | 0.6 | 2.0 | 2.6 |
| 11871 | 0.0 | 0.6 | 2.0 | 2.6 |
| 12317 | 0.0 | 0.7 | 2.0 | 2.7 |
| 12726 | 0.0 | 0.7 | 2.0 | 2.7 |
| 13200 | 0.0 | 0.6 | 2.0 | 2.6 |
| 13733 | 0.0 | 0.5 | 2.0 | 2.5 |
| 14335 | 0.0 | 0.5 | 2.0 | 2.5 |
| 14920 | 0.0 | 0.5 | 2.0 | 2.5 |
| 15347 | 0.0 | 0.5 | 2.0 | 2.5 |

| **Table 11-1** – Other Scour Components (FT): Local Scour (LS, Bedform Height (H/2), Low-Flow Incisement (I) | | | | |
|---|---|---|---|---|
| **SECTION** | **LS** | **H/2** | **I** | **TOTAL** |
| 15682 | 0.0 | 0.6 | 2.0 | 2.6 |
| 16028 | 0.0 | 0.5 | 2.0 | 2.5 |
| 16476 | 0.0 | 0.7 | 2.0 | 2.7 |
| 16913 | 0.0 | 0.8 | 2.0 | 2.8 |
| 17330 | 0.0 | 1.0 | 2.0 | 3.0 |
| 17768 | 0.0 | 0.8 | 2.0 | 2.8 |
| 18399 | 0.0 | 0.7 | 2.0 | 2.7 |
| 18929 | 0.0 | 0.6 | 2.0 | 2.6 |
| 19200 | 0.0 | 0.5 | 2.0 | 2.5 |
| 19813 | 0.0 | 0.5 | 2.0 | 2.5 |
| 20179 | 0.0 | 0.4 | 2.0 | 2.4 |
| 20654 | 0.0 | 0.4 | 2.0 | 2.4 |
| 20754 | 3.4 | 0.4 | 2.0 | 5.8 |
| 20853 | 0.0 | 0.5 | 2.0 | 2.5 |
| 20953 | 0.0 | 0.8 | 2.0 | 2.8 |
| 21459 | 0.0 | 0.6 | 2.0 | 2.6 |
| 21912 | 0.0 | 0.5 | 2.0 | 2.5 |
| 22448 | 0.0 | 0.5 | 2.0 | 2.5 |
| 22909 | 0.0 | 0.3 | 2.0 | 2.3 |
| 23406 | 0.0 | 0.2 | 2.0 | 2.2 |
| 23817 | 0.0 | 0.2 | 2.0 | 2.2 |
| 24190 | 0.0 | 0.2 | 2.0 | 2.2 |
| 24469 | 0.0 | 0.2 | 2.0 | 2.2 |
| 24895 | 0.0 | 0.1 | 2.0 | 2.1 |
| 25246 | 0.0 | 0.1 | 2.0 | 2.1 |
| 25846 | 0.0 | 0.2 | 2.0 | 2.2 |
| 26500 | 0.0 | 0.2 | 2.0 | 2.2 |
| 27263 | 0.0 | 0.2 | 2.0 | 2.2 |
| 28104 | 0.0 | 0.2 | 2.0 | 2.2 |
| 29025 | 0.0 | 0.1 | 2.0 | 2.1 |
| 29945 | 0.0 | 0.2 | 2.0 | 2.2 |
| 30361 | 0.0 | 0.3 | 2.0 | 2.3 |

### 11.4 Other Aggradation

Other aggradation comprises the local aggradation components. Other aggradation is determined by calculating the sum of super elevation, which was found to be zero for all sections, and bed from height (H/2).

# 12 Levee Design Toedown and Top Elevation

## 12.1 Levee Toedown Requirements Analysis

The design levee toedown was based on the summing the maximum scour from the different components evaluated which included: (1) Long-Term, (2) General, (3) Local Scour/Bridge, (4) Bedform, and (5) Low-flow Incisement. There was no safety factor applied value of the total scour since all the different components and the recommended toedown was placed below the total scour. Inherently there are already safety factors imbedded in the (1) hydrology values/procedures, (2) hydraulic analysis and parameters, and (3) estimation of values such as the low-flow incisement. In general, there was always some residual vertical difference between the toe-down depth and the estimated total scour, which can be considered the safety factor. In addition, a minimum toedown of four-feet is recommended for those locations where the total scour depth is less than four feet based on discussions with the District and comparison of general minimum design recommendations in the industry.

The **total scour** is based on the following components and a discussion of the values selected in the analysis:

1. General and Long-Term Scour – The maximum negative bed adjustment was evaluated for determining both the General and Long-Term adjustment individually and also evaluating a combined simulation using both the Long-Term hydrograph and General single event 100-year hydrograph. A comparison was made of summing the individual contribution from the General and Long-Term simulation and the combined simulation to determine the maximum scour from the HEC-6T simulations.
2. Local Bridge Scour – The local bridge scour evaluated the abutment, pier, and contraction scour following the procedures outlined in *HEC-18 Evaluating Scour at Bridges-4th Edition* (FHWA, May 2001). The contraction scour calculated using the FHWA procedures was compared to the value computed with HEC-T since the cross-section geometry will also compute contraction scour since it is a sediment continuity balance. The maximum value of these two procedures was utilized and other value eliminated. The pier scour has been included at both bridges for the toedown depth for conservative estimate. However, the pier scour may be eliminated for the toedown estimate at the Sanderson Avenue Bridge since the pier scour hole geometry will be well outside of any influence to the channel bank since the pier is 110 feet from the abutment. It should not be eliminated at State Street bridge since the distance from the abutment to the pier is only 32.5 feet and would be in the zone of influence to the adjacent bank.
3. Other Scour Components – Low flow incisement was estimated from field reconnaissance of the existing conditions and the bedform was calculated for the trough height of an anti-dune.

The following table presents the tabular results and data used in the development of the total scour and toedown value. The recommended toedown was always set below the maximum total scour value.

**Table 12-1 –** Summary of Levee Toedown Components and Recommended Design Toedown Elevation

| River Sta | Initial Thalweg Elevation | Max General Scour (ft) | Max Long-Term Scour (ft) | Bedform Height (ft) | Low-flow Incisement (ft) | Local Scour (Bridge Pier) (ft) | Total Est. Scour (ft) | Min. Toedown Depth (ft) | Design Toedown Elev. | Safety Factor (Residual Freeboard) (ft) |
|---|---|---|---|---|---|---|---|---|---|---|
| 30361.69 | 1538 | 0.0 | 0.0 | -0.5 | -2.0 | | **-2.5** | -4 | 1534.0 | 1.4 |
| 29945.89 | 1535 | -0.1 | 0.0 | -0.5 | -2.0 | | **-2.6** | -4 | 1531.0 | 1.4 |
| 29025.39 | 1530 | 0.0 | -0.5 | -0.4 | -2.0 | | **-2.9** | -4 | 1526.0 | 1.1 |
| 28104.69 | 1525 | -0.2 | -2.8 | -0.9 | -2.0 | | **-5.9** | -6 | 1519.0 | 0.1 |
| 27263.37 | 1517 | -1.1 | -1.7 | -0.9 | -2.0 | | **-5.7** | -6 | 1511.0 | 0.3 |
| 26500.53 | 1513 | 0.0 | 0.0 | -0.6 | -2.0 | | **-2.6** | -4 | 1509.0 | 1.4 |
| 25846.05 | 1512.5 | 0.0 | 0.0 | -0.7 | -2.0 | | **-2.7** | -4 | 1508.5 | 1.3 |
| 25246.64 | 1512 | -0.4 | -0.3 | -0.9 | -2.0 | | **-3.6** | -4 | 1508.0 | 0.4 |
| 24895.09 | 1511 | -0.9 | -1.7 | -0.8 | -2.0 | | **-5.4** | -6 | 1505.0 | 0.6 |
| 24469.84 | 1510 | 0.0 | -1.0 | -0.9 | -2.0 | | **-4.0** | -4 | 1506.0 | 0.0 |
| 24190.24 | 1508 | 0.1 | 0.0 | -0.8 | -2.0 | | **-2.7** | -4 | 1504.0 | 1.3 |
| 23817.09 | 1506 | -0.7 | -0.5 | -1.0 | -2.0 | | **-4.1** | -4 | 1502.0 | 0.0 |
| 23406.44 | 1505 | -0.1 | -0.7 | -0.7 | -2.0 | | **-3.5** | -4 | 1501.0 | 0.5 |
| 22909.46 | 1502 | -0.1 | -1.4 | -0.6 | -2.0 | | **-4.0** | -4 | 1498.0 | 0.0 |
| 22448.18 | 1500 | -0.3 | -1.4 | -0.8 | -2.0 | | **-4.5** | -7 | 1493.0 | 2.5 |
| 21912.02 | 1497.51 | -0.4 | -3.5 | -0.6 | -2.0 | | **-6.6** | -7 | 1490.5 | 0.4 |
| 21459.26 | 1496 | 0.0 | -0.1 | -0.8 | -2.0 | | **-2.9** | -7 | 1489.0 | 4.1 |
| 20953.16 | 1494.19 | -0.7 | -3.6 | -2.1 | -2.0 | | **-8.5** | -9 | 1485.2 | 0.5 |
| 20853.6* | 1493.79 | -1.5 | -2.0 | -1.9 | -2.0 | -3.4 | **-10.8** | -12 | 1481.8 | 1.2 |
| 20802.68 | **State Street Bridge** | | | | | | | -12 | | |
| 20754.2* | 1493.4 | -1.5 | -3.1 | -1.8 | -2.0 | -3.4 | **-11.8** | -12 | 1481.4 | 0.2 |
| 20654.72 | 1493 | 0.0 | -2.9 | -2.4 | -2.0 | | **-7.3** | -8 | 1485.0 | 0.7 |

| **Table 12-1 –** Summary of Levee Toedown Components and Recommended Design Toedown Elevation | | | | | | | | | | |
|---|---|---|---|---|---|---|---|---|---|---|
| **River Sta** | **Initial Thalweg Elevation** | **Max General Scour** (ft) | **Max Long-Term Scour** (ft) | **Bedform Height** (ft) | **Low-flow Incisement** (ft) | **Local Scour (Bridge Pier)** (ft) | **Total Est. Scour** (ft) | **Min. Toedown Depth (ft)** | **Design Toedown Elev.** | **Safety Factor (Residual Freeboard)** (ft) |
| 20179.46 | 1490 | 0.0 | -0.9 | -1.4 | -2.0 | | **-4.3** | -6 | 1484.0 | 1.7 |
| 19813.26 | 1489.4 | -0.1 | -1.9 | -1.7 | -2.0 | | **-5.7** | -6 | 1483.4 | 0.3 |
| 19200.76 | 1488.2 | 0.0 | -0.6 | -0.6 | -2.0 | | **-3.2** | -4 | 1484.2 | 0.8 |
| 18929.32 | 1488 | 0.0 | -0.8 | -0.4 | -2.0 | | **-3.2** | -4 | 1484.0 | 0.8 |
| 18399.16 | 1486 | -0.7 | -2.7 | -0.5 | -2.0 | | **-5.9** | -6 | 1480.0 | 0.1 |
| 17768.32 | 1485 | -0.5 | -2.1 | -0.6 | -2.0 | | **-5.2** | -6 | 1479.0 | 0.8 |
| 17330.97 | 1483 | -0.1 | -3.6 | -0.6 | -2.0 | | **-6.3** | -7 | 1476.0 | 0.7 |
| 16913.42 | 1482 | 0.0 | -2.2 | -0.7 | -2.0 | | **-4.9** | -6 | 1476.0 | 1.1 |
| 16476.12 | 1480 | -0.7 | -2.2 | -0.7 | -2.0 | | **-5.6** | -6 | 1474.0 | 0.4 |
| 16028.82 | 1478 | 0.0 | -1.4 | -0.6 | -2.0 | | **-4.0** | -4 | 1474.0 | 0.0 |
| 15682.82 | 1477 | -0.3 | -1.3 | -0.5 | -2.0 | | **-4.1** | -4 | 1473.0 | 0.0 |
| 15347.98 | 1476 | 0.0 | -0.8 | -0.5 | -2.0 | | **-3.3** | -4 | 1472.0 | 0.7 |
| 14920.48 | 1474 | -0.3 | -1.6 | -0.5 | -2.0 | | **-4.5** | -5 | 1469.0 | 0.5 |
| 14335.42 | 1472 | 0.0 | -0.8 | -0.5 | -2.0 | | **-3.3** | -4 | 1468.0 | 0.7 |
| 13733.7 | 1470 | -0.4 | -1.0 | -0.6 | -2.0 | | **-4.0** | -4 | 1466.0 | 0.0 |
| 13200.36 | 1467 | 0.0 | -0.2 | -0.5 | -2.0 | | **-2.7** | -4 | 1463.0 | 1.3 |
| 12726.18 | 1466 | 0.0 | -0.8 | -0.7 | -2.0 | | **-3.5** | -4 | 1462.0 | 0.5 |
| 12317.58 | 1464 | -1.1 | -4.1 | -0.8 | -2.0 | | **-8.1** | -9 | 1455.0 | 0.9 |
| 11871.18 | 1463 | 0.0 | -3.2 | -1.0 | -2.0 | | **-6.1** | -6 | 1457.0 | 0.0 |
| 11396.58 | 1461 | -0.1 | 0.0 | -0.8 | -2.0 | | **-2.8** | -6 | 1455.0 | 3.2 |
| 11003.2* | 1460 | -0.9 | 0.0 | -0.7 | -2.0 | -3.4 | **-7.0** | -7 | 1453.0 | 0.0 |
| 10687.71 | **Sanderson Bridge** | | | | | | | -7 | | |
| 10609.8* | 1459 | -0.9 | 0.0 | -0.6 | -2.0 | -3.4 | **-6.9** | -7 | 1452.0 | 0.1 |

| **Table 12-1 –** Summary of Levee Toedown Components and Recommended Design Toedown Elevation | | | | | | | | | | |
|---|---|---|---|---|---|---|---|---|---|---|
| **River Sta** | **Initial Thalweg Elevation** | **Max General Scour** (ft) | **Max Long-Term Scour** (ft) | **Bedform Height** (ft) | **Low-flow Incisement** (ft) | **Local Scour (Bridge Pier)** (ft) | **Total Est. Scour** (ft) | **Min. Toedown Depth (ft)** | **Design Toedown Elev.** | **Safety Factor (Residual Freeboard)** (ft) |
| 10216.47 | 1458 | 0.0 | 0.0 | -0.5 | -2.0 | | **-2.5** | -4 | 1454.0 | 1.5 |
| 9716.61 | 1457 | 0.0 | 0.0 | -0.5 | -2.0 | | **-2.5** | -4 | 1453.0 | 1.5 |
| 9359.16 | 1455.75 | 0.0 | 0.0 | -0.4 | -2.0 | | **-2.4** | -4 | 1451.8 | 1.6 |
| 8867.34 | 1454 | 0.0 | 0.0 | -0.4 | -2.0 | | **-2.4** | -4 | 1450.0 | 1.6 |
| 8175.9 | 1452 | 0.0 | 0.0 | -0.4 | -2.0 | | **-2.4** | -4 | 1448.0 | 1.6 |
| 7758.4 | 1451 | 0.0 | 0.0 | -0.5 | -2.0 | | **-2.5** | -4 | 1447.0 | 1.5 |
| 7418.76 | 1450.3 | -0.3 | -0.2 | -0.8 | -2.0 | | **-3.3** | -4 | 1446.3 | 0.7 |
| 6710.68 | 1448 | 0.0 | 0.0 | -0.6 | -2.0 | | **-2.6** | -4 | 1444.0 | 1.4 |
| 6166.06 | 1447.43 | 0.0 | 0.0 | -0.5 | -2.0 | | **-2.5** | -4 | 1443.4 | 1.5 |
| 5941.03 | 1447.24 | -0.3 | 0.0 | -0.5 | -2.0 | | **-2.8** | -4 | 1443.2 | 1.2 |
| 5609.07 | 1447.06 | 0.0 | 0.0 | -0.3 | -2.0 | | **-2.3** | -4 | 1443.1 | 1.7 |
| 5183.62 | 1446.88 | 0.0 | 0.0 | -0.2 | -2.0 | | **-2.2** | -4 | 1442.9 | 1.8 |
| 4684.24 | 1446.7 | 0.0 | 0.0 | -0.2 | -2.0 | | **-2.2** | -4 | 1442.7 | 1.8 |
| 4327.64 | 1446.7 | 0.0 | 0.0 | -0.2 | -2.0 | | **-2.2** | -4 | 1442.7 | 1.8 |
| 3997.36 | 1446.7 | 0.0 | 0.0 | -0.2 | -2.0 | | **-2.2** | -4 | 1442.7 | 1.8 |
| 3670.6 | 1446.7 | 0.0 | 0.0 | -0.1 | -2.0 | | **-2.1** | -4 | 1442.7 | 1.9 |
| 3284.55 | 1446.2 | 0.0 | 0.0 | -0.1 | -2.0 | | **-2.1** | -4 | 1442.2 | 1.9 |
| 2960.91 | 1445.7 | -0.1 | -0.7 | -0.2 | -2.0 | | **-3.0** | -4 | 1441.7 | 1.0 |
| 2580.91 | 1445.2 | -0.1 | -0.6 | -0.2 | -2.0 | | **-2.8** | -4 | 1441.2 | 1.2 |
| 2298.35 | 1444.7 | -0.1 | -0.4 | -0.2 | -2.0 | | **-2.6** | -4 | 1440.7 | 1.4 |
| 2072.69 | 1444.2 | 0.0 | -0.2 | -0.2 | -2.0 | | **-2.4** | -4 | 1440.2 | 1.6 |
| 1677.04 | 1443.7 | 0.0 | 0.0 | -0.1 | -2.0 | | **-2.1** | -4 | 1439.7 | 1.9 |
| 1284.64 | 1442.58 | -0.4 | -0.2 | -0.2 | -2.0 | | **-2.8** | -4 | 1438.6 | 1.2 |

| Table 12-1 – Summary of Levee Toedown Components and Recommended Design Toedown Elevation | | | | | | | | | | |
|---|---|---|---|---|---|---|---|---|---|---|
| **River Sta** | **Initial Thalweg Elevation** | **Max General Scour** (ft) | **Max Long-Term Scour** (ft) | **Bedform Height** (ft) | **Low-flow Incisement** (ft) | **Local Scour (Bridge Pier)** (ft) | **Total Est. Scour** (ft) | **Min. Toedown Depth (ft)** | **Design Toedown Elev.** | **Safety Factor (Residual Freeboard)** (ft) |
| 1000 | 1442.7 | 0.0 | 0.0 | -0.3 | -2.0 | | **-2.3** | -4 | 1438.7 | 1.7 |

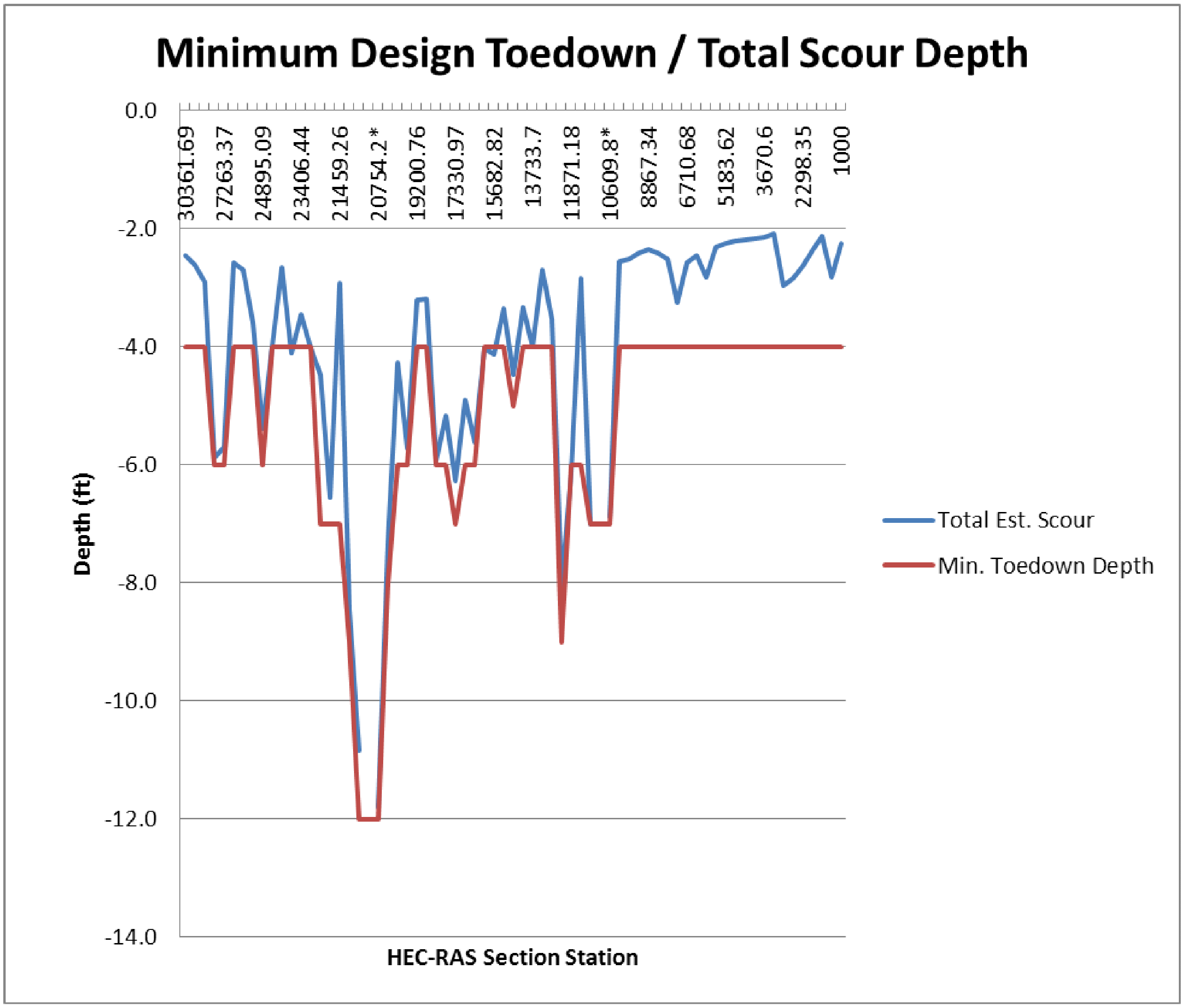


**Figure 12-1 –** Horizontal variation of estimated "total" maximum depth of the different scour components compared to minimum recommended design toedown of levee revetment

The design toedown recommended in the table and graph represents the minimum suggested values. The levee revetment must extend far enough below the existing ground elevation in order to prevent undermining by multiple processes that occur both on a short and long-term basis. The profile may be adjusted based on constructability considerations as long as the minimum criterion is maintained. Additional recommendations include:

- Maintain the maximum toedown depths upstream and downstream of the bridge for a distance four times the estimated scour depth or minimum of 25 feet and then transition at a 5:1 slope in the toedown profile to the next toedown depth upstream and downstream. (Additional similar guidance can be found in bridge scour countermeasure design outlined in *Bridge Scour* (Melville,2000))
- At other locations transition between different toedown depths at a 5:1 profile. (For example, to transition between the 7.0 foot toedown and 4.0 foot toedown would result in a 15-foot horizontal transition)

- Minimum depth of toedown at the Sanderson Bridge location may be reduced with the elimination of the pier scour component.

### 12.2 Design Minimum Top of Levee Requirements and Freeboard

The top of levee was evaluated to ensure that if sediment deposition occurred during a 100-year event then sufficient minimum freeboard as required by FEMA. The National Flood Insurance Program (NFIP) regulations indicate in 44 CFR § 65.10 *Mapping of Areas Protected by Levee Systems* the minimum freeboard requirements for a levee. Riverine levee must provide a minimum freeboard of three feet above the base flood which will be the design 100-year flood event. An additional one-foot above the minimum is required within 100-feet in either side of structures, such as bridges, riverward of the levee. An additional one-half foot above the minimum is required at the upstream end of the levee.

A separate “top of levee” 100-year HEC-RAS was prepared which modified/adjusted each of the “proposed condition” HEC-RAS cross-section with the maximum vertical aggradation amounts determined as the total of the maximum general and long-term adjustment HEC-6T simulations. The maximum aggradation amount was applied uniformly across the cross-section by vertically adjusting the section by that amount. The results of that analysis are illustrated in the following table. This table also provides the minimum recommended top of levee elevation which includes in the minimum freeboard as required by FEMA, except at the upstream end. The upstream location of the levee should have the additional one-half foot added to the value indicated in the table. This table only illustrates the minimum point values along the levee and the final profile should be adjusted to “smooth” the profile and minimize grade breaks.

**Table 12-2 –** Top of Levee Design Elevation
Modified 100-year HEC-RAS Water Surface with Maximum Sediment Deposition Added to Section

| River Sta | Agradation HEC-RAS | | Original HEC-RAS | | Difference | | Design Top Levee Elv (ft) | Design Freeboard (ft) | Total Levee Height (ft) |
|---|---|---|---|---|---|---|---|---|---|
| | Min Ch El (ft) | W.S. Elev (ft) | Min Ch El (ft) | W.S. Elev (ft) | WS (ft) | Invert (ft) | | | |
| 30361.69 | 1541.1 | 1546.09 | 1538 | 1544.42 | 1.67 | 3.1 | 1549.09 | 4.67 | 11.09 |
| 29945.89 | 1535.9 | 1542.99 | 1535 | 1542.34 | 0.65 | 0.9 | 1545.99 | 3.65 | 10.99 |
| 29025.39 | 1530.4 | 1538.95 | 1530 | 1538.79 | 0.16 | 0.4 | 1541.95 | 3.16 | 11.95 |
| 28104.69 | 1525 | 1533.2 | 1525 | 1532.65 | 0.55 | 0 | 1536.2 | 3.55 | 11.2 |
| 27263.37 | 1517.75 | 1530.87 | 1517 | 1527.96 | 2.91 | 0.75 | 1533.87 | 5.91 | 16.87 |
| 26500.53 | 1518.1 | 1528.25 | 1513 | 1526.95 | 1.3 | 5.1 | 1531.25 | 4.3 | 18.25 |
| 25846.05 | 1514.1 | 1525.97 | 1512.5 | 1525.3 | 0.67 | 1.6 | 1528.97 | 3.67 | 16.47 |
| 25246.64 | 1512.72 | 1523.44 | 1512 | 1523.07 | 0.37 | 0.72 | 1526.44 | 3.37 | 14.44 |
| 24895.09 | 1511 | 1522.69 | 1511 | 1522.02 | 0.67 | 0 | 1525.69 | 3.67 | 14.69 |
| 24469.84 | 1510.2 | 1521.31 | 1510 | 1520.23 | 1.08 | 0.2 | 1524.31 | 4.08 | 14.31 |
| 24190.24 | 1509.8 | 1519.22 | 1508 | 1519.02 | 0.2 | 1.8 | 1522.22 | 3.2 | 14.22 |
| 23817.09 | 1506.1 | 1516.62 | 1506 | 1516.6 | 0.02 | 0.1 | 1519.62 | 3.02 | 13.62 |
| 23406.44 | 1505 | 1514.36 | 1505 | 1514.16 | 0.2 | 0 | 1517.36 | 3.2 | 12.36 |
| 22909.46 | 1502.3 | 1512.81 | 1502 | 1512.79 | 0.02 | 0.3 | 1515.81 | 3.02 | 13.81 |
| 22448.18 | 1500 | 1510.06 | 1500 | 1510.02 | 0.04 | 0 | 1513.06 | 3.04 | 13.06 |
| 21912.02 | 1497.51 | 1508.36 | 1497.51 | 1508.14 | 0.22 | 0 | 1511.36 | 3.22 | 13.85 |
| 21459.26 | 1496.3 | 1507.02 | 1496 | 1506.83 | 0.19 | 0.3 | 1510.02 | 3.19 | 14.02 |

**Table 12-2 –** Top of Levee Design Elevation
Modified 100-year HEC-RAS Water Surface with Maximum Sediment Deposition Added to Section

| River Sta | Agradation HEC-RAS | | Original HEC-RAS | | Difference | | Design Top Levee Elv (ft) | Design Freeboard (ft) | Total Levee Height (ft) |
|---|---|---|---|---|---|---|---|---|---|
| | Min Ch El (ft) | W.S. Elev (ft) | Min Ch El (ft) | W.S. Elev (ft) | WS (ft) | Invert (ft) | | | |
| 20953.16 | 1494.19 | 1505.62 | 1494.19 | 1505.13 | 0.49 | 0 | 1508.62 | 3.49 | 14.43 |
| 20853.6* | 1493.99 | 1505.49 | 1493.79 | 1505 | 0.49 | 0.2 | 1509.49 | 4.49 | 15.7 |
| 20802.68 | **State Street Bridge** | | | | | | | | |
| 20754.2* | 1493.5 | 1504.27 | 1493.4 | 1503.07 | 1.2 | 0.1 | 1508.27 | 5.2 | 14.87 |
| 20654.72 | 1493.1 | 1504.07 | 1493 | 1502.75 | 1.32 | 0.1 | 1507.07 | 4.32 | 14.07 |
| 20179.46 | 1491 | 1500.3 | 1490 | 1500.02 | 0.28 | 1 | 1503.3 | 3.28 | 13.3 |
| 19813.26 | 1489.4 | 1498.83 | 1489.4 | 1498 | 0.83 | 0 | 1501.83 | 3.83 | 12.43 |
| 19200.76 | 1489.3 | 1496.9 | 1488.2 | 1496.3 | 0.6 | 1.1 | 1499.9 | 3.6 | 11.7 |
| 18929.32 | 1489.5 | 1495.93 | 1488 | 1495.74 | 0.19 | 1.5 | 1498.93 | 3.19 | 10.93 |
| 18399.16 | 1486 | 1494.25 | 1486 | 1494.25 | 0 | 0 | 1497.25 | 3 | 11.25 |
| 17768.32 | 1485 | 1491.75 | 1485 | 1491.59 | 0.16 | 0 | 1494.75 | 3.16 | 9.75 |
| 17330.97 | 1483.2 | 1489.5 | 1483 | 1489.47 | 0.03 | 0.2 | 1492.5 | 3.03 | 9.5 |
| 16913.42 | 1482 | 1487.48 | 1482 | 1487.43 | 0.05 | 0 | 1490.48 | 3.05 | 8.48 |
| 16476.12 | 1480 | 1485.8 | 1480 | 1485.53 | 0.27 | 0 | 1488.8 | 3.27 | 8.8 |
| 16028.82 | 1478.3 | 1483.96 | 1478 | 1483.63 | 0.33 | 0.3 | 1486.96 | 3.33 | 8.96 |
| 15682.82 | 1477.1 | 1482.98 | 1477 | 1482.4 | 0.58 | 0.1 | 1485.98 | 3.58 | 8.98 |
| 15347.98 | 1476.9 | 1481.57 | 1476 | 1481.47 | 0.1 | 0.9 | 1484.57 | 3.1 | 8.57 |
| 14920.48 | 1474 | 1480.12 | 1474 | 1479.98 | 0.14 | 0 | 1483.12 | 3.14 | 9.12 |
| 14335.42 | 1472.2 | 1478.4 | 1472 | 1478.29 | 0.11 | 0.2 | 1481.4 | 3.11 | 9.4 |
| 13733.7 | 1470 | 1476.66 | 1470 | 1476.44 | 0.22 | 0 | 1479.66 | 3.22 | 9.66 |
| 13200.36 | 1467.3 | 1474.74 | 1467 | 1474.58 | 0.16 | 0.3 | 1477.74 | 3.16 | 10.74 |
| 12726.18 | 1466.1 | 1472.63 | 1466 | 1472.26 | 0.37 | 0.1 | 1475.63 | 3.37 | 9.63 |
| 12317.58 | 1464 | 1471.76 | 1464 | 1470.92 | 0.84 | 0 | 1474.76 | 3.84 | 10.76 |
| 11871.18 | 1463.4 | 1470.93 | 1463 | 1469.64 | 1.29 | 0.4 | 1473.93 | 4.29 | 10.93 |
| 11396.58 | 1462.03 | 1469.99 | 1461 | 1468.33 | 1.66 | 1.03 | 1472.99 | 4.66 | 11.99 |
| 11003.2* | 1461.46 | 1469.29 | 1460 | 1467.47 | 1.82 | 1.46 | 1473.29 | 5.82 | 13.29 |
| 10687.71 | **Sanderson Bridge** | | | | | | | | 0 |
| 10609.8* | 1461.12 | 1468.08 | 1459 | 1465.71 | 2.37 | 2.12 | 1472.08 | 6.37 | 13.08 |
| 10216.47 | 1460.48 | 1466.7 | 1458 | 1464.54 | 2.16 | 2.48 | 1469.7 | 5.16 | 11.7 |
| 9716.61 | 1459.1 | 1465.44 | 1457 | 1463.34 | 2.1 | 2.1 | 1468.44 | 5.1 | 11.44 |
| 9359.16 | 1458.49 | 1464.16 | 1455.75 | 1462.67 | 1.49 | 2.74 | 1467.16 | 4.49 | 11.41 |
| 8867.34 | 1455.92 | 1462.8 | 1454 | 1461.82 | 0.98 | 1.92 | 1465.8 | 3.98 | 11.8 |
| 8175.9 | 1452.98 | 1461.01 | 1452 | 1460.4 | 0.61 | 0.98 | 1464.01 | 3.61 | 12.01 |
| 7758.4 | 1451.67 | 1459.71 | 1451 | 1459.21 | 0.5 | 0.67 | 1462.71 | 3.5 | 11.71 |
| 7418.76 | 1450.72 | 1458.4 | 1450.3 | 1457.67 | 0.73 | 0.42 | 1461.4 | 3.73 | 11.1 |
| 6710.68 | 1448.88 | 1456.21 | 1448 | 1455.08 | 1.13 | 0.88 | 1459.21 | 4.13 | 11.21 |

**Table 12-2 –** Top of Levee Design Elevation
Modified 100-year HEC-RAS Water Surface with Maximum Sediment Deposition Added to Section

| River Sta | Agradation HEC-RAS | | Original HEC-RAS | | Difference | | Design Top Levee Elv (ft) | Design Freeboard (ft) | Total Levee Height (ft) |
|---|---|---|---|---|---|---|---|---|---|
| | Min Ch El (ft) | W.S. Elev (ft) | Min Ch El (ft) | W.S. Elev (ft) | WS (ft) | Invert (ft) | | | |
| 6166.06 | 1448.61 | 1454.78 | 1447.43 | 1453.39 | 1.39 | 1.18 | 1457.78 | 4.39 | 10.35 |
| 5941.03 | 1448.29 | 1454.3 | 1447.24 | 1452.63 | 1.67 | 1.05 | 1457.3 | 4.67 | 10.06 |
| 5609.07 | 1448.96 | 1453.31 | 1447.06 | 1451.75 | 1.56 | 1.9 | 1456.31 | 4.56 | 9.25 |
| 5183.62 | 1448.63 | 1452.37 | 1446.88 | 1451.1 | 1.27 | 1.75 | 1455.37 | 4.27 | 8.49 |
| 4684.24 | 1448.22 | 1451.54 | 1446.7 | 1450.57 | 0.97 | 1.52 | 1454.54 | 3.97 | 7.84 |
| 4327.64 | 1447.93 | 1451.02 | 1446.7 | 1450.22 | 0.8 | 1.23 | 1454.02 | 3.8 | 7.32 |
| 3997.36 | 1447.86 | 1450.56 | 1446.7 | 1449.92 | 0.64 | 1.16 | 1453.56 | 3.64 | 6.86 |
| 3670.6 | 1447.39 | 1450.26 | 1446.7 | 1449.67 | 0.59 | 0.69 | 1453.26 | 3.59 | 6.56 |
| 3284.55 | 1448.47 | 1449.72 | 1446.2 | 1449.52 | 0.2 | 2.27 | 1452.72 | 3.2 | 6.52 |
| 2960.91 | 1445.7 | 1449.28 | 1445.7 | 1449.2 | 0.08 | 0 | 1452.28 | 3.08 | 6.58 |
| 2580.91 | 1445.2 | 1448.8 | 1445.2 | 1448.64 | 0.16 | 0 | 1451.8 | 3.16 | 6.6 |
| 2298.35 | 1444.7 | 1448.47 | 1444.7 | 1448.24 | 0.23 | 0 | 1451.47 | 3.23 | 6.77 |
| 2072.69 | 1444.2 | 1448.29 | 1444.2 | 1448 | 0.29 | 0 | 1451.29 | 3.29 | 7.09 |
| 1677.04 | 1444.3 | 1447.53 | 1443.7 | 1447.39 | 0.14 | 0.6 | 1450.53 | 3.14 | 6.83 |
| 1284.64 | 1442.58 | 1446.53 | 1442.58 | 1446.53 | 0 | 0 | 1449.53 | 3 | 6.95 |
| 1000 | 1442.7 | 1445.85 | 1442.7 | 1445.85 | 0 | 0 | 1448.85 | 3 | 6.15 |

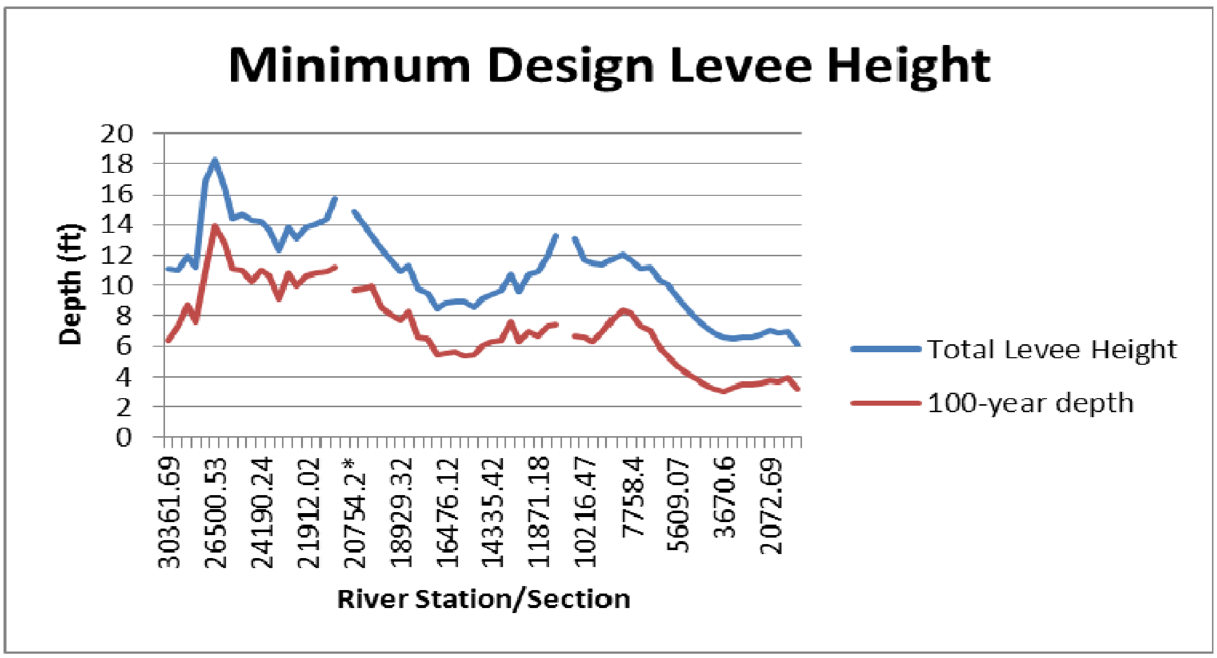


**Figure 12-2 –** Horizontal variation of the minimum total levee height measured from the thalweg elevation compared to the maximum100-year flow depths.

# 13 Mystic Lake

## 13.1 HEC-6T Implications for Mystic Lake Management

Results presented in *Table 9 5 – Comparison of Existing and Proposed Conditions General Adjustment Bed Elevation* illustrates changes between existing and proposed conditions which suggest that only minor ($\Delta z<0.1$ft) changes in bed elevation are expected between the two conditions at the downstream end of the project. This is the expected result since the proposed levee width increases at the downstream end of the project from the design width to the existing floodplain width. Since no major change in bed change is expected between the existing and proposed conditions downstream of the project, and since the project does not divert from or confluence flows to the River only local sediment transport changes are expected as a result of the proposed project. Therefore, management of sediment exchange between San Jacinto River and Mystic Lake can be expected to continue without alteration following the completion of the proposed project.

## 13.2 Discussion of Anticipated Effects of Downstream In-Stream Sediment Basin

There is a proposal as part of the “San Jacinto Stage IV Levee Preliminary Design” to potentially implement an in-channel sedimentation basin within the downstream reach of a portion of the floodplain as part of the overall sediment management plan for the river system. The basin would be located in the downstream transition zone for levee where the levee alignment is expanding to the original floodplain. The initial conceptual layout of the basin proposes an approximately 70-acre shallow basin that would be excavated three-feet and the basin would occur outside of the main active channel, within the southerly overbank area. The conceptual basin is illustrated below and is shown as the orange hatched triangular area along the downstream levee expansion transition.


**Figure 13-1 –** Conceptual footprint of in-channel sedimentation basin located at the downstream reach of the levee system

The general trends of sediment transport for the proposed levee system can be utilized to develop a qualitative assessment and general prediction of the impacts from this type of facility. The qualitative assessment was then verified with a preliminary HEC-6T model for the 100-year storm which incorporated modified cross-sections within the overbank that reflected the proposed basin. A general qualitative assessment of the basin performance and effect on the river system is outlined in the following points from an understanding of the river characteristics using the previous analysis. However, **the basin should not have any significant influence on the downstream stream stability.**

- The basin does not result in any significant influence to the average channel hydraulics because basin geometry occurs over (1) a large area within the overbank, and (2) basin relatively shallow.
- The original sediment transport modeling for the proposed levee system indicates that the system is aggrading and approximately 24% of the entire 100-year volume in trapped within the channel, so the basin should not change the general trends of the channel, but should increase the trap efficiency of the system.
- The active channel invert and geometry is still maintained so only sediment transport within the overbank would be influenced.

The proposed levee conditions HEC-6T model was adjusted to create a new preliminary model with the general configuration of the basin incorporated in the sections, so the hydraulic influence can be reflected in the sediment continuity analysis. Approximately 11 different cross-sections within the model were modified to reflect the excavation of a 70-acre basin approximately 3 feet deep. The HEC-6T River Stations where the basin is located occur between upstream Station 74+19 and downstream Station 36+71. This model is just intended as an initial assessment tool to confirm the qualitative predictions. More detailed fluvial analysis should be performed as part of the final design. The model generally indicated the following:

- The basin would increase the amount of sediment trapped within the “system” and during a 100-year storm it increased to 36% (from 24%) which is not a significant change based on comparison of the aggradation trends anyways in the channel system.
- There was localized degradation which occurred upstream of the basin for two sections, or approximately 800 feet until it appeared to stabilize.
- The cross-section upstream of the basin resulted in the most degradation which was about 1.5 feet.
- The amount of degradation that occurred downstream of the basin appeared to be the same as the original proposed conditions model and was generally less than 0.1 feet.

The following Table 13-1 illustrates a comparison of the General Storm streambed variation based on the HEC-6T models for the proposed conditions with and without the sedimentation basin. The highlighted sections numbers indicated the sections in which the geometry was modified to include the excavation of the basin.

**Table 13-1** – Comparison of HEC-6T Results for General Storm Streambed Adjustments between Proposed Conditions Wide Model and Same Model Modified with Sedimentation Basin

| HEC-6T Section | Initial Thalweg Elevation | Change In Thalweg Elevation at End of Hydrograph | |
|---|---|---|---|
| | | Proposed (Final) (ft) | Proposed with Basin (Final) (ft) |
| 1000 | 1442.7 | 0.0 | 0.0 |
| 1285 | 1442.6 | -0.4 | -0.4 |
| 1677 | 1442.7 | 0.0 | 0.0 |

| **Table 13-1** – Comparison of HEC-6T Results for General Storm Streambed Adjustments between Proposed Conditions Wide Model and Same Model Modified with Sedimentation Basin | | | |
|---|---|---|---|
| **HEC-6T Section** | **Initial Thalweg Elevation** | **Change In Thalweg Elevation at End of Hydrograph** | |
| | | **Proposed (Final) (ft)** | **Proposed with Basin (Final) (ft)** |
| 2073 | 1444.2 | 0.0 | 0.0 |
| 2298 | 1444.7 | -0.1 | -0.1 |
| 2581 | 1445.2 | -0.1 | -0.1 |
| 2961 | 1445.7 | -0.1 | -0.1 |
| 3285 | 1442.7 | 0.2 | 0.0 |
| 3671 | 1444.1 | 0.2 | 0.1 |
| 3997 | 1445.0 | 0.2 | 0.1 |
| 4328 | 1445.0 | 0.1 | 0.1 |
| 4684 | 1446.0 | 0.2 | 0.2 |
| 5184 | 1446.0 | 0.1 | 0.7 |
| 5609 | 1447.0 | 0.2 | 0.6 |
| 5941 | 1447.2 | -0.3 | 0.2 |
| 6166 | 1447.4 | 0.0 | 0.1 |
| 6711 | 1449.8 | 0.1 | 0.0 |
| 7419 | 1451.0 | -0.3 | 0.7 |
| 7758 | 1452.0 | 0.0 | -1.5 |
| 8176 | 1452.0 | 0.0 | -0.2 |
| 8867 | 1453.4 | 0.0 | 0.0 |
| 9359 | 1454.5 | 0.1 | 0.1 |
| 9717 | 1455.9 | 0.0 | 0.0 |
| 10216 | 1456.8 | 0.1 | 0.1 |

### 13.3 Comparison of Current Study to the Previous USBR 2008 Sediment Transport Study

A previous study, *Upper San Jacinto River Sediment Transport Study, San Jacinto River, California* (USBR/Tetra Tech, 2008) was performed for the portion of the San Jacinto River from near Lake Park Drive to Bridge Street in order to evaluate the sediment transport effect from a proposed channel connection to Mystic Lake. The purpose of the report was to analyze the flow of sediment through the proposed channel connection to the terminus just upstream of Bridge Street near Mystic Lake. This was a comprehensive study which followed a similar work program and analytical process to the current PACE study, however, the objective of the report was not for performed to a level of detail levee design, but was to understand the general trends in sediment transport through the system. The basic elements of the USBR work program and analysis included:

- Sediment sampling of **bed material sizes**
- Evaluation of the “long term” **hydrology evaluation** of the 87-years of flow gage data
- **Hydraulic characteristics** of the floodplain with HEC-RAS

- Dividing the channel into discrete reaches representative of similar hydraulic characteristics
- **Sediment budget** analysis of the five identified channel reaches to determine the change in sediment transport/delivery long term using “flow-duration” analysis (bins). (provides a simplified procedure in order to evaluate average changes of the channel reaches in a time period and the results can be used to check the results of the more detailed sediment transport model)
- **Sediment transport moveable bed model** using SRH-1D to evaluate changes in the streambed for the long term condition using the 87-years of record flow data which was reduced in order to eliminate the zero flow days.

The results of the USBR study indicated general trends which included that (1) aggradation was predicted for all the reaches and cross sections, (2) an average of 1 ft of aggradation under three years of flow which was the equivalent to the 87-years of record, and (3) 6,000 tons of bed material per year was estimated to be delivered long term downstream to Mystic Lake at Bridge Street.

The current study differs in several areas of the work from the previous USBR study since a more detailed assessment was performed including various sensitivity analysis evaluating the effects of various conditions and parameters. In addition, the objective of the current study was to evaluate the maximum potential change in the streambed both from aggradation and degradation, since during the passage of a storm hydrograph both conditions can occur and not just to focus on the condition of the streambed at the end of the hydrograph. Some of the differences between the current and USBR study include the following:

- Current study utilized HEC-6T for the moveable bed model while the USBR used SRH-1D
- Long term hydrology for the current only used flowrates from the 87-years of record which exceeded 5,000 cfs since this provided flow depths in the HEC-RAS models and resulted in a linearized hydrograph of 18 days. The USBR study used any flowrate which exceeded zero which resulted in a synthesized continuous hydrograph was 3.2 years, but most flows were relatively small.
- The sediment grain size characteristics were observed to change between the upstream and downstream reach of the channel based on the most current field sampling done for the levee study. The upstream reach had a median gran size 0.7 mm which is the same as the USBR study while the downstream reach of the channel had a median grain size of 0.3 mm. It is expected as you proceed downstream that the grain size will become smaller as you have correspondingly flatter slope and less sediment transport capacity. However, the USBR used the single representative grain size distribution.
- Both the “general storm” and “long term” hydrology was evaluated in the current fluvial analysis which evaluated the associated streambed changes with each. The general scour evaluated the design 100-year hydrograph of 57,000 cfs while the USBR study only evaluated the long term hydrology.
- The long term hydrology used in the USBR mobile bed model only used the average daily flows and did not include a peak flowrate during the daily period which was evaluated as one of the sensitivity analysis in the current analysis.
- Current study used different sediment transport equations to evaluate the fluvial hydraulics in the model which included Toffaleti as the primary relationship, but Yang and Ackers-White was also evaluated. The USBR study used Ackers-White, Yang, Laursen, and Engelund-Hansen.
- Using the “recirculation” option of HEC-6T to determine the upstream boundary condition for the inflowing sediment hydrograph, while the USBR study appeared to have used the sediment transport capacity upstream.
- The hydraulic parameters used were generally similar including the cross section spacing and manning’s coefficient, however, it is not known how the USBR analysis handled the divided flow or if the flow was assumed to be contained within the levees.

| **Summary Comparison Difference in Analyses for PACE Study to USBR/Tetra Tech Study** | | |
|---|---|---|
| **Analysis Element** | **PACE** | **USBR** |
| Fluvial Model | HEC6-T | SRH-1D |

| | | |
|---|---|---|
| 100-year Storm | Yes | No |
| Long term analysis | Yes | Yes |
| Long Term Hydrology | Considered only flows greater than 5,000 cfs during 87-year period of record data – 18 days linearized hydrograph | Considered all flows greater than zero – 3.2 year linearized hydrograph |
| Long Term Hydrology | Peak flows with average daily | Only average daily |
| Upstream Sediment Inflow | HEC-6T recirculation option | Sediment transport capacity |
| Sediment transport equation | Toffaleti (also Yang, Ackers-White) | Yange, Laursen, Ackers-White, Engelund-Hansen |
| Channel Geometry | Webb Levee Design | Levee and proposed downstream channel connection to Bridge Street |

**The general trends related to sediment transport between the two studies are essentially the same** which indicated that aggradation is expected to occur along different reach, except where there are contractions or bridges. In addition, the amount of sediment entering the upstream reach of the channel is less than is delivered at the downstream because of the diminished slope and corresponding sediment transport capacity. However, the current study goes into more detail evaluating not only the long term conditions but the effect of a single 100-year storm event or "general storm." In addition, the current study evaluated a variety of different scenarios and sensitivity analyses which include (1) wide and narrow channel, (2) long term hydrology with peaks added to daily average flows, (3) general storm included in the time period of the long term flows, (4) separate bridge hydraulic and scour analysis, (5) existing and proposed channel geometry, and (6) evaluation of the maximum aggradation and degradation during the storm hydrograph. It is difficult to compare the total quantity of long term sediment delivery at the downstream reach between the two studies since the downstream points are different and the application of the long term hydrology is also different. In addition, the current study evaluates the maximum positive and vertical change at a cross section during the passage of a storm hydrograph so this can be used to evaluate the required levee toedown, since scour is observed during the passage of a storm and in particular at contractions in the levee alignment and at bridges. The increased level of detail to evaluate these different conditions and changes in the streambed elevation were necessary as part of the "design" information for the levee improvements. The work program and level of analysis is expected to be different between the two studies since the objectives of these studies were different because the current study is for the top and toedown requirements of a levee while the previous study focused on the change in sediment delivery to Mystic Lake.

# 14 References


CHJ (2008) In Progress Report Sediment Transport Sampling and Testing San Jacinto Area San Jacinto River, Riverside County California. July 23.

Federal Emergency Management Agency (1999) Riverine Erosion Hazard Areas Mapping Feasibility Study. September.

Federal Highway Administration (2001) Hydraulic Engineering Circular Number 18. May.

Federal Register (2003) V. 22, N. 139, p. 39802.

Jaffe, D. A. (2009) A comparison of long-term sediment transport numerical model results using historical and statistical hydrograph data in the arid southwestern United States. Headwaters to Ocean Conference, Long Beach, CA Conference abstract.

Mobile Boundary Hydraulics (2002) Sedimentation in stream network (HEC-6T).

McCuen, R. H. (1998) Hydrologic Analysis and Design, 2$^{nd}$. ed. Prentice Hall.

Riverside County Flood Control and Water Conservation District (RCFCD) (1975) Report on San Jacinto River Hydrology, Zone 4. March.

Riverside County Flood Control and Water Conservation District (RCFCD) (1994) Report on San Jacinto River Hydrology, Zone 4. January.

Riverside County Flood Control and Water Conservation District (RCFCD) (2000) Evaluation of the Hydrologic and Hydraulic Effects of San Jacinto River Channelization on Ordinary Flood Events in the Lower Perris Valley California. June.

Simons, D. B., and F. Senturk (1992) Sediment Transport Technology, revised edition. Water Resources Publications, Chelsea, Michigan, USA.

United States Army Corps of Engineers (ACOE) (2008) HEC-RAS River Analysis System. March.

United States Army Corps of Engineers (ACOE) (2002) SAM Hydraulic Design Package for Channels. September.

Yang, C. T., and C.-A. Huang (2001) Applicability of sediment transport formulas. Int. J. of Sediment Res., Vol 16, No 3, pp. 335-353.